



01 Feb 1981

Behavior of C- and Z-purlins under wind uplift

Parviz Soroushian

Teoman Peköz

Follow this and additional works at: <https://scholarsmine.mst.edu/ccfss-library>



Part of the [Structural Engineering Commons](#)

Recommended Citation

Soroushian, Parviz and Peköz, Teoman, "Behavior of C- and Z-purlins under wind uplift" (1981). *Center for Cold-Formed Steel Structures Library*. 157.

<https://scholarsmine.mst.edu/ccfss-library/157>

This Technical Report is brought to you for free and open access by Scholars' Mine. It has been accepted for inclusion in Center for Cold-Formed Steel Structures Library by an authorized administrator of Scholars' Mine. This work is protected by U. S. Copyright Law. Unauthorized use including reproduction for redistribution requires the permission of the copyright holder. For more information, please contact scholarsmine@mst.edu.

Department of Structural Engineering
School of Civil and Environmental Engineering
Cornell University

Report No. 81-2

R 7/20/81

BEHAVIOR OF C- AND Z-PURLINS
UNDER WIND UPLIFT

by
Teoman Peköz
Project Director
and
P. Soroushian

A Research Project Sponsored by the
Metal Building Manufacturers Association
and
American Iron and Steel Institute

CCFSS LIBRARY Teoman Pekoz, P. Soroushian,
22 1 * 2047 BEHAVIOR OF C- AND Z- PURLINS
February UNDER WIND UPLIFT
1981

CCFSS LIBRARY Teoman Pekoz, P. Soroushian,
22 1 * 2047 BEHAVIOR OF C- AND Z- PURLINS
February UNDER WIND UPLIFT
1981

DATE	ISSUED TO

Technical Library
Center for Cold-Formed Steel Structures
University of Missouri-Rolla
Rolla, MO 65401

PREFACE

This is the second major and final report of the Ultimate Strength of Cold-Formed Steel Z- and C-Purlins subjected to wind uplift loading. The first major progress report was by M.A.A. Razak and T. Peköz dated February 1980 (Ref. 1). The present final report presents the results of work conducted since the earlier major report. To the extent possible the material presented in the earlier report is not repeated here. This final report does contain an up-dated version of all the material presented in several intermediate progress reports issued since February 1980.

The authors wish to thank Mr. Erol Peköz for his expert computer programming and support to produce all the plots in this report, Mr. Bao-kang He for his help in the project, and Mrs. Oneita I. Weeks for her patient and competent typing of this report.

The sponsorship of the American Iron and Steel Institute and of the Metal Building Manufacturers Association as well as the cooperation of the committees of the sponsors is gratefully acknowledged.

TABLE OF CONTENTS

	Page
PREFACE	
1. INTRODUCTION	1
2. GENERAL THEORY AND SOLUTIONS	3
2.1 The Analytical Model	4
2.2 The Solutions	9
2.2.1 Simply Supported Purlins Without Intermediate Braces	10
2.2.2 Simply Supported Purlins With Midspan Bracing	13
2.2.3 Simply Supported Purlins With Third Point Bracing	14
2.3 Failure Criteria	15
2.3.1 Full Depth, Failure Stress Approach	16
2.3.2 Effective Depth Approach (Ref. 6)	17
3. SIMPLIFICATIONS OF THE SOLUTIONS AND NUMERIC STUDIES	19
3.1 Simply Supported Purlins Without Intermediate Braces	19
3.1.1 Simplified Form of the Equations and the Moment of Inertia	19
3.1.2 A Possible Design Approach	21
3.1.3 Parametric Studies	23
4. EXPERIMENTAL INVESTIGATION	27
4.1 Large Scale Tests	27
4.1.1 Z-Purlin Tests at Cornell University	28
4.1.2 Z-Purlin Tests by a Metal Building Manufacturer	28
4.1.3 C-Purlin Tests at Cornell University	28
4.2 Component Tests	29

	Page
4.2.1 Rotational Restraint Tests	29
4.2.2 Roof Panel Shear Rigidity (Cantilever Tests)	31
5. COMPARISON OF CALCULATED AND EXPERIMENTALLY OBSERVED RESULTS	32
5.1 Comparison of Ultimate Loads	33
5.2 Comparison of Deflections and Stresses at Midspan	34
5.3 Summary and Conclusions	35
6. SUMMARY AND CONCLUSIONS	36
REFERENCES	38
TABLES	39
FIGURES	53

CHAPTER 1

INTRODUCTION

Cold-formed steel lipped channel (C-) and Z-purlins are used widely in the roofs of metal buildings. They are easy and economical to fabricate and erect. However these sections are weak in the lateral direction and in torsion. In order to use their full bending capacity in the strong direction, they must be braced in the lateral direction and against twisting. Roof panels which are connected to the purlins do provide to some extent such bracing effect by virtue of their shear rigidity and resistance to local bending at the connections.

Wind uplift is an important design condition for roof purlins. The objective of the research reported herein was to develop simple design equations for C- and Z-purlins subjected to uplift.

The previous work reported in Refs. 2 through 4 based on the classical theory of torsional-flexure resulted in computer programs for the analysis of the problem. The classical theory of torsional-flexure due to its complexity was not suitable for treating the effects of local buckling and post-buckling behavior on the overall behavior. Furthermore, this approach was not extended to include the effects of initial sweep and twist of purlins. The importance of these parameters was observed in several large scale tests. The theory was shown to be satisfactory for predicting deflections but not the ultimate loads. The discrepancies were larger for thinner sections indicating the importance of local behavior of the component plate elements of the sections.

In the first phase of the present research reported in Ref. 1, work was initiated to include the above parameters in a design formulation. The basic

approach used in Ref. 1 was that given in Section 3 of Part III of Ref. 5. This approach also has several deficiencies. First, a sudden bifurcation type is the basic behavior mode assumed in that approach. Namely, it is assumed that the compression flange of a purlin does not deflect laterally until failure. The actual behavior is clearly not so. The compression flange deflects laterally from the start of loading. Second, the effect of initial sweep and twist is not accounted for. These and several other additional deficiencies of that approach have been eliminated by the new approach derived in the present research. This new approach will be discussed in detail in Chapter 2. Failure criteria will also be discussed in this chapter.

Simplifications to the general solutions obtained in Chapter 2 will be presented in Chapter 3.

Large scale and component tests by the authors and by a steel manufacturer will be described in Chapter 4. The experimental and analytical results will be compared in Chapter 5. Finally, a summary of the work and the conclusions will be presented in Chapter 6.

CHAPTER 2

GENERAL THEORY AND SOLUTIONS

The previous work reported in Refs. 2 through 4 has taken into account the bracing action of the roof panels due to their shear rigidity as well as the resistance to rotation to local bending at the purlin-to-roof-panel connection. The latter action will be referred to as the rotational restraint. The rotational restraint is also provided by the cross-bending rigidity of the panels. However, in the previous tests it was concluded that the cross-bending rigidity is an order of magnitude higher than the local rigidity at the connection. For this reason the rotations of the purlin due to cross-bending of the panels will be ignored.

In order to reach a simple solution and based on an intuitive assessment of the overall behavior in the building, the purlins will be assumed fixed against deflection in the plane of the roof at the purlin-to-roof-panel connection. This is equivalent to taking the value of the shear rigidity to be infinite in the method of analysis of Refs. 2 through 4. This assumption appears reasonable because studies such as those reported in Ref. 9 based on the computer program of Ref. 3 show that as long as the value of Q is larger than a reasonable minimum, the results are not sensitive to the value of Q . As the correlation with the test results indicate this assumption appears satisfactory within the framework of the simple solutions obtained in this research.

In a great majority of metal building applications, the purlins are continuous over the building frames which serve as intermediate supports for the purlins. The continuity is accomplished by lapping the purlins over the

supports. The Z-purlins are lapped by nesting one inside the other. C-purlins are lapped by placing them back-to-back over the supports. In each case the purlins are bolted together and the screws connecting the roof panels to the purlins penetrate through both purlins. The research reported herein dealt with only simply-supported purlins. The solutions can be extended to continuous purlins as will be discussed below.

In principle, the model developed for analyzing the lateral deflection and twisting isolates a portion of the part of the purlin subjected to compressive stresses and treats it as a beam-column on an elastic foundation. The elastic foundation is provided by the remaining portion of the purlin and the roof panels. The lateral loading on the beam-column results from the shear flow in the section and varies along the length of the member. The axial load in the beam-column results from the compressive stresses in the purlin. These too can vary along the length. In general, the component plate elements of purlins can be quite thin. Consequently, the post-buckling behavior of the plate elements can influence the overall behavior significantly. This effect will be included by using the effective width approach. Furthermore, the post-buckling interaction of the plate elements is, to some degree, reflected in the failure criteria to be used.

2.1 The Analytical Model

The analytical model described above in principle, will be developed quantitatively in this section. The C- and Z-purlins undergo vertical deflections (in the original plane of the web) and twisting. The twisting results in lateral deflections of the compression flange. Deflected configurations are shown in Fig. 2.1.a. For the purposes of our discussion and the derivation of the analytical model the deformations can be considered in two stages.

These stages will be referred to as the torsion and the vertical bending stages. These stages are illustrated in Fig. 2.1.b.

The vertical bending stage can be analyzed using the simple flexure theory. However, the moment of inertia is to be computed for the twisted section. Twisting does introduce some small vertical deflection component which will be added to the vertical deflections obtained for the vertical bending stage.

The torsion stage involves lateral deflection and twisting which will be analyzed through the use of an idealized analytical model. The model involves the assumption of a beam-column on elastic foundation. The beam-column section consists of the compression flange and a portion of the web. The spring constraint for the elastic foundation is obtained as follows. The purlin to panel connection can be idealized to act as a rotational spring located at the center of rotation of each purlin as shown in Fig. 2.2.a. Further simplification is made by converting this spring into a linear extensional spring of stiffness k located at the level of the compression flange shown in Fig. 2.2.a. This linear spring combines the effect of the restraint provided by the roof panels and the web of the purlin to the compression portion of the purlin. The roof panel restraint is best determined by test.

As discussed above, the lateral force on the idealized beam-column results from the variation of the shear flow along the member. In the case of Z-purlins, the center of rotation can be assumed to be the corner between the web and the tension flange (Fig. 2.3) and the flange shear flow force resultant causes a twisting moment about the center of rotation. The shear flow force in the web goes through the center of rotation and hence causes no twisting moment. On the other hand, the center of rotation for C-purlins can be assumed as the junction of the tension flange and its stiffener. In this case, the shear

flow force in the web does not go through the center of rotation (Fig. 2.3). Thus the shear force in the web in addition to the shear force in the flange causes twisting moment about the center of rotation. The change in the shear force in the web per unit length is equal to the applied uniform vertical load.

The distributed lateral load on the beam column $w(x)$ results from the differences in the shear flow forces along the length of the member and can be expressed as

$$w(x) = \frac{\text{Flange Shear Force at } (x + dx) - \text{Flange Shear Force at } (x)}{dx} + \alpha q \quad (2.1-1)$$

$$= \frac{d\left(\frac{VQb}{2I}\right)}{dx} + \alpha q \quad (2.1-2)$$

$$= q\left(\frac{Qb}{2I} + \alpha\right) \quad (2.1-3)$$

where:

q = Distributed uplift load on the Z or C section

b = Flange width (see Fig. 4)

Q = Static moment of the flange and the stiffening lip around the centroidal axis of the purlin

I = Moment of inertia about the horizontal axis (normal to the undeflected web) of the section in the deflected configuration. Either the entire gross or the effective section is to be used as applicable. Different approaches for determining I will be discussed in Sections 2.2.1, 2.3, and 3.1.

V = Shear force

H = Height of the section

$\alpha = \frac{b}{H}$ for C purlins and 0 for Z purlins

flow force in the web does not go through the center of rotation (Fig. 2.3). Thus the shear force in the web in addition to the shear force in the flange causes twisting moment about the center of rotation. The change in the shear force in the web per unit length is equal to the applied uniform vertical load q .

The distributed lateral load on the beam column $w(x)$ results from the differences in the shear flow forces along the length of the member and can be expressed as

$$w(x) = \frac{\text{Flange Shear Force at } (x + dx) - \text{Flange Shear Force at } (x)}{dx} + \alpha q \quad (2.1-1)$$

$$= \frac{d\left(\frac{VQb}{2I}\right)}{dx} + \alpha q \quad (2.1-2)$$

$$= q\left(\frac{Qb}{2I} + \alpha\right) \quad (2.1-3)$$

where:

q = Distributed uplift load on the Z or C section

b = Flange width (see Fig. 4)

Q = Static moment of the flange and the stiffening lip around the centroidal axis of the purlin

I = Moment of inertia about the horizontal axis (normal to the undeflected web) of the section in the deflected configuration. Either the entire gross or the effective section is to be used as applicable. Different approaches for determining I will be discussed in Sections 2.2.1, 2.3, and 3.1.

V = Shear force

H = Height of the section

$\alpha = \frac{b}{H}$ for C purlins and 0 for Z purlins

The first term of the right hand side of Eq. 2.1-1 represents the lateral loading on the idealized beam-column due to the shear flow in the compression flange and is the same for both the C- and the Z-purlin. For the sake of simplicity, the flange is assumed to be a flat element of width b (see Fig. 2.4). This simplification is used only in determining $w(x)$ and $p(x)$ derived below. The second term of the same equation is to account for the twisting moment due to the shear force in the web. To facilitate the derivation below the loading in the web is converted to a load applied at the flange level and which results in the same twisting moment as the load in the web.

The distributed axial force $p(x)$ results from the variation of the compression stress along the length of the member. The beam-column section is assumed to be the flange and part of the flat width of the compression portion of the web $BB(\frac{H}{2} - R_1)$ as shown in Fig. 2.4. BB indicates the percentage of the flat width. The axial force can be expressed as follows:

$$p(x) = \frac{\text{Beam-Column Axial Force } (x + dx) - \text{Beam-Column Axial Force } (x)}{dx} \quad (2.1-4)$$

$$= \frac{d \left(\int_A \frac{My}{I} dA \right)}{dx} \quad (2.1-5)$$

$$= V \frac{1}{I} \int_A y dA \quad (2.1-6)$$

$$= V \cdot G \quad (2.1-7)$$

where

M = Bending moment at the section

G = Static moment of the beam-column area about the

centroidal axis of the purlin divided by the moment

$$\text{of inertia} = \left(\int_A y dA \right) / I \quad (2.1-8)$$

S = Section modulus of the total or the effective section--
depending on the approach. This will be discussed in
Section 2.3.

\bar{A} = Area of the beam-column

V = Shear force at any point in the span
(function of x) = dM/dx

b = Flange width (Fig. 2.4)

With the above idealizations the analysis of C- and Z-purlins for lateral deflections and twisting (torsion stage) is reduced to the analysis of the beam-column section shown in Fig. 2.4 with the loading shown in Fig. 2.2.b.

The idealized beam-column will be analyzed using the principle of stationary potential energy.

It can be shown that the potential energy (U) consists of two parts: the internal strain energy (V) and the work of the external loads (W). The strain energy itself consists of two parts: the flexural strain energy (V_f), and the elastic foundation strain energy (V_k). Their values are:

$$V_f = 2 \int_0^{\ell/2} \frac{EI_f}{2} \left(\frac{d^2 u}{dx^2} - \frac{d^2 u_0}{dx^2} \right)^2 dx \quad (2.1-9)$$

$$V_k = 2 \int_0^{\ell/2} \frac{K(u - u_0)^2}{2} dx \quad (2.1-10)$$

where

I_f = Moment of inertia of beam-column around its own centroidal
axis parallel to the web

ℓ = Span of the beam-column

K = Stiffness of the linear spring = F/H^2

u = Deflection of the beam-column (in the plane of the flange)

u_0 = Initial sweep of the beam-column (in the plane of the flange)

The work performed by the external loads also has two parts: the work of the lateral loads (W_w), and the work of the axial loads (W_p). Their values are:

$$W_w = -2 \int_0^{\ell/2} w(x) \cdot (u - u_0) dx \quad (2.1-11)$$

$$W_p = -2 \int_0^{\ell/2} \left\{ p(x) \cdot \frac{1}{2} \int_x^{\ell/2} \left[\left(\frac{du}{dx} \right)^2 - \left(\frac{du_0}{dx} \right)^2 \right] dx \right\} dx \quad (2.1-12)$$

Thus, the total potential energy U is:

$$U = V + W \quad (2.1-13)$$

$$= V_f + V_k + W_w + W_p \quad (2.1-14)$$

$$\begin{aligned} &= 2 \int_0^{\ell/2} \frac{EI_f}{2} \left(\frac{d^2u}{dx^2} - \frac{d^2u_0}{dx^2} \right)^2 dx + 2 \int_0^{\ell/2} \frac{K(u - u_0)^2}{2} dx \\ &- 2 \int_0^{\ell/2} w(x) \cdot (u - u_0) dx \\ &- 2 \int_0^{\ell/2} \left\{ p(x) \cdot \frac{1}{2} \int_x^{\ell/2} \left[\left(\frac{du}{dx} \right)^2 - \left(\frac{du_0}{dx} \right)^2 \right] dx \right\} dx \end{aligned} \quad (2.1-15)$$

2.2 The Solutions

In this section the total potential energy equations derived above will be used to obtain expressions for various bracing conditions. The general procedure involves the use of trigonometric functions satisfying the end conditions as well as the conditions at intermediate braces where applicable.

Frequently, one or more intermediate braces are used to facilitate the erection of the roof system and to reduce the lateral deflections. These

braces will be referred to as the intermediate braces and the application of the energy method will be demonstrated for certain cases.

2.2.1 Simply Supported Purlins Without Intermediate Braces

The following displacement functions satisfy the end conditions for the simply supported purlins:

$$u = \sum_{n=1,3,\dots} a_n \cdot \sin \frac{n\pi x}{l} \quad (2.2-1)$$

$$u_0 = \sum_{n=1,3,\dots} a_{no} \sin \frac{n\pi x}{l} \quad (2.2-2)$$

where a_n are the amplitude of deflections to be computed using the energy expressions and a_{no} are the amplitudes which can be obtained from the measured values of the sweep (in the plane of the flange). Since the lateral deflections are symmetric with respect to the midspan, only the odd values of n are used in the solution.

Substituting the above functions for u and u_0 in the total potential energy equation (Eq. 2.1-16), the following is obtained:

$$\begin{aligned}
 U = & \frac{EI_f \pi^4}{4l^3} \cdot \sum_{n=1,3,\dots} [n^4 (a_n - a_{no})^2] + \frac{Kl}{4} \sum_{n=1,3,\dots} (a_n - a_{no})^2 \\
 & - \left(\frac{2qQb}{I} + 2\alpha q \right) \cdot \frac{l}{\pi} \cdot \sum_{n=1,3,\dots} \frac{a_n - a_{no}}{n} \\
 & - Gql \cdot \sum_{n=1,3,\dots} [(a_n^2 - a_{no}^2) \cdot (.206n^2 - .063)] \quad (2.2-3)
 \end{aligned}$$

The amplitudes a_n can be determined by the Ritz procedure as follows:

$$\frac{\partial U}{\partial a_n} = 0$$

$$a_n = \frac{4q\ell^4 \left(\frac{Qb}{2I} + \alpha \right) + a_{no} (n^5 EI_f \pi^5 + nK\ell^4 \pi)}{EI_f \pi^5 n^5 + K\ell^4 n\pi - 4Gq\ell^4 n\pi (.206n^2 - .063)} \quad (2.2-4)$$

*Rev Ritz procedure
9/17/81*

The lateral deflection shape can now be obtained by substituting a_n from Eq. 2.2-4 into Eq. 2.2-1. The lateral deflection Δu in addition to the initial sweep can be determined by subtracting u_0 from u .

$$\Delta u = u - u_0 \quad (2.2-5)$$

$$= \sum_{n=1,3,\dots} q \frac{4\ell^4 \left(\frac{Qb}{2I} + \alpha \right) + 4a_{n0} G\ell^4 n\pi (.206n^2 - .063)}{EI_f \pi^5 n^5 + K\ell^4 n\pi - 4Gq\ell^4 n\pi (.206n^2 - .063)} \sin \frac{n\pi x}{\ell} \quad (2.2-6)$$

It should be noted that the lateral deflection, u , is the total lateral deflection of the compression flange. The deflections of the vertical bending stage does not have a component in the plane of the flange. In contrast with this, the lateral deflection, u , causes a deflection component in the vertical direction (in the plane of the web). The vertical deflection component is shown in Fig. 2.5. The main part of the vertical deflection, v , results from the vertical bending. The total vertical deflection, v , can be expressed as follows:

$$v = \frac{qx}{24EI} (\ell^3 - 2\ell x^2 + x^3) + \frac{\psi u^2}{2H} \quad (2.2-7)$$

where ψ is a correction factor which will be discussed in Section 3.1.2.

The last term in the right hand side of the above equation is the vertical component resulting from the torsion stage. The rest pertains to the vertical bending stage.

In the above equations the moment of inertia I is to be taken about the original axis perpendicular to the web before twisting or lateral deflection. Since significant deflections are possible, the section is to be taken in the deflected and rotated configuration. The determination of I is discussed further in Sections 2.3 and 3.1 below. Since the moment of inertia is

reduced as a result of the rotation (horizontal deflection) of the section and the horizontal deflection itself is a function of the reduced moment of inertia the following iterative procedure is needed:

- 1) Calculate u with the original dimensions.
- 2) Using the computed u get the value of I , and recompute u .
- 3) Repeat step 2, until the starting and the resulting values of u about equal. Then calculate the vertical deflection and the maximum stresses with the final u .

The total stresses in the purlin are obtained by superposing the stresses due to bending in the plane of the web (the vertical bending stage) on the stresses due to twisting and lateral deflection (torsion stage). Thus the total stress can be expressed as

$$\sigma = \frac{M}{S} + \frac{M_f}{S_f} \quad (2.2-8)$$

where

M = Moment resulting from the vertical bending stage
 $= q \times (\ell - x)/2$

S = Section modulus based on the moment of inertia I

S_f = Section modulus of the beam-column about its centroidal axis parallel to the web

M_f = Beam-column bending moment

The beam-column bending moment M_f can be determined as follows:

$$M_f = EI_f(u'' - u''_0) \quad (2.2-9)$$

$$= \frac{EI_f \pi^2}{\ell^2} \cdot \sum_{n=1,3,\dots} n^2 (a_n - a_{n0}) \sin \frac{n\pi x}{\ell} \quad (2.2-10)$$

where I_f is the moment of inertia of the beam-column about its axis parallel to the web.

The maximum compressive stress occurs at the junction of the compression flange with the web. Thus, S_f to be used in Eq. 2.2-8 should be the appropriate section modulus for that point.

2.2.2 Simply Supported Purlins With Midspan Bracing

The equations for the vertical deflections are the same as those for purlins without intermediate braces. The shape of the lateral deflection curve for the compression flange is changed because of the brace at midspan. The assumed deflection and initial sweep curves are illustrated in Fig. 2.6.a. The initial sweep is still taken as

$$u_0 = a_0 \sin \frac{\pi X}{\ell} \quad (2.2-11a)$$

However, the deflected shape is now taken as

$$u = (a + a_0) \sin \frac{\pi X}{\ell} + a \sin \frac{3\pi X}{\ell} \quad (2.2-11b)$$

It may be noted that the deflected shapes were taken as infinite series for the case without bracing. Here, only two or three terms are taken for the sake of simplicity.

Substituting the assumed deflection functions above into the total potential energy equation (Eq. 2.1-15), the following is obtained:

$$U = \frac{EI_f \pi^4}{4\ell^3} \left(82a^2 \right) + \frac{K\ell}{2} a^2 - \frac{2q\ell}{\pi I} \left(\frac{Qb}{2} + \alpha I \right) \cdot \frac{4a}{3} - Gq\ell(1.93a^2 + .29a_0 a) \quad (2.2-11c)$$

The amplitude a can be determined by the Ritz procedure as follows:

$$\frac{\partial U}{\partial a} = 0 \quad (2.2-12)$$

reduced as a result of the rotation (horizontal deflection) of the section and the horizontal deflection itself is a function of the reduced moment of inertia, the following iterative procedure is needed:

- 1) Calculate u with the original dimensions.
- 2) Using the computed u get the value of I , and recompute u .
- 3) Repeat step 2, until the starting and the resulting values of u about equal. Then calculate the vertical deflection and the maximum stresses with the final u .

The total stresses in the purlin are obtained by superposing the stresses due to bending in the plane of the web (the vertical bending stage) on the stresses due to twisting and lateral deflection (torsion stage). Thus the total stress can be expressed as

$$\sigma = \frac{M}{S} + \frac{M_f}{S_f} \quad (2.2-8)$$

where

M = Moment resulting from the vertical bending stage

$$= q \times (\ell - x)/2$$

S = Section modulus based on the moment of inertia I

S_f = Section modulus of the beam-column about its centroidal axis parallel to the web

M_f = Beam-column bending moment

The beam-column bending moment M_f can be determined as follows:

$$M_f = EI_f(u'' - u_0'') \quad (2.2-9)$$

$$= \frac{EI_f \pi^2}{\ell^2} \cdot \sum_{n=1,3,\dots} n^2 (a_n - a_{n0}) \sin \frac{n\pi x}{\ell} \quad (2.2-10)$$

where I_f is the moment of inertia of the beam-column about its axis parallel to the web.

The maximum compressive stress occurs at the junction of the compression flange with the web. Thus, S_f to be used in Eq. 2.2-8 should be the appropriate section modulus for that point.

2.2.2 Simply Supported Purlins With Midspan Bracing

The equations for the vertical deflections are the same as those for purlins without intermediate braces. The shape of the lateral deflection curve for the compression flange is changed because of the brace at midspan. The assumed deflection and initial sweep curves are illustrated in Fig. 2.6.a. The initial sweep is still taken as

$$u_0 = a_0 \sin \frac{\pi X}{\ell} \quad (2.2-11a)$$

However, the deflected shape is now taken as

$$u = (a + a_0) \sin \frac{\pi X}{\ell} + a \sin \frac{3\pi X}{\ell} \quad (2.2-11b)$$

It may be noted that the deflected shapes were taken as infinite series for the case without bracing. Here, only two or three terms are taken for the sake of simplicity.

Substituting the assumed deflection functions above into the total potential energy equation (Eq. 2.1-15), the following is obtained:

$$U = \frac{EI_f \pi^4}{4\ell^3} \left(82a^2 \right) + \frac{K\ell}{2} a^2 - \frac{2q\ell}{\pi I} \left(\frac{Qb}{2} + \alpha I \right) \cdot \frac{4a}{3} - Gq\ell(1.93a^2 + .29a_0 a) \quad (2.2-11c)$$

The amplitude a can be determined by the Ritz procedure as follows:

$$\frac{\partial U}{\partial a} = 0 \quad (2.2-12)$$

reduced as a result of the rotation (horizontal deflection) of the section and the horizontal deflection itself is a function of the reduced moment of inertia, the following iterative procedure is needed:

- 1) Calculate u with the original dimensions.
- 2) Using the computed u get the value of I , and recompute u .
- 3) Repeat step 2, until the starting and the resulting values of u about equal. Then calculate the vertical deflection and the maximum stresses with the final u .

The total stresses in the purlin are obtained by superposing the stresses due to bending in the plane of the web (the vertical bending stage) on the stresses due to twisting and lateral deflection (torsion stage). Thus the total stress can be expressed as

$$\sigma = \frac{M}{S} + \frac{M_f}{S_f} \quad (2.2-8)$$

where

M = Moment resulting from the vertical bending stage
 $= q \times (\ell - x)/2$

S = Section modulus based on the moment of inertia I

S_f = Section modulus of the beam-column about its centroidal axis parallel to the web

M_f = Beam-column bending moment

The beam-column bending moment M_f can be determined as follows:

$$M_f = EI_f(u'' - u_0'') \quad (2.2-9)$$

$$= \frac{EI_f \pi^2}{\ell^2} \cdot \sum_{n=1,3,\dots} n^2 (a_n - a_{n0}) \sin \frac{n\pi x}{\ell} \quad (2.2-10)$$

where I_f is the moment of inertia of the beam-column about its axis parallel to the web.

The maximum compressive stress occurs at the junction of the compression flange with the web. Thus, S_f to be used in Eq. 2.2-8 should be the appropriate section modulus for that point.

2.2.2 Simply Supported Purlins With Midspan Bracing

The equations for the vertical deflections are the same as those for purlins without intermediate braces. The shape of the lateral deflection curve for the compression flange is changed because of the brace at midspan. The assumed deflection and initial sweep curves are illustrated in Fig. 2.6.a. The initial sweep is still taken as

$$u_0 = a_0 \sin \frac{\pi X}{\ell} \quad (2.2-11a)$$

However, the deflected shape is now taken as

$$u = (a + a_0) \sin \frac{\pi X}{\ell} + a \sin \frac{3\pi X}{\ell} \quad (2.2-11b)$$

It may be noted that the deflected shapes were taken as infinite series for the case without bracing. Here, only two or three terms are taken for the sake of simplicity.

Substituting the assumed deflection functions above into the total potential energy equation (Eq. 2.1-15), the following is obtained:

$$U = \frac{EI_f \pi^4}{4\ell^3} \left(82a^2 \right) + \frac{K\ell}{2} a^2 - \frac{2q\ell}{\pi I} \left(\frac{Qb}{2} + \alpha I \right) \cdot \frac{4a}{3} - Gq\ell (1.93a^2 + .29a_0 a) \quad (2.2-11c)$$

The amplitude a can be determined by the Ritz procedure as follows:

$$\frac{\partial U}{\partial a} = 0 \quad (2.2-12)$$

*for Labouche
3/4/62*

$$a = \frac{8q\ell \left(\frac{Qb}{2} + \alpha I \right) + .29Gq\ell a_0}{\frac{4EI_f \pi^4}{\ell^3} + K\ell - 3.86Gq\ell} \quad (2.2-13)$$

Now, the deflection u can be determined by substituting a from Eq. 2.2-13 into Eq. 2.2-10. It may be noted that now the maximum u occurs at $x = .2\ell$ and is equal to $1.54a$.

Proceeding in the same manner as was done in Section 2.2.1, the following is obtained:

$$v = \frac{qx(\ell^3 - 2\ell x^2 + x^3)}{24EI} + \frac{\psi u^2}{2H} \quad (2.2-14)$$

and

$$\sigma = \frac{qx(\ell - x) \cdot H}{4I} + \frac{EI_f \pi^2}{\ell^2 S_f} \cdot u \cdot \left(\sin \frac{\pi x}{\ell} + 9 \sin \frac{3\pi x}{\ell} \right) \quad (2.2-15)$$

As in Section 2.2.1, an iterative approach may be used to determine the moment of inertia I .

2.2.3 Simply Supported Purlins With Third Point Bracing

As in Section 2.2.2, only the function used for lateral deflection is changed. The initial sweep is still taken as:

$$u_0 = a_0 \sin \frac{\pi x}{\ell} \quad (2.2-16)$$

The deflected shape is now taken as:

$$u = (a + a_0) \cdot \sin \frac{\pi x}{\ell} + .81a \sin \frac{5\pi x}{\ell} \quad (2.2-17)$$

This deflected shape satisfies lateral deflection conditions at the brace points and at the ends (see Fig. 2.6.b).

With the above displacement functions, the total potential energy equation (Eq. 2.1-15) gives:

$$U = \frac{EI_f \pi^4}{4\ell^3} (410a^2) + \frac{K\ell}{4} (1.65a^2) - 1.16 \frac{q\ell}{\pi I} (Qb + 2\alpha I) \cdot a - Gq\ell\pi^2 (.35a^2 + .03a_0 a) \quad (2.2-18)$$

Applying the Ritz procedure

$$\frac{\partial U}{\partial a} = 0 \quad (2.2-19)$$

The following is obtained

$$a = \frac{.37 \frac{q\ell}{I} (Qb + 2\alpha I) + .29Gq\ell a_0}{19971 \frac{EI_f}{\ell^3} - 6.93Gq\ell + .83K\ell} \quad (2.2-20)$$

The following expressions for v and σ are obtained using the procedure discussed in Section 2.2.1.

$$v = \frac{qx(\ell^3 - 2\ell x^2 + x^3)}{24EI} + \frac{\psi u^2}{2H} \quad (2.2-21)$$

$$\sigma = \frac{qx(\ell - x)H}{4I} + \frac{EI_f \pi^2}{\ell^2 S_f} u \left(\sin \frac{\pi x}{\ell} + 20.25 \sin \frac{5\pi x}{\ell} \right) \quad (2.2-22)$$

2.3 Failure Criteria

Under uplift loading simply supported purlins deflect as shown in Fig. 1.a. Thus, in general the maximum compressive stress occurs at the junction of the web to compression flange. With only a few exceptions, the dominant failure mechanism observed in the large scale tests was the formation of an inelastic local buckle at the web to compression flange junction. For this reason various procedures of predicting web failure were used to formulate a purlin failure criterion. The two procedures discussed below were developed by LaBoube and are given in Ref. 6.

2.3.1 Full Depth, Failure Stress Approach

In this approach that has been adopted in the 1980 AISI Specification (Ref. 8), a failure stress is defined. The web is taken as fully effective. In the application of this approach, the beam-column section was assumed to be the compression portion of the section with BB taken equal to zero.

If the compression flange is a stiffened plate element, the failure stress, F_{wu} , taken as

$$F_{wu} = [1.210 - .000337 \left(\frac{H}{t}\right) \cdot \sqrt{F_y}] \cdot F_y \leq F_y \quad (2.3-1)$$

where F_y is the yield stress of the material.

If the compression flange is an unstiffened plate element the F_{wu} becomes

$$F_{wu} = [1.259 - .000508 \left(\frac{H}{t}\right) \cdot \sqrt{F_y}] \cdot F_y \leq F_y \quad (2.3-2)$$

For the Z-purlins with inclined stiffeners, the web failure stress equation for unstiffened flanges was used in all cases.

For the C-purlins the decision whether the flange is stiffened or not was based on the procedure proposed by Desmond (Ref. 7) as follows:

$$\text{Define } R = \frac{w}{t}, R_\alpha = \frac{221}{\sqrt{F_y}}, R_\beta = \frac{77.23}{\sqrt{F_y}} \quad (2.3-3)$$

where

w = Flat width of flange

t = Thickness

$$\text{If } R \leq R_\beta \quad : \quad I_{s_{adeq.}} = 0 \quad (2.3-4)$$

$$\text{If } R_\beta \leq R \leq R_\alpha \quad : \quad I_{s_{adeq.}} = 389t^4 \left(\frac{R}{R_\alpha} - .324\right)^3 \quad (2.3-5)$$

$$\text{If } R \geq R_\alpha \quad : \quad I_{s_{adeq.}} = t^4 \left(\frac{115R}{R_\alpha} + 5\right) \quad (2.3-6)$$

If I_s is $< I_{s_{adeq}}$, assume the flange to be unstiffened.

If $I_s \geq I_{s_{adeq}}$, assume the flange to be stiffened.

2.3.2 Effective Depth Approach (Ref. 6)

This is an extension of the well known (Ref. 5) effective width concept. The post-buckling behavior is predicted through the use of the effective depth approach.

The following determination of effective depth is taken from Ref. 6.

$$h_e = 0.358t \sqrt{\frac{\kappa' E}{f_c}} \leq h \quad (2.3-7)$$

where

h_e = Effective depth of the compression portion of web

h = Total depth of the compression portion of web

f_c = Maximum compressive stress in the web

$$\kappa' = 4 + 2(1 + \beta)^3 + 2(1 + \beta), \quad \beta = |f_t/f_c| \quad (2.3-8)$$

f_t = Maximum tensile stress in web

Since h_e and f_c both depend on each other, the following iterative approach needs to be used:

- 1) Calculate stresses assuming the web to be fully effective.
- 2) Calculate the effective depth by Eq. 2.3-7.
- 3) Based on the effective area of the web, compute the neutral axis position, and calculate the new stresses for bending about the centroidal and parallel to flange.
- 4) Repeat (2), then (3), until h_e converges.
- 5) If this calculated h_e is less than the full compression depth, use $BB = 0.0$ instead of 0.33 for determining the beam-column section to be used

in computing the horizontal deflections and the stresses resulting from the horizontal deflection.

6) Calculate stresses and deflections with these values of h_e , BB, and compare the stress with the following ultimate stress used for this approach:

For stiffened compression flanges, the ultimate stress is:

$$F_{\max} = S'F_y \quad (2.3-9)$$

where

$$S' = \text{Stress reduction factor} = \gamma_1\gamma_2 \leq 1.0$$

$$\gamma_1 = 1.037 - .000125 \left(\frac{h}{t}\right) \cdot \sqrt{F_y} \quad (2.3-10)$$

$$\gamma_2 = 1.0735 - .0735 \left(\frac{w}{t}\right) / \left(\frac{w}{t}\right)_{\text{lim}}, \text{ when: } 1.0 < \left(\frac{w}{t}\right) / \left(\frac{w}{t}\right)_{\text{lim}} < 2.0 \quad (2.3-11)$$

$$\gamma_2 = 1.0, \text{ when } \left(\frac{w}{t}\right)_{\text{lim}} \leq 1.0 \quad (2.3-12)$$

$$\left(\frac{w}{t}\right)_{\text{lim}} = \frac{221}{\sqrt{F_y}}, \text{ w = flat width of the compression flange.}$$

For unstiffened compression flange, the above formulas become:

$$F_{\max} = S'F_y \quad (2.3-13)$$

$$S' = \text{Stress reduction factor} = \gamma_1\gamma_2 \leq 1.0 \quad (2.3-14)$$

$$\gamma_1 = 0.80$$

$$\gamma_2 = 1.024 - .024 \left(\frac{w}{t}\right) / \left(\frac{w}{t}\right)_{\text{lim}}, \text{ when } \left(\frac{w}{t}\right) / \left(\frac{w}{t}\right)_{\text{lim}} > 1.0 \quad (2.3-15)$$

$$\gamma_2 = 1.0, \text{ when } \left(\frac{w}{t}\right) / \left(\frac{w}{t}\right)_{\text{lim}} \leq 1.0 \quad (2.3-16)$$

$$\left(\frac{w}{t}\right)_{\text{lim}} = \frac{63.3}{\sqrt{F_y}} \quad (2.3-17)$$

CHAPTER 3

SIMPLIFICATIONS OF THE SOLUTIONS AND NUMERIC STUDIES

In this chapter numeric studies carried out to simplify the solutions of Chapter 2 will be discussed.

3.1 Simply Supported Purlins Without Intermediate Braces

3.1.1 Simplified Form of the Equations and the Moment of Inertia

Equation 2.2-4 can be written as

$$a_n = \frac{C_n \left(\frac{Qb}{2I} + \alpha \right) + a_{n0}}{1 - C_n G \pi n (.206n^2 - .063)} \quad (3.1-1)$$

where

$$C_n = \frac{\frac{4q\ell^4}{EI_f}}{n^5 \pi^5 + \frac{nKL^4 \pi}{EI_f}} \quad (3.1-2)$$

$$= \frac{4q}{\frac{n^5 \pi^5 EI_f}{\ell^4} + nK\pi} \quad (3.1-3)$$

The series

$$u = \sum_{n=1,3,\dots} a_n \sin \frac{n\pi x}{\ell} \quad (3.1-4)$$

converge rapidly. In numeric studies conducted with practical values of the parameters involved taking only one term led to errors less than 5% in u . For $n=1$, Eqs. 3.1-1 and -3 become

$$a_1 = \frac{C_1 \left(\frac{Qb}{2I} + \alpha \right) + a_{10}}{1 - .45C_1 G} \quad (3.1-5)$$

and

$$C_1 = \frac{1.27q}{\frac{94.41EI_f}{l^4} + K} \quad (3.1-6)$$

The flange bending moment can now be found using Eq. 2.2-10. Due to the term n^2 in the summation, taking only the term with $n=1$ leads to less accurate results. Namely, the convergence is less rapid for the flange bending moment than that for the lateral deflection. However, with proper simplifications, as will be described below, taking $n=1$ even for the flange bending moment gives excellent results.

Before further simplifications are introduced into the above equations, a brief discussion of the moment of inertia I is in order. Moment of inertia I was first defined in connection with Eq. 2.1-3 in Section 2.1 and used throughout the rest of the preceding chapter. As a result of lateral deflections and twist, the moment of inertia I with respect to the centroidal axis perpendicular to the original position of the web will be reduced. An approximate expression for the reduction can be obtained by assuming the Z- or C-section to be without lips (Fig. 3.2). The moment of inertia before twisting, I_0 , can be expressed as

$$I_0 = I_{web} + I_{flange} \quad (3.1-7)$$

$$\approx t \frac{H^3}{12} + 2(bt) \cdot \left(\frac{H}{2}\right)^2 \quad (3.1-8)$$

The moment of inertia after twisting may be approximated as

$$I = I_{web} + I_{flange} \quad (3.1-9)$$

$$= \frac{tH^3}{12} \cos^2 \theta + 2(bt) \cdot \left(\frac{H \cos \theta}{2}\right)^2 \quad (3.1-10)$$

$$= \left[\frac{tH^3}{12} + 2(bt) \cdot \left(\frac{H}{2}\right)^2 \right] \cdot \cos^2 \theta = I_0 \cos^2 \theta \quad (3.1-11)$$

where θ is the angle of twist as shown in Fig. 3.1.

Noting that

$$\sin \theta \approx \frac{u}{H} ; \cos^2 \theta = 1 - \sin^2 \theta = 1 - \left(\frac{u}{H}\right)^2 \quad (3.1-12)$$

the reduced moment of inertia I becomes

$$I = I_0 \left[1 - \left(\frac{u}{H}\right)^2 \right] \quad (3.1-13)$$

In the actual computations, I for the actual section with the stiffeners is used. However, the reduction factor used is the one derived above.

3.1.2 A Possible Design Approach

Parametric studies which will be discussed below and the evaluation of the test results discussed in Chapter 5 lead to the following simple approach. If the portion of the web contributing to I_f , Q , and G is ignored and the compression flange width is taken to be equal to b (shown in Fig. 23) then

$$I_f = tb^3/12 \quad (3.1-14)$$

$$G = btH/(2I_0) \quad (3.1-15)$$

and

$$Q = btH/2 \quad (3.1-16)$$

Substituting Eq. 3.1-14 through 3.1-16 into Eqns. 3.1-5 and 3.1-6, the following is obtained

$$a = \frac{C(Zb + \alpha) + a_0}{1 - .9ZC} \quad (3.1-17)$$

where

$$Z = \frac{tHb}{4I_0} \quad (3.1-18a)$$

$$C = \frac{1.27q}{\frac{7.87Etb^3}{l^4} + K} \quad (3.1-18b)$$

α was defined in connection with Eq. 2.1-3. All parameters should have consistent units.

In the above equations the notation has been simplified by expressing C_1 as C , a_1 as a , and a_0 as a_{10} . Furthermore, for simplicity, the reduction in the moment of inertia can be ignored. Therefore, depending on the approach taken, I_0 is the gross or effective moment of inertia of the undeformed purlin about the centroidal axis parallel to the flanges. Using Eqs. 2.2-10, and the simplifications discussed above, Eq. 2.2-8 for the maximum stress at the flange to web junction for Z-purlins and flange to stiffening lip junction of C-purlins becomes

$$\sigma = \frac{MH}{2I} + \frac{Eb\pi^2}{2l^2} (a - a_0) \quad (3.1-19)$$

M is defined in connection with Eq. 2.2-8, I is defined by Eq. 3.1-13 with $u = a$

The value of the restraint factor K is not a constant but varies with the amount of lateral deflection or lateral load q . The following procedure for determining the value of K in the above equations gave excellent results. The horizontal force, $w(x)$, at which the value of K is determined can be found by Eq. 2.1-3. With the simplifications above this equation becomes

$$w = q \left(\frac{b^2 tH}{4I_0} + \alpha \right) \quad (3.1-20)$$

Units of w are lbs/in.

The solution therefore involves a very rapidly converging iteration. The steps are as follows:

Step 1 — Assume a failure load q .

Step 2 — Using Eq. 3.1-20 find the value of w .

- Step 3 — From a plot of lateral load versus lateral displacement in an F test determine the value of K at a lateral load equal to w per unit length of the test specimen.
- Step 4 — Determine a by Eq. 3.1-17. This is the maximum lateral deflection.
- Step 5 — Determine σ by equation 3.1-19.
- Step 6 — Repeat steps 1 through 5 until σ obtained is equal to one of the failure stresses defined in Section 2.3.
- Step 7 — The design load is the failure load obtained above divided by an appropriate factor of safety.

The total maximum vertical deflection can be obtained from Eq. 2.2-7 by setting $x = \ell/2$

$$v_{\max} = \frac{5q\ell^3}{384EI} + \frac{\psi a^2}{2H} \quad (3.1-21)$$

The first term in the above equation is the component due to vertical bending. $a^2/(2H)$ in the second term is due to lateral bending as shown in Fig. 3.3. The factor ψ is to account for the cross-sectional distortion effects. It should depend on the cross-sectional dimensions. However, a regression analysis conducted on the test results indicated that taking a value of 3.4 for ψ leads to excellent agreement between the computed and observed results.

3.1.3 Parametric Studies

The convergence of the series solutions and the validity of the simplifications outlined in Section 3.1.2 were studied numerically. For this purpose, the simple computer programs given in this chapter in Tables 3.1 and 3.7 as well as the rather large computer program prepared to evaluate the test results were used. In this section the results of studies using

the programs given in this chapter will be discussed. The results of the larger program will be discussed in Chapter 5.

The programs given in this chapter take the section to have sharp corners and determines stresses and displacements. The idealized beam-column is assumed to include one sixth of the web depth for the unsimplified approach.

The results of analyses on 51 Z- and 68 C-purlin sections are given in this chapter. Many more sections were analyzed but the results given here are typical and were thought to be sufficient. The dimensions of 17 Z-purlins are given in Table 3.2. The results of the analyses for these sections are given in Table 3.3. In Tables 3.4 through 3.6 results are given for sections that have the same dimensions as those given in Table 3.2 except for the flange width W (see Fig. 3.1). In each of these tables a different flange width is assumed. C-purlins have basically the same dimensions as the Z-purlins except for the angle between the flange and the stiffening lip. This angle is taken as 90 degrees except for sections 8 and 17 where it was taken as 50 degrees. Tables 3.8 through 3.11 give the results for C-purlins listed in Table 3.2 except for W and the angle β_e . Each table is for a different W value. All the tables given in this chapter are for a span length of 20 ft and a uniform load of 144 lbs/ft.

The following notation is used in these tables.

- U7 maximum u determined by Eqs. 3.1-1 and 3.1-4 taking 7 terms (in.).
- U1 maximum u determined by Eqs. 3.1-5 and 3.1-4 taking 1 term (in.).
- US maximum u determined by simplified Eq. 3.1-17 (in.).
- S7 maximum stress in the flange due to lateral bending only, determined by Eq. 2.2-10 using 7 terms of the series (ksi).

- S1 same as S7 except only one term of the series is used (ksi).
 SS same as S7 except the lateral bending part (last term on the right hand side) of Eq. 3.1-19 is used (ksi).
 St7 S7 plus vertical bending stress (ksi).
 St1 S1 plus vertical bending stress (ksi).
 StS SS plus vertical bending stress (ksi).

The stresses St7, St1, and StS are the total stresses. A lower estimate will of course lead to a higher estimate of the ultimate load.

Since a very wide range of values of the geometric parameters were used, some of the sections may have rather nontypical dimensions. Sections having typical dimensions are listed in Table 4.1. These were the sections tested. Comparing the dimensions of Table 4.1 with those of this chapter, it is seen that Table 3.3 contains the results for typical Z-purlins and Tables 3.8 and 3.10 for typical C-purlins. The following general conclusions can be drawn from these tables.

There is no question that the agreement between U1, U7, and US is excellent for every one of the 119 sections tested numerically. The following table summarizes the correlation of stresses computed by different approaches.

		S1/S7	SS/S7	StS/St7
Z-purlins (Table 3.4)	Avg.	.82	1.10	1.03
	St. Dev.	.06	.11	.04
C-purlins (Tables 3.8 and 3.10)	Avg.	.68	.98	1.00
	St. Dev.	.11	.15	.08

The above values are given only to show the trends. It is seen that the simplified formulas compared with more complicated formulas estimate stresses excellently. It is also seen that in general the unconservatism

involved in taking one term of the series solution is compensated by the conservative simplifying assumptions made.

It is very important to note that for some value of q the denominator of Eq. 3.1-5 may be equal to zero which indicates a buckling condition. For values of q greater than that the equations are not valid. This situation, however, was not encountered in any of the cases studied.

3.2 Intermediate Braces

Though equations for the cases of intermediate braces were derived in Section 2.2.2 and 2.2.3, this subject was outside the scope of the research. Therefore no parametric or experimental studies were conducted. However it appears reasonable that the simplifications discussed in Section 3.1 would also be applicable to the equations of Sections 2.2.2 and 2.2.3. Further work on this subject appears desirable.

CHAPTER 4

EXPERIMENTAL INVESTIGATION

As discussed in the preceding chapters, the behavior of purlins is quite complex. A test program was carried out to check the theory and the simplifying assumptions made. Both C- and Z-purlins were used in the test program.

The types of tests conducted can be categorized into two groups: large scale assembly tests and component tests. Large scale assembly tests involved testing 20-foot spans of purlins under vacuum and point loadings. The purlins were tested simply supported and the span was chosen to represent the typical distance from the end support to the first inflection point in a continuous system with 25-foot spans.

Component tests included tests for rotational restraint, roof panel shear rigidity, and material properties.

The cross-sectional dimensions of all the tests evaluated in this report are listed in Table 4.1. The cross-sectional notation is illustrated in Fig. 2.4. Each section is referred to by its dimensions $H \times t \times a_0$. a_0 is the maximum sweep of the compression flange of the purlin that failed in the vacuum test.

4.1 Large Scale Tests

The results of the large scale tests are presented and evaluated in Chapter 5.

4.1.1 Z-Purlin Tests at Cornell University

The first major progress report (Ref. 1) describes the first phase of the experimental investigation in detail. The reader is referred to that report for a description of the test procedures, test specimens and results. Table 5.3 compares the specimen designations of Ref. 1 and the present report.

In the first phase only Z-purlin assemblies were tested under vacuum and point loadings. These tests will be referred to as the vacuum and beam tests, respectively. Six vacuum and seven beam tests were conducted in the first phase.

4.1.2 Z-Purlin Tests by a Metal Building Manufacturer

Since the first major progress report a total of nine vacuum tests were conducted by a metal building manufacturer and the results were made available to the researchers. Some of these tests were witnessed by T. Peköz. They were conducted competently and in accordance with the procedures used in the Cornell research.

The dimensions of the sections tested are listed in Table 4.1. The results are plotted in Chapter 5 along with the calculated values. In these tests only displacements were measured.

4.1.3 C-Purlin Tests at Cornell University

Since the first major progress report (Ref. 1), three vacuum tests were conducted using C-purlins. The test procedures and the overall test assembly dimensions were exactly the same as those described in detail in Ref. 1.

4.1.1 Z-Purlin Tests at Cornell University

The first major progress report (Ref. 1) describes the first phase of the experimental investigation in detail. The reader is referred to that report for a description of the test procedures, test specimens and results. Table 5.3 compares the specimen designations of Ref. 1 and the present report.

In the first phase only Z-purlin assemblies were tested under vacuum and point loadings. These tests will be referred to as the vacuum and beam tests, respectively. Six vacuum and seven beam tests were conducted in the first phase.

4.1.2 Z-Purlin Tests by a Metal Building Manufacturer

Since the first major progress report a total of nine vacuum tests were conducted by a metal building manufacturer and the results were made available to the researchers. Some of these tests were witnessed by T. Peköz. They were conducted competently and in accordance with the procedures used in the Cornell research.

The dimensions of the sections tested are listed in Table 4.1. The results are plotted in Chapter 5 along with the calculated values. In these tests only displacements were measured.

4.1.3 C-Purlin Tests at Cornell University

Since the first major progress report (Ref. 1), three vacuum tests were conducted using C-purlins. The test procedures and the overall test assembly dimensions were exactly the same as those described in detail in Ref. 1.

The results of the C-purlin tests are plotted in Figs. 4.1 through 4.7. Stresses and deflections were measured in the tests on C 7 x .075 and 9 x .075. Only deflections were measured in the test on C 9 x .077.. The initial sweeps are shown in Fig. 4.8.

All the test results were corrected to account for the dead load of the roof system. The dead load was taken as 7.5 lb/ft. The initial strain and dial gage readings were taken at this load. Thus the initial readings were corrected by estimating the reading at dead load and plotting it as the initial reading.

All failures took place within 6 in. of the midspan and with an apparent local buckle at the web to flange junction.

4.2 Component Tests

4.2.1 Rotational Restraint Tests

The objective of these tests was to determine the spring constant K used in the beam-column idealization. These tests are also referred to as F-tests. Some tests were conducted in the first phase of the research and the results were reported in Ref. 1. These test results were reported in terms of the section rotation versus twisting moment. The approach taken in the final phase of the research necessitated the determination of the relationship between the lateral force applied to the tension flange and the lateral displacement of the tension flange. The schematic for the type of test conducted is shown in Fig. 4.9 taken from Ref. 1. Further discussion of the test procedure can be found in Ref. 1. Several tests were conducted on Z- and C-purlins. The results are plotted in Figs. 4.10 through 4.14 for Z-purlins and Figs. 4.15 through 4.17 for C-purlins.

For the sections tested the following expressions gave surprisingly good estimates of the value of K at loads corresponding to the shear flow loads at failure. (The shear flow forces are discussed in Chapters 2 and 3.) These expressions are

$$K = \frac{1}{42H + \frac{4H^3}{Et^3}} \quad (4.2-1)$$

for C-purlins and

$$K = \frac{1}{58H + \frac{4H^3}{Et^3}} \quad (4.2-2)$$

for Z-purlins. The second term in the denominators of these expressions was derived taking the web of the purlin as a cantilever. The calculated results are plotted along with the observed results in the figures. Further work using different types of panels seem necessary before a general expression is recommended.

The rotational restraint tests for C-purlins were carried out using two different approaches. One was the same as the procedure and set-up used for the Z-purlins. The other was by changing the set-up shown in Fig. 4.9 as follows: the 18 in. distance shown in the figure was increased to one half the purlin spacing and the dial gage was mounted to a stand that was not on the panel. This arrangement was thought to represent the behavior of the C-purlins assembled in an alternating fashion. The first set-up is referred to in the plots as "gage on panel" and the latter as "gage outside panel." However, the two different procedures did not show any significant difference. Therefore, the procedure using gages "outside panel" seem unnecessary.

For the sections tested the following expressions gave surprisingly good estimates of the value of K at loads corresponding to the shear flow loads at failure. (The shear flow forces are discussed in Chapters 2 and 3.) These expressions are

$$K = \frac{1}{42H + \frac{4H^3}{Et^3}} \quad (4.2-1)$$

for C-purlins and

$$K = \frac{1}{58H + \frac{4H^3}{Et^3}} \quad (4.2-2)$$

for Z-purlins. The second term in the denominators of these expressions was derived taking the web of the purlin as a cantilever. The calculated results are plotted along with the observed results in the figures. Further work using different types of panels seem necessary before a general expression is recommended.

The rotational restraint tests for C-purlins were carried out using two different approaches. One was the same as the procedure and set-up used for the Z-purlins. The other was by changing the set-up shown in Fig. 4.9 as follows: the 18 in. distance shown in the figure was increased to one half the purlin spacing and the dial gage was mounted to a stand that was not on the panel. This arrangement was thought to represent the behavior of the C-purlins assembled in an alternating fashion. The first set-up is referred to in the plots as "gage on panel" and the latter as "gage outside panel." However, the two different procedures did not show any significant difference. Therefore, the procedure using gages "outside panel" seem unnecessary.

Figure 4.17 shows the importance of the location of the screw (or bolt) on the value of K obtained. In all the tests the screws were placed within about 1/4" of the flange centerline

4.2.2 Roof Panel Shear Rigidity (Cantilever Tests)

The tests conducted and their results are described in detail in Ref. 1.

CHAPTER 5

COMPARISON OF CALCULATED AND EXPERIMENTALLY OBSERVED RESULTS

The ultimate loads observed in thirteen Z-purlin and three C-purlin vacuum tests are compared with calculated ultimate loads in Tables 5.1 and 5.2. The sections used were those of Ref. 1 as well as those tested by a metal building manufacturer and the C-purlins tested since Ref. 1. The test section designations used in Ref. 1 and the present report are compared in Table 5.3. Observed and calculated stresses and deflections are compared graphically in the figures of this chapter.

The beam tests (see Chapter 4) were shown in Ref. 1 to be in good agreement with the vacuum tests. Thus only the vacuum tests are considered in this chapter. Purlin Type E (Test V6) of Ref. 1 was excluded from consideration. This type of purlin had an unusual sweep. It was both quite large (.91 in) and in the direction from the lip to the web. The local buckle occurred at the stiffening lip of this specimen whereas in all the other specimens the local buckle occurred at the flange to web junction. This case needs further study.

As described in Chapter 4, all the test results including those by a metal building manufacturer were corrected to account for the dead load of the roof system. The dead load was taken to be 7.5 lb/ft. The initial strain and dial gage readings were taken at this load. Therefore the initial readings were corrected by estimating the deflection or the strain at dead load and taking this as the initial reading.

The types of comparison calculations used in this chapter are designated as follows:

CHAPTER 5

COMPARISON OF CALCULATED AND EXPERIMENTALLY OBSERVED RESULTS

The ultimate loads observed in thirteen Z-purlin and three C-purlin vacuum tests are compared with calculated ultimate loads in Tables 5.1 and 5.2. The sections used were those of Ref. 1 as well as those tested by a metal building manufacturer and the C-purlins tested since Ref. 1. The test section designations used in Ref. 1 and the present report are compared in Table 5.3. Observed and calculated stresses and deflections are compared graphically in the figures of this chapter.

The beam tests (see Chapter 4) were shown in Ref. 1 to be in good agreement with the vacuum tests. Thus only the vacuum tests are considered in this chapter. Purlin Type E (Test V6) of Ref. 1 was excluded from consideration. This type of purlin had an unusual sweep. It was both quite large (.91 in) and in the direction from the lip to the web. The local buckle occurred at the stiffening lip of this specimen whereas in all the other specimens the local buckle occurred at the flange to web junction. This case needs further study.

As described in Chapter 4, all the test results including those by a metal building manufacturer were corrected to account for the dead load of the roof system. The dead load was taken to be 7.5 lb/ft. The initial strain and dial gage readings were taken at this load. Therefore the initial readings were corrected by estimating the deflection or the strain at dead load and taking this as the initial reading.

The types of comparison calculations used in this chapter are designated as follows:

"Simple" or "Simplified":

Equations of Section 3.1.2 and the failure criteria of Section 2.3.1 were used.

"Full Depth" or "Full":

Equations of Section 3.1.1 and the failure criteria of Section 2.3.1 were used. In all cases only one term of the series solutions ($n=1$) and $BB=0$ (see Fig. 2.4) was taken.

"Eff. Depth" or "Eff.":

Equations of Section 3.1.1 and the failure criteria of Section 2.3.2 were used. The number of series terms is indicated in each case.

5.1 Comparison of Ultimate Loads

The observed ultimate loads are compared with ultimate loads calculated with three different approaches in Table 5.1. The simple approach is seen to be just as accurate as the other two approaches. The mean of the ratio of the ultimate load calculated with the simple approach to that observed is 1.02 for Z-purlins and .89 for C-purlins. The standard deviations for these are .12 and .06, respectively. The mean and standard deviation for all specimens are .99 and .13, respectively. The results for C-purlins are seen to be less conservative and in excellent agreement with the full depth approach. This is certainly a point to consider. However, in view of the fact that there relatively fewer number of tests on C-purlins, it may be desirable to use the simple approach which is a bit more conservative.

The most unconservative results (by 19%) for the simplified approach were observed for Sections Z 8.053 x .063 x .25 and Z 7.93 x .115 x .25. The discrepancy for the first section can be attributed in part to the fact

that a premature failure might have been caused by the local buckling at a sag rod perforation.

The convergence of solutions is studied in Table 5.2 for the effective depth approach. It is seen that the most significant change in the solution takes place between $n=1$ and $n=2$. However, on the basis of Table 5.1, it can be concluded that the simplified approach is just as accurate as the more detailed calculations.

5.2 Comparison of Deflections and Stresses at Midspan

The observed horizontal and vertical deflections of the web to compression flange junction are compared with those calculated in Figs. 5.1 through 5.24. The calculated and observed ultimate loads are marked by horizontal lines on the load axis of each figure. The correlation is seen to be satisfactory. There is a relatively larger discrepancy between the calculated and observed deflections at lower loads. This can be attributed to the fact that the value of K was chosen for the ultimate load condition as explained in Section 3.1.2.

The observed and calculated values of the maximum stress which occurs at the web to flange junction are plotted in Figs. 5.25 through 5.30. These ultimate loads are marked also on these figures. Again the correlation is seen to be satisfactory.

It should be noted the graphs of this chapter were plotted using a minicomputer. The observed and calculated results were specified at discrete points. Straight lines were drawn between these points. For this reason the curves have discontinuities which actually do not exist.

that a premature failure might have been caused by the local buckling at a sag rod perforation.

The convergence of solutions is studied in Table 5.2 for the effective depth approach. It is seen that the most significant change in the solution takes place between $n=1$ and $n=2$. However, on the basis of Table 5.1, it can be concluded that the simplified approach is just as accurate as the more detailed calculations.

5.2 Comparison of Deflections and Stresses at Midspan

The observed horizontal and vertical deflections of the web to compression flange junction are compared with those calculated in Figs. 5.1 through 5.24. The calculated and observed ultimate loads are marked by horizontal lines on the load axis of each figure. The correlation is seen to be satisfactory. There is a relatively larger discrepancy between the calculated and observed deflections at lower loads. This can be attributed to the fact that the value of K was chosen for the ultimate load condition as explained in Section 3.1.2.

The observed and calculated values of the maximum stress which occurs at the web to flange junction are plotted in Figs. 5.25 through 5.30. These ultimate loads are marked also on these figures. Again the correlation is seen to be satisfactory.

It should be noted the graphs of this chapter were plotted using a minicomputer. The observed and calculated results were specified at discrete points. Straight lines were drawn between these points. For this reason the curves have discontinuities which actually do not exist.

5.3 Summary and Conclusions

It is seen in this chapter that the correlation between the computed and the observed ultimate loads is excellent. The correlation between the calculated and observed deflections is satisfactory for design purposes. The iteration caused by the determination of the spring constant K is a rapidly converging one. This rapid convergence can also be predicted from Table 4.2 where it is shown that K is not too sensitive to the value of the flange shear flow force assumed.

CHAPTER 6

SUMMARY AND CONCLUSIONS

The behavior of C- and Z-purlins braced by roof panels was studied for wind uplift loading. The analytical formulation of the behavior included several important parameters that have not been considered previously. A brief discussion of these parameters was given in Chapter 1.

A very simple approach was developed to predict behavior. This approach correlated very well with the results of a rather extensive experimental program.

The research dealt primarily with simply supported purlins. However, the results can readily be extended to multiple span continuous purlins by considering the portions between the inflection points as simply supported.

Though it was not in the original scope of the investigation, some solutions for the intermediately braced purlins were developed.

It appears very feasible and desirable to extend the ideas developed and used in this research to the case of gravity loading. However, in the case of gravity loading taking proper account of the roof shear rigidity and the behavior of stiffening lips is essential. The latter point is due to the fact that under gravity loading the lateral bending stress adds to the vertical bending stress at the stiffening lip. In the case of uplift loading, the lateral bending stress reduces the total stress at the stiffening lip. Significant amount of unsponsored research has recently been concluded at Cornell University on this subject. The results will be available shortly.

Finally, the best test of the analytical approach will be by observing the behavior of a full scale building. Only in this manner, the effect of the interaction of many complex elements of a roof system can be evaluated.

REFERENCES

1. Razak, M.A.A. and Peköz, T., "Progress Report - Ultimate Strength of Cold-Formed Steel Z-Purlins," Dept. of Structural Engineering Report No. 80-3, Cornell University, February 1980.
2. Celebi, N., Peköz, T. and Winter, G., "Behavior of Channel and Z-Section Beams Braced by Diaphragms," Proc. of First Specialty Conference on Cold-Formed Steel Structures, University of Missouri, Rolla, 1971.
3. Peköz, T., "Diaphragm Braced Channel and Z-Section Purlins," Report and Computer Program prepared for MBMA and AISI, 1973.
4. Peköz, T., "Progress Report on Cold-Formed Steel Purlin Design," Proceedings of the Third International Conference on Cold-Formed Steel Structures, Dept. of Civil Engineering, University of Missouri-Rolla, November 1975.
5. "Cold-Formed Steel Design Manual," American Iron and Steel Institute, Washington, D.C., 1977 edition.
6. LaBoube, R.A. and Yu, W-W., "Webs for Cold Formed Steel Flexural Members," Civil Engineering Study 78-1, Structural Series, University of Missouri-Rolla, Final Report June 1978.
7. Desmond, T.P., "The Behavior and Strength of Thin-Walled Compression Elements with Longitudinal Stiffeners," Report No. 369, Dept. of Structural Engineering, Cornell University, February 1978.
8. "Specification for the Design of Cold-Formed Steel Structural Members," American Iron and Steel Institute, Washington, D.C., September 3, 1980 Edition.
9. Ellifritt, D.S., "A Computer Study of Purlin Stresses," MBMA, 1978.

Table 3.1

Z-PURLIN PARAMETRIC STUDY PROGRAM

```

5 PRINT "SECTION      U7      U1 U7      U6 U7      S1      S1 S4      S4 S7      St7 St1 St7 St8 St
7"
6 PRINT " "
10 DIM B(2), Uo(2), U(2), So(2), S(2), S1(2), St(2)
20 DEG
30 A1=0
40 L=210
50 E=500000
60 FOR Jj=1 TO 17
70 READ H,W,Cc,Be,T,Ro,K,F
71   Ch=Cc*COS(Be)
72   Cv=Cc*SIN(Be)
73   B=W+Ch
74   I=H^3/12+2*(W*(H/2)^2+Cc*Cv^2/12+Cc*(H/2-Cv/2)^2)
75   I=I*T
80 IF Jj=2 THEN H=7
90 IF Jj=3 THEN T=.06
100 IF Jj=3 THEN Ro=1
110 IF Jj=4 THEN K=3
120 IF Jj=5 THEN K=1
130 IF Jj=6 THEN K=3
140 IF Jj=6 THEN T=.07
150 IF Jj=7 THEN Ro=0
160 IF Jj=8 THEN Be=50
170 IF Jj=9 THEN Cc=1
171 IF Jj>9 THEN H=7
172 IF Jj=10 THEN T=.06
173 IF Jj=11 THEN Ro=1
174 IF Jj=12 THEN K=3
175 IF Jj=13 THEN K=1
176 IF Jj=14 THEN K=3
177 IF Jj=15 THEN T=.07
178 IF Jj=17 THEN Be=50
180 RESTORE 740
190 FOR J=1 TO 2
200 IF J=2 THEN Cc=0
210 IF J=2 THEN F=0
215 IF J=2 THEN W=B
220 GOTO 250
230 IMAGE XXXXX,DD,XXX,D.DD,XXX,DD.DD,XXX,DD.DD,XXX,DD,XXX,.DDD,XXX.DD.DDD,XXX,
   DDD.DD,XXX,DD.DDD
240 PRINT USING 230;Jj,H,W,Cc,Be,T,Ro,K,F
250 REM GOTO 720
260 Ch=Cc*COS(Be)
270 Cv=Cc*SIN(Be)
280   B=W+Ch

```

REFERENCES

1. Razak, M.A.A. and Peköz, T., "Progress Report - Ultimate Strength of Cold-Formed Steel Z-Purlins," Dept. of Structural Engineering Report No. 80-3, Cornell University, February 1980.
2. Celebi, N., Peköz, T. and Winter, G., "Behavior of Channel and Z-Section Beams Braced by Diaphragms," Proc. of First Specialty Conference on Cold-Formed Steel Structures, University of Missouri, Rolla, 1971.
3. Peköz, T., "Diaphragm Braced Channel and Z-Section Purlins," Report and Computer Program prepared for MBMA and AISI, 1973.
4. Peköz, T., "Progress Report on Cold-Formed Steel Purlin Design," Proceedings of the Third International Conference on Cold-Formed Steel Structures, Dept. of Civil Engineering, University of Missouri-Rolla, November 1975.
5. "Cold-Formed Steel Design Manual," American Iron and Steel Institute, Washington, D.C., 1977 edition.
6. LaBoube, R.A. and Yu, W-W., "Webs for Cold Formed Steel Flexural Members," Civil Engineering Study 78-1, Structural Series, University of Missouri-Rolla, Final Report June 1978.
7. Desmond, T.P., "The Behavior and Strength of Thin-Walled Compression Elements with Longitudinal Stiffeners," Report No. 369, Dept. of Structural Engineering, Cornell University, February 1978.
8. "Specification for the Design of Cold-Formed Steel Structural Members," American Iron and Steel Institute, Washington, D.C., September 3, 1980 Edition.
9. Ellifritt, D.S., "A Computer Study of Purlin Stresses," MBMA, 1978.

Table 3.1

Z-PURLIN PARAMETRIC STUDY PROGRAM

```

5 PRINT "SECTION      U7      U1 U7      U6 U7      S1      S1-S2      S2-S3      S3-S4      S4-S5      S5-S6      S6-S7      S7-S8      S8-S9
7"
6 PRINT " "
10 DIM B(20),Uo(20),U(20),So(20),S(20),S1(20),S2(20)
20 DEG
30 A1=0
40 L=210
50 E=2000000
60 FOR Jj=1 TO 17
70 READ H,W,Cc,Be,T,Ro,K,F
71   Ch=Cc+COS(Be)
72   Cv=Cc+SIN(Be)
73   B=W+Ch
74   I=H^3/12+2*(W*(H/2)^2+Cc*Cv^2/12+Cc*(H/2-Cv/2)^2)
75   I=I*T
80 IF Jj=2 THEN H=7
90 IF Jj=3 THEN T=.06
100 IF Jj=3 THEN Ro=1
110 IF Jj=4 THEN K=3
120 IF Jj=5 THEN K=1
130 IF Jj=6 THEN K=3
140 IF Jj=6 THEN T=.07
150 IF Jj=7 THEN Ro=0
160 IF Jj=8 THEN Be=50
170 IF Jj=9 THEN Cc=1
171 IF Jj>9 THEN H=7
172 IF Jj=10 THEN T=.06
173 IF Jj=11 THEN Ro=1
174 IF Jj=12 THEN K=3
175 IF Jj=13 THEN K=1
176 IF Jj=14 THEN K=3
177 IF Jj=15 THEN T=.07
178 IF Jj=17 THEN Be=50
180 RESTORE 740
190 FOR J=1 TO 2
200 IF J=2 THEN Cc=0
210 IF J=2 THEN F=0
215 IF J=2 THEN W=B
220 GOTO 250
230 IMAGE XXXXX,DD,XXX,B.DD,XXX,DD.DD,XXX,DD.DD,XXX,DD,XXX,.DDD,XXX.DD.DDD,XXX,
DDD.DD,XXX,DD.DDD
240 PRINT USING 230;Jj,H,W,Cc,Be,T,Ro,K,F
250 REM GOTO 720
260 Ch=Cc+COS(Be)
270 Cv=Cc+SIN(Be)
280   B=W+Ch

```

Table 3.1

Z-PURLIN PARAMETRIC STUDY PROGRAM (CONTINUING)

```

      Fi:
      Fi:
360  Qb=Hf*(H/2-Hf/2)+W*H/2+Cc*(H/2-Cc/2)
370  Qb=Qb*T
380  G=Qb/I
390  Qf=T*B*H/2
400  Q=12
410  U=0
420  S=0
430  FOR N=1 TO 7 STEP 2
440  An=0
450  IF N=1 THEN An=Ao
460  Ln=(N*PI)^5+N*K*L^4*PI/(E*Fi)
470  Gn=4*Q*L^4/(E*Fi)
480  C=Gn/Ln
490  U1=C*(Qf*B/(2*I)+A1)+An
500  U2=1-C*G*PI*N*(.206*N^2-.063)
510  U=U+U1/U2
520  S=N^2*(U1/U2-An)+S
530  IF U2<0 THEN PRINT "BUCKLING*****"
540  IF N=1 THEN Uo=U
550  IF N=1 THEN So=S
560  NEXT N
570  Sa=E*Fi*PI^2/L^2*Xb/Fi
580  So=So+Sa
590  S=S+Sa
600  Sf=Q*L^2/8*(H/2)/I
610  St=S+Sf
620  S1=So+Sf
630  Uo(J)=Uo
640  U(J)=U
650  So(J)=So/1000
660  S(J)=S/1000
670  S1(J)=S1/1000
680  St(J)=St/1000
690  NEXT J
700  IMAGE  XXXXX, DD, XX, D. DD, XXX, D. DD, XXXX, D. DD, XXX, DD. D, XXX, D. DD, XXX, D. DD, XXX
D, XXXX, D. DD, XXXX, D. DD
710  PRINT USING 700; Jj, U(J), Uo(J)/U(J), Uo(2)/U(J), S(J), So(J)/S(J), So(2)/S(J)
1), S1(J)/St(J), S1(2)/St(J)
720  NEXT Jj
730  END

```

Table 3.2

Z-PURLIN PARAMETERS

Section	H (in)	W (in)	Cc (in)	Be (deg)	T (in)	Ao (in)	K (lb-in/in)	F *
3	9.49	2.00	.80	45	.060	1.000	1.91	.167
4	9.49	2.00	.80	45	.100	.250	3.00	.167
5	9.49	2.00	.80	45	.100	.250	1.00	.167
6	9.49	2.00	.80	45	.070	.250	3.00	.167
7	9.49	2.00	.80	45	.100	0.000	1.91	.167
8	9.49	2.00	.80	50	.100	.250	1.91	.167
9	9.49	2.00	1.00	45	.100	.250	1.91	.167
10	7.00	2.00	.80	45	.060	.250	1.91	.167
11	7.00	2.00	.80	45	.100	1.000	1.91	.167
12	7.00	2.00	.80	45	.100	.250	3.00	.167
13	7.00	2.00	.80	45	.100	.250	1.00	.167
14	7.00	2.00	.80	45	.100	.250	3.00	.167
15	7.00	2.00	.80	45	.070	.250	1.91	.167
16	7.00	2.00	.80	45	.100	.250	1.91	.167
17	7.00	2.00	.80	50	.100	.250	1.91	.167

* Portion of web height used in the beam-column (F x H)

Table 3.3

Z-PURLIN ANALYSIS
(W = 2.0 in)

SECTION	U7	U1/U7	U5/U7	S7	S1/S7	S5/S7	St7	St1/St7	St5/St7
1	1.20	.98	.91	5.2	.78	1.05	26.4	.96	1.01
2	.87	.98	.96	3.8	.76	.98	19.5	.95	1.00
3	1.71	.99	.92	4.1	.74	.92	25.3	.96	.99
4	.81	.97	.92	3.4	.69	.94	24.7	.96	.99
5	2.55	.99	.86	11.2	.90	1.13	32.4	.96	1.04
6	.63	.97	.93	2.6	.61	.84	23.8	.96	.98
7	.84	.97	.93	4.7	.76	1.07	25.9	.96	1.01
8	1.17	.99	.91	5.0	.78	1.02	26.2	.96	1.00
9	1.28	.99	.93	6.0	.81	1.07	27.2	.96	1.02
10	.61	.97	.95	2.5	.66	.85	18.2	.95	.98
11	1.82	.99	.95	4.8	.81	.97	20.5	.96	.99
12	.63	.97	.96	2.7	.67	.86	18.3	.95	.98
13	1.53	.99	.92	7.1	.87	1.13	22.8	.96	1.04
14	.63	.97	.96	2.7	.67	.86	18.3	.95	.98
15	.67	.97	.96	2.7	.67	.86	18.3	.95	.98

Table 3.4
Z-PURLIN ANALYSIS
(W = 2.5 in)

SECTION	U7	U1/U7	US/U7	S7	S1/S7	S8/S7	St7	St1	St7	St8	S17
1	1.38	.99	.98	6.7	.85	1.18	25.8		.96		1.05
2	.95	.99	1.01	5.0	.83	1.09	19.0		.95		1.02
3	1.78	.99	.95	5.2	.81	1.04	24.2		.96		1.01
4	.89	.98	.97	4.5	.78	1.07	23.5		.96		1.01
5	2.48	.99	1.02	13.3	.92	1.32	32.3		.97		1.13
6	.70	.98	.96	3.3	.71	.97	22.4		.96		1.00
7	.95	.98	1.01	6.2	.83	1.20	25.2		.96		1.05
8	1.27	.99	.98	6.6	.85	1.16	25.6		.96		1.04
9	1.36	.99	1.00	7.6	.86	1.20	26.6		.96		1.06
10	.67	.98	.98	3.3	.75	.96	17.3		.95		.99
11	1.89	.99	.98	6.2	.86	1.07	20.2		.96		1.02
12	.70	.98	.99	3.5	.76	.98	17.5		.95		1.00
13	1.59	.99	1.06	8.9	.90	1.25	22.9		.96		1.10
14	.70	.98	.99	3.5	.76	.98	17.5		.95		.99

Table 3.5
Z-PURLIN ANALYSIS
(W = 1.75 in)

SECTION	U7	U1/U7	US/U7	S7	S1/S7	S8/S7	St7	St1	St7	St8	S17
1	1.13	.97	.88	4.5	.73	.96	27.1		.95		.99
2	.82	.97	.93	3.3	.71	.91	19.9		.95		.98
3	1.67	.98	.91	3.6	.69	.84	26.2		.96		.98
4	.76	.96	.90	3.0	.62	.85	25.6		.96		.98
5	2.54	.99	.78	10.0	.87	1.01	32.6		.96		1.00
6	.60	.96	.91	2.3	.54	.75	24.8		.96		.99
7	.77	.96	.88	4.1	.70	.97	26.6		.95		1.06
8	1.10	.97	.87	4.4	.72	.93	26.9		.96		.99
9	1.22	.98	.89	5.2	.77	.99	27.7		.96		1.00
10	.58	.97	.94	2.2	.60	.77	18.8		.95		.97
11	1.77	.99	.93	4.2	.77	.91	20.8		.95		.98
12	.60	.97	.94	2.3	.61	.79	18.9		.95		.97
13	1.47	.98	.92	6.2	.83	1.05	22.8		.96		1.01
14	.60	.97	.94	2.3	.61	.79	18.9		.95		.97
15	.63	.97	.94	2.5	.63	.81	19.1		.95		.98
16	.82	.97	.93	3.3	.71	.91	19.9		.95		.98
17	.66	.97	.93	3.2	.70	.88	19.8		.95		.98

Table 3.4
Z-PURLIN ANALYSIS
(w = 2.5 in)

SECTION	U7	U1/U7	U3/U7	S7	S1/S7	S3/S7	St7	St1/St7	St3/St7
1	1.38	.99	.98	6.7	.85	1.18	25.8	.96	1.05
2	.95	.99	1.01	5.0	.83	1.09	19.0	.95	1.02
3	1.78	.99	.95	5.2	.81	1.04	24.2	.96	1.01
4	.89	.98	.97	4.5	.78	1.07	23.5	.96	1.01
5	2.48	.99	1.02	13.3	.92	1.32	32.3	.97	1.13
6	.70	.98	.96	3.3	.71	.97	22.4	.96	1.00
7	.95	.98	1.01	6.2	.83	1.20	25.2	.96	1.05
8	1.27	.99	.98	6.6	.85	1.16	25.6	.96	1.04
9	1.36	.99	1.00	7.6	.86	1.20	26.6	.96	1.06
10	.67	.98	.98	3.3	.75	.96	17.3	.95	.99
11	1.89	.99	.98	6.2	.86	1.07	20.2	.96	1.02
12	.70	.98	.99	3.5	.76	.98	17.5	.95	1.00
13	1.59	.99	1.06	8.9	.90	1.25	22.9	.96	1.10
14	.70	.98	.99	3.5	.76	.98	17.5	.95	1.00

Table 3.5
Z-PURLIN ANALYSIS
(W = 1.75 in)

SECTION	U7	U1/U7	U3/U7	S7	S1/S7	S3/S7	St7	St1/St7	St3/St7
1	1.13	.97	.88	4.5	.73	.96	27.1	.95	.99
2	.82	.97	.93	3.3	.71	.91	19.9	.95	.98
3	1.67	.98	.91	3.6	.69	.84	26.2	.96	.98
4	.76	.95	.90	3.0	.62	.85	25.6	.96	.98
5	2.54	.99	.78	10.0	.87	1.01	32.6	.96	1.00
6	.60	.96	.91	2.3	.54	.75	24.8	.96	.98
7	.77	.96	.88	4.1	.70	.97	26.6	.95	1.00
8	1.10	.97	.87	4.4	.72	.93	26.9	.96	.98
9	1.22	.98	.89	5.2	.77	.99	27.7	.96	1.00
10	.58	.97	.94	2.2	.60	.77	18.8	.95	.97
11	1.77	.99	.93	4.2	.77	.91	20.8	.95	.98
12	.60	.97	.94	2.3	.61	.79	18.9	.95	.97
13	1.47	.98	.92	5.2	.83	1.05	22.8	.96	1.01
14	.60	.97	.94	2.3	.61	.79	18.9	.95	.97
15	.60	.97	.94	2.5	.63	.81	19.1	.95	.98
16	.60	.97	.93	3.3	.71	.81	19.9	.95	.98
17	.60	.97	.93	3.3	.71	.81	19.9	.95	.98

Table 3.6

Z-PURLIN ANALYSIS
(W = 3.00 in)

SECTION	U7	U1/U7	US/U7	S7	S1/S7	SS/S7	St7	St1/St7	StS/St7
1	1.36	.99	1.05	8.3	.88	1.28	25.5	.96	1.09
2	1.01	.99	1.05	6.2	.87	1.17	18.9	.96	1.06
3	1.84	.99	.98	6.5	.85	1.12	23.7	.96	1.03
4	.96	.99	1.01	5.6	.83	1.16	22.8	.96	1.04
5	2.34	.99	1.16	14.9	.93	1.49	32.1	.97	1.23
6	.75	.98	.99	4.2	.78	1.07	21.4	.96	1.01
7	1.02	.99	1.09	7.7	.87	1.30	24.9	.96	1.09
8	1.33	.99	1.05	8.1	.88	1.26	25.3	.96	1.08
9	1.41	.99	1.07	9.1	.89	1.29	26.3	.96	1.10
10	.72	.99	1.01	4.2	.81	1.04	16.9	.95	1.01
11	1.93	.99	1.01	7.5	.89	1.15	20.2	.96	1.02
12	.75	.99	1.02	4.4	.81	1.06	17.0	.95	1.01
13	1.58	.99	1.15	10.4	.92	1.35	23.1	.96	1.16
14	.75	.99	1.02	4.4	.81	1.06	17.0	.95	1.01
15	.80	.99	1.02	4.7	.83	1.08	17.4	.95	1.02
16	1.01	.99	1.05	6.2	.87	1.17	18.9	.96	1.06

Table 3.7

C-PURLIN PARAMETRIC STUDY PROGRAM

```

6 PRINT " "
10 DIM B(2),Uo(2),U(2),So(2),S(2),S1(2),St(2)
20 DEG
30 A1=0
40 L=240
50 E=29500000
60 FOR Jj=1 TO 17
70 READ H,W,Cc,Be,T,Ro,K,F
71   Ch=Cc*COS(Be)
72   Cv=Cc*SIN(Be)
73   B=W+Ch
74   I=H^3/12+2*(W*(H/2)^2+Cc*Cv^2/12+Cc*(H/2-Cv/2)^2)
75   I=I*T
80 IF Jj=2 THEN H=7
90 IF Jj=3 THEN T=.06
100 IF Jj=3 THEN Ro=1
110 IF Jj=4 THEN K=3
120 IF Jj=5 THEN K=1
130 IF Jj=6 THEN K=3
140 IF Jj=6 THEN T=.07
150 IF Jj=7 THEN Ro=0
160 IF Jj=8 THEN Be=50
170 IF Jj=9 THEN Cc=1
171 IF Jj>9 THEN H=7
172 IF Jj=10 THEN T=.06
173 IF Jj=11 THEN Ro=1
174 IF Jj=12 THEN K=3
175 IF Jj=13 THEN K=1
176 IF Jj=14 THEN K=3
177 IF Jj=15 THEN T=.07
178 IF Jj=17 THEN Be=50
180 RESTORE 740
190 FOR J=1 TO 2
200 IF J=2 THEN Cc=0
210 IF J=2 THEN F=0
215 IF J=2 THEN W=B
216   GOTO 250
230 IMAGE XXXXX,DD,XXX,D.DD,XXX,DD.DD,XXX,DD.DD,XXX,DD,XXX,.DDD,XXX,DD.D
   DDD.DD,XXX,DD.DDD
240 PRINT USING 230;Jj,H,W,Cc,Be,T,Ro,K,F
250 REM GOTO 720
260 Ch=Cc*COS(Be)
270 Cv=Cc*SIN(Be)
280   B=W+Ch
290   Wc=F*H
      40)*1
      +Cc*1

```

Table 3.7

C-PURLIN PARAMETRIC STUDY PROGRAM (CONTINUING)

```

360 Qb=Hf*(H/2-Hf/2)+W*H/2+Cc*(H/2-Cv/2)
370 Qb=Qb*T
380 G=Qb/I
390 Qf=T*B*H/2
400 Q=12
410 U=0
420 S=0
430 FOR N=1 TO 7 STEP 2
440 An=0
450 IF N=1 THEN An=Ro
460 Ln=(N*PI)^5+N*K*L^4*PI/(E*Fi)
470 Gn=4*Q*L^4/(E*Fi)
480 C=Gn/Ln
481 A1=B/H
490 U1=C*(Qf*B/(2*I)+A1)+An
500 U2=1-C*G*PI*N*(.206*N^2-.063)
510 U=U+U1/U2
520 S=N^2*(U1/U2-An)+S
530 IF U2<0 THEN PRINT "BUCKLING*****"
540 IF N=1 THEN Uo=U
550 IF N=1 THEN So=S
560 NEXT N
570 Ss=E*Fi*PI^2/L^2*Xb/Fi
580 So=So*Ss
590 S=S*Ss
600 Sf=Q*L^2/8*(H/2)/I
610 St=S+Sf
620 S1=So+Sf
630 Uo(J)=Uo
640 U(J)=U
650 So(J)=So/1000
660 S(J)=S/1000
670 S1(J)=S1/1000
680 St(J)=St/1000
690 NEXT J
700 IMAGE XXXXX,DD,XX,D.DD,XXX,D.DD,XXXX,D.DD,XXX,DD.D,XXX,D.DD,XXX,D.DD,XXX,DD.
D,XXXX,D.DD,XXXX,D.DD
710 PRINT USING 700;Jj,U(1),Uo(1)/U(1),Uo(2)/U(1),S(1),So(1)/S(1),So(2)/S(1),St(
1),S1(1)/St(1),S1(2)/St(1)
720 NEXT Jj
730 END

```

Table 3.8

C-PURLIN ANALYSIS
(W = 2.0 in)

1	4.29	.98	.94	22.8	.78	1.18	43.6	.89	1.09
2	4.56	.97	.98	27.6	.76	1.08	42.9	.84	1.05
3	4.56	.97	.94	22.6	.68	1.03	43.3	.84	1.01
4	2.66	.95	.94	15.2	.69	1.05	36.0	.87	1.02
5	9.77	.99	.92	47.7	.89	1.29	68.5	.92	1.20
6	2.42	.95	.93	15.3	.60	.93	36.1	.83	.97
7	3.93	.97	.95	22.3	.78	1.18	43.1	.88	1.09
8	3.86	.97	.92	20.2	.76	1.04	41.0	.88	1.02
9	4.54	.98	.96	25.6	.81	1.22	46.4	.90	1.12
10	4.21	.96	.96	28.8	.65	.93	44.2	.77	.95
11	5.50	.98	.97	28.6	.77	1.08	43.9	.85	1.05
12	2.94	.96	.96	19.2	.67	.95	34.6	.81	.97
13	9.07	.99	1.01	50.4	.86	1.25	65.7	.89	1.19
14	2.94	.96	.96	19.2	.67	.95	34.6	.81	.97
15	4.69	.97	.97	34.6	.77	1.06	49.4	.85	1.05

Table 3.9

C-PURLIN ANALYSIS
(W = 2.5 in)

1	4.53	.98	1.01	28.1	.84	1.28	46.7	.91	1.17
2	4.89	.98	1.03	34.0	.82	1.17	47.8	.87	1.12
3	4.88	.98	.98	27.6	.77	1.14	46.3	.86	1.08
4	2.90	.98	.99	18.8	.77	1.16	37.4	.89	1.08
5	9.13	.99	1.06	54.1	.92	1.45	72.7	.94	1.33
6	2.67	.97	.97	18.6	.71	1.05	37.2	.85	1.03
7	4.18	.98	1.02	27.5	.84	1.29	46.2	.91	1.17
8	4.15	.98	1.00	25.3	.84	1.18	43.9	.91	1.10
9	4.69	.99	1.03	30.9	.86	1.31	49.6	.91	1.19
10	4.63	.97	1.00	35.2	.74	1.03	49.0	.81	1.02
11	5.82	.98	1.02	35.2	.83	1.17	48.9	.88	1.12
12	3.22	.97	1.00	23.6	.75	1.05	37.4	.84	1.03
13	9.03	.99	1.09	59.6	.90	1.34	73.4	.92	1.28
14	3.22	.97	1.00	23.6	.75	1.05	37.4	.84	1.03
15	4.69	.97	1.01	34.6	.77	1.06	49.4	.85	1.05

Table 3.10

C-PURLIN ANALYSIS
(W = 1.5 in)

1	3.72	.90	.86	18.5	.65	.99	41.9	.85	.99
2	4.09	.95	.92	22.0	.64	.93	39.3	.80	.96
3	4.19	.94	.89	18.9	.54	.83	42.4	.79	.93
4	2.39	.93	.88	12.7	.54	.85	36.1	.84	.95
5	9.99	.98	.77	39.9	.82	1.08	63.3	.89	1.05
6	2.17	.91	.87	13.0	.46	.73	36.5	.81	.91
7	3.55	.95	.86	18.0	.64	.99	41.5	.84	.99
8	3.46	.94	.83	16.5	.60	.81	39.9	.84	.92
9	4.22	.96	.89	20.7	.71	1.07	44.2	.87	1.03
10	3.73	.92	.91	23.8	.52	.77	41.1	.72	.87
11	5.05	.96	.92	22.8	.65	.93	40.1	.80	.96
12	2.61	.93	.91	15.7	.53	.79	33.0	.78	.90
13	8.64	.98	.91	40.1	.79	1.11	57.4	.85	1.03
14	2.61	.93	.91	15.7	.53	.79	33.0	.78	.90
15	3.81	.93	.91	20.2	.55	.77	38.0	.78	.90

Table 3.11

C-PURLIN ANALYSIS
(W = 3.00 in)

1	4.61	.99	1.07	33.2	.88	1.36	50.1	.92	1.24
2	5.07	.99	1.07	40.4	.86	1.23	52.9	.90	1.18
3	5.12	.98	1.02	33.2	.82	1.22	50.1	.88	1.14
4	3.07	.98	1.03	22.7	.83	1.23	39.6	.90	1.13
5	8.30	.99	1.17	53.2	.93	1.57	75.2	.95	1.44
6	2.87	.98	1.01	22.4	.77	1.14	39.3	.87	1.08
7	4.27	.99	1.08	32.6	.88	1.36	49.5	.92	1.24
8	4.29	.99	1.08	30.4	.87	1.28	47.3	.92	1.18
9	4.71	.99	1.09	35.9	.89	1.38	52.0	.93	1.26
10	4.96	.98	1.03	42.2	.80	1.10	54.7	.85	1.08
11	5.99	.99	1.06	41.6	.87	1.23	54.1	.90	1.18
12	3.44	.98	1.03	28.4	.81	1.12	40.9	.87	1.08
13	8.65	.99	1.16	66.8	.92	1.41	79.2	.93	1.34
14	3.44	.98	1.03	28.4	.81	1.12	40.9	.87	1.08
15	4.98	.98	1.04	41.5	.82	1.14	54.0	.86	1.11

Table 4.1

CROSS-SECTIONAL DIMENSIONS**

Section (H x t x a_0)	H (in)	t (in)	w (in)	α (rad)	R (in)	R_1 (in)	S (in)	F_y (ksi)
Z 8 x .059 x .1	8	.059	1.961	.624	.49	.578	.624	66.00
Z 7.92 x .06 x .56*	7.92	.060	2.01	.698	.392	.300	.640	61.50
Z 8.055 x .063 x .25	8.055	.063	2.059	.873	.477	.279	.602	56.89
Z 7.97 x .07 x .25	7.97	.070	1.875	.698	.715	.527	.766	64.60
Z 8 x .075 x .25	8.00	.075	1.891	.716	.738	.551	.734	64.70
Z 8.031 x .088 x .25	8.031	.088	1.953	.707	.762	.461	.727	63.80
Z 8 x .089 x .00	8.00	.089	1.938	.751	.688	.498	.797	64.00
Z 7.94 x .114 x .25	7.94	.114	2.051	.831	.746	.309	.773	56.1
Z 7.93 x .115 x .47*	7.93	.115	1.860	.620	.805	.445	.810	65.90
Z 9.625 x .062 x .125	9.625	.062	2.141	.799	.656	.402	.875	57.44
Z 9.45 x .063 x .66*	9.45	.063	2.030	.733	.512	.326	.600	57.3
Z 9.578 x .106 x -.0625	9.578	.106	2.141	.712	.523	.367	.602	52.90
Z 9.49 x .109 x .25*	9.49	.109	2.020	.698	.680	.34	.900	57.60
C 7 x .075 x .00*	7.00	.075	1.656	1.571	.406	.406	.359	55.0
C 9 x .075 x .25*	9.00	.075	1.750	1.571	.320	.306	.445	55.25
C 9 x .077 x 1.0*	9.00	.077	1.820	1.571	.328	.318	.420	55.25

* All sections marked by an asterisk were tested at Cornell University. All others were tested by a metal building manufacturer.

** Cross-sectional notation is illustrated in Fig. 2.4.
 α is the angle of the stiffening lip with the horizontal (flange).

Table 4.2
OBSERVED VALUES OF K
(lb/in/in)

Section Tested (H x t)	at (*) w_u			K at w_u used in the Evaluation of Vacuum Test Section: (H x t x a_o)
	$.75w_u$	w_u	$1.25w_u$	
Z 8 x .062	1.28	1.28	1.28	Z 8 x .059 x .10 Z 8 x .06 x .56 Z 8 x .063 x .25
Z 8 x .073	1.53	1.57	1.64	Z 7.97 x .07 x .25 Z 8 x .075 x .25
Z 8 x .106	1.67	1.78	1.88	Z 8.031 x .088 x .25 Z 8 x .089 x .00
Z 8 x .117	2.08	2.15	2.29	Z 7.94 x .114 x .25 Z 7.93 x .115 x .47
Z 9.5 x .065	.97	.97	1.01	Z 9.625 x .062 x .125 Z 9.45 x .063 x .66
Z 9.5 x .107	1.56	1.62	1.69	Z 9.578 x .106 x -.0625 Z 9.49 x .109 x .25
C 7 x .075	3.00 2.88 2.67 2.00	3.10 3.00 2.80 2.29	3.17 3.10 2.96 2.38	C 7 x .075 x .00
average	2.64	2.80	2.82	
C 9 x .077	1.60 1.48 1.48 1.32	1.63 1.63 1.51 1.48	1.71 1.67 1.60 1.56	C 9 x .075 x .25 C 9 x .077 x 1.00
average	1.47	1.56	1.64	

* w_u is the value of w defined by Eq. 3.1-20 with q equal to vacuum test ultimate load

Table 5.1

COMPARISON OF OBSERVED AND CALCULATED ULTIMATE LOADS*

Section (H x t x a _o)	Test	Simple	Full, n=1	Eff. n=1	Simple Test	Full Test	Eff. Test
Z 8 x .059 x .1	90.7	102	109.2	108	1.12	1.20	1.19
Z 7.92 x .06 x .56**	83	98.4	102.0	99.6	1.19	1.23	1.20**
Z 8.053 x .063 x .25	96.2	105.6	108	102	1.10	1.12	1.06
Z 7.97 x .07 x .25	118.35	128.4	138.0	127.2	1.08	1.17	1.07
Z 8 x .075 x .25	137.9	136.8	146.4	133.2	0.99	1.06	0.97
Z 8.031 x .088 x .25	165.8	168.0	176.4	154.8	1.01	1.06	0.93
Z 8 x .089 x .00	162.7	174.0	181.2	158.4	1.05	1.09	0.96
Z 7.94 x .114 x .25	214.5	210.0	213.6	176.4	0.98	1.00	0.82
Z 7.93 x .115 x .47	184.0	218.4	229.2	194.4	1.19	1.25	1.06
Z 9.625 x .062 x .125	119.0	103.2	104.4	105.6	0.87	0.88	0.89
Z 9.45 x .063 x .66	114.0	102.0	103.2	104.4	0.89	0.91	0.92
Z 9.578 x .106 x -.0625	266.7	218.4	220.8	190.8	0.82	0.83	0.72
Z 9.49 x .109 x .25**	218.0	201.6	205.2	178.8	0.92	0.94	0.82**
C 7 x .075 x .00	127.3	102.0	116.4	106.8	0.80	0.91	0.84
C 9 x .075 x .25	117.2	102.0	109.2	121.2	0.87	0.93	1.03
C 9 x .077 x 1.0	103.2	94.8	103.2	116.4	0.92	1.00	1.12
Average					0.99	1.04	0.98
Coefficient of variation (%)					12	12	14

*All loads in lbs/ft; all dimensions in inches.

**Failure with local buckling at a perforation for sag rods.

Table 5.2

CONVERGENCE OF SOLUTION
(Effective Depth Approach)

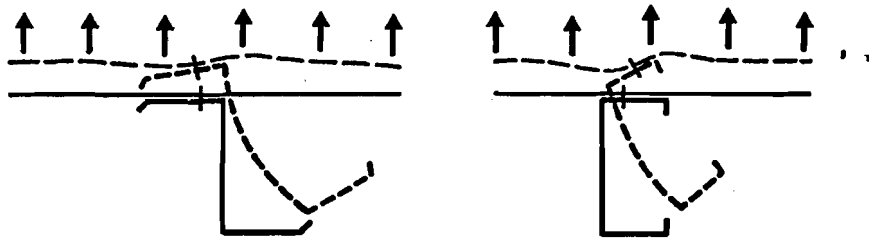
Section	Test Ult. Load	Calculated Ult. Loads*					Eff. (n=5) Test
		1	2	3	4	5	
Z 8 x .059 x .1	90.7	108.0	121.2	118.8	120.0	118.8	1.31
Z 7.92 x .06 x .56	83	99.6	115.2	118.8	114.0	112.8	1.36
Z 8.055 x .063 x .25	96.2	102	116.4	114	114	114	1.19
Z 7.97 x .07 x .25	118.35	127.2	138	136.8	136.8	136.8	1.16
Z 8 x .075 x .25	137.9	133.2	142.8	141.6	141.6	141.6	1.03
Z 8.031 x .088 x .25	165.8	154.8	166.8	164.4	165.6	164.4	0.99
Z 8 x .089 x .00	162.7	158.4	170.4	168.0	169.2	168.0	1.03
Z 7.94 x .114 x .25	214.5	176.4	190.8	188.4	188.4	188.4	0.88
Z 7.93 x .115 x .47	184.0	194.4	206.4	205.2	205.2	205.2	1.12
Z 9.625 x .062 x .125	119.0	105.6	112.8	111.6	111.6	111.6	0.94
Z 9.45 x .063 x .66	114.0	104.4	114	111.6	112.8	111.6	0.98
Z 9.578 x .106 x -.0625	266.7	190.8	207.6	204.0	205.2	205.2	0.77
Z 9.49 x .109 x .25	218.0	178.8	188.4	187.2	187.2	187.2	0.86
Average							1.05
Coefficient of variation (%)							16

* All loads in lbs/ft; all dimensions in inches.

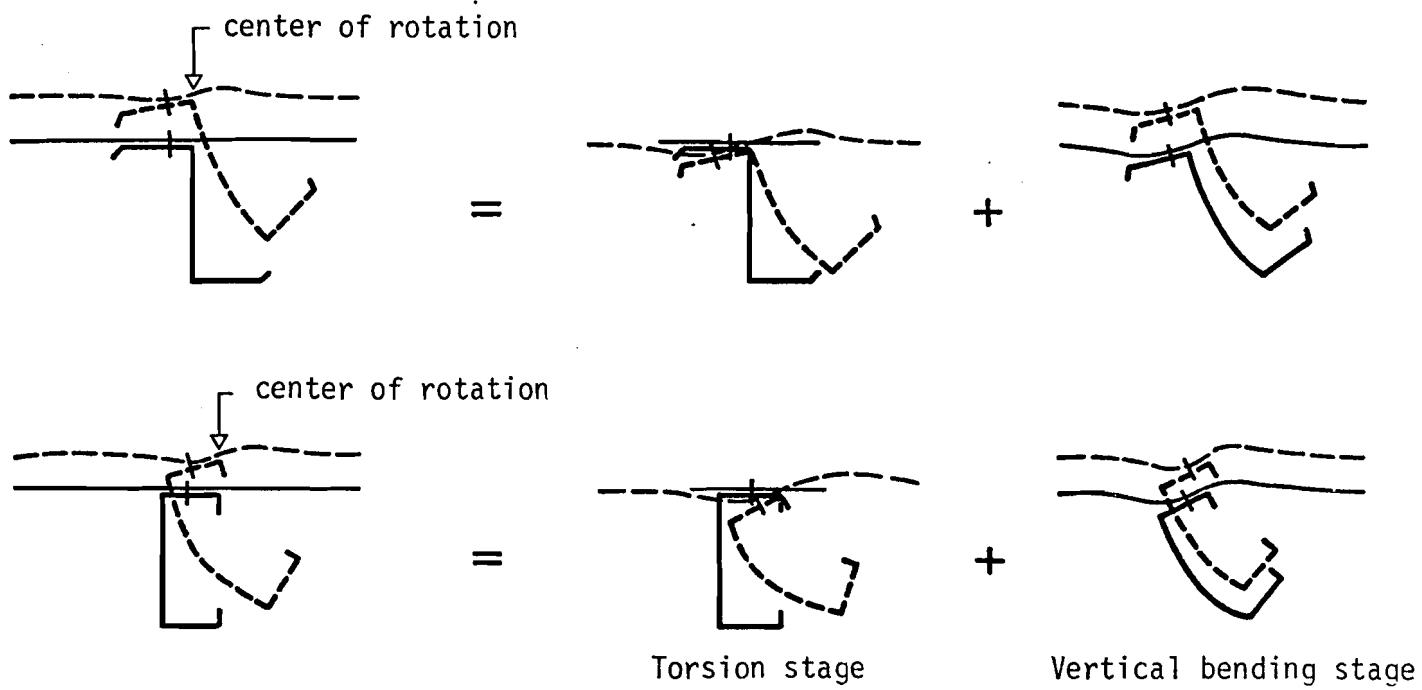
Table 5.3
TEST AND SECTION DESIGNATIONS

Section (Designation of this Report)	Test (Designation of Ref. 1)	Section (Designation of Ref. 1)
Z 9.45 x .063 x .66	V5	A
Z 9.49 x .109 x .25	V7	B
Z 7.92 x .06 x .56	V4	C *
Z 7.93 x .115 x .47	V3	D *

*The failure loads used in this report are slightly different from those given in Ref. 1. Some errors in pressure recording and dead load correction in Ref. 1 were discovered.

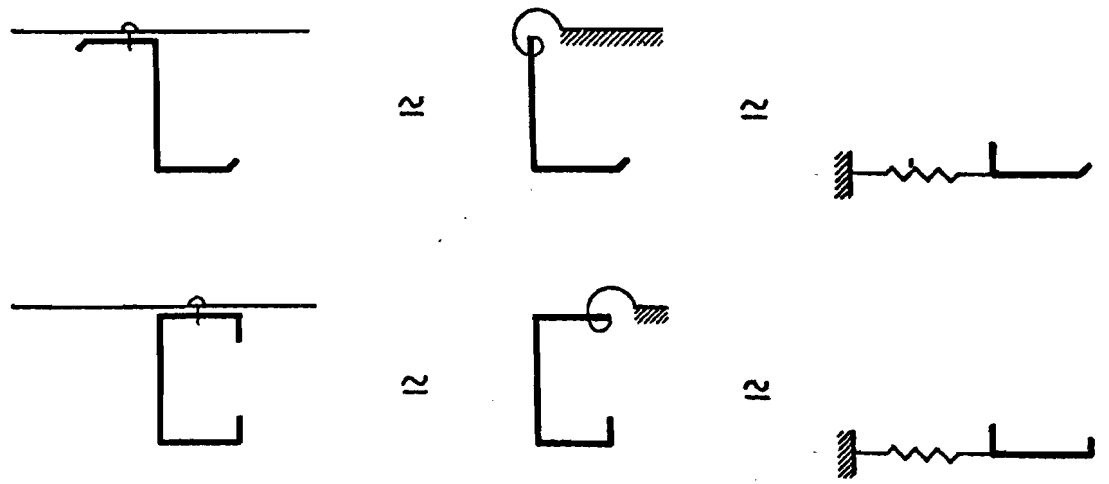


a. Total deflection

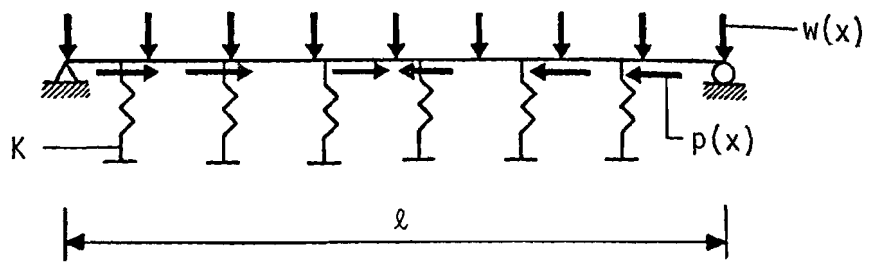


b. Components of total deflection

Fig. 2.1 Idealized behavior of purlins



a. Idealization of rotational restraint



b. Beam-column idealization

Fig. 2.2 Behavior idealization

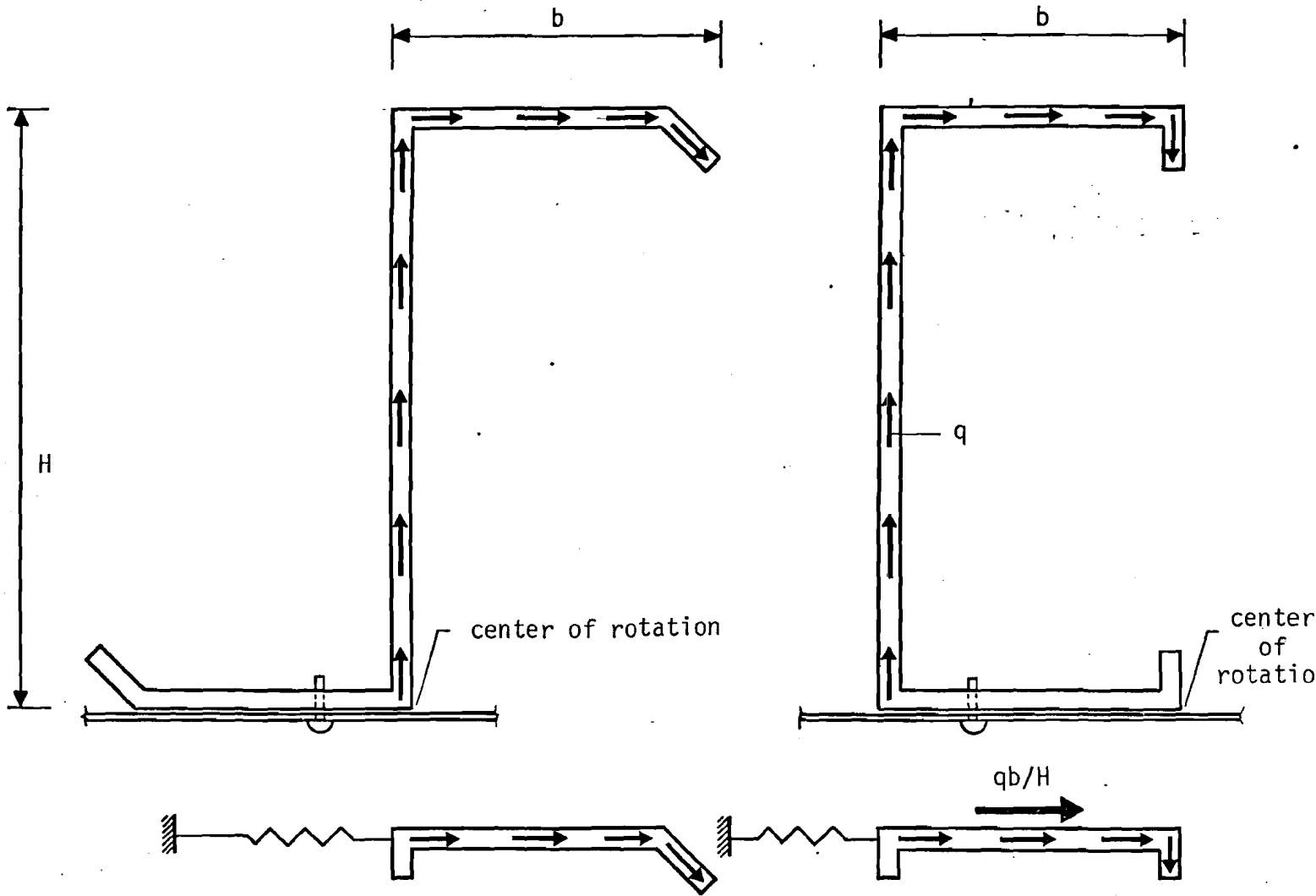


Fig. 2.3 Lateral forces on the beam-column

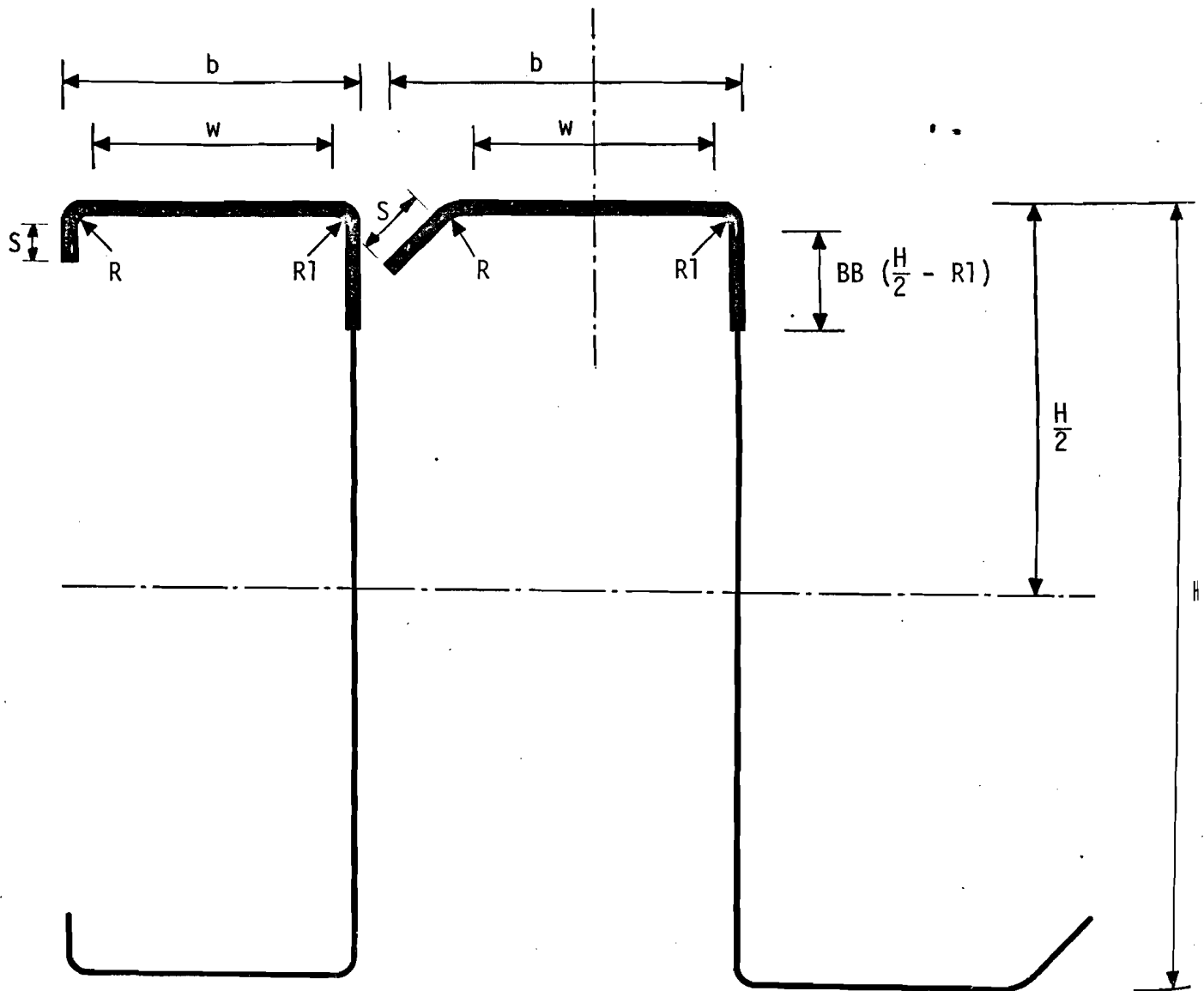


Fig. 2.4 Cross-sectional dimensions. The heavy lines indicate the idealized beam-column section

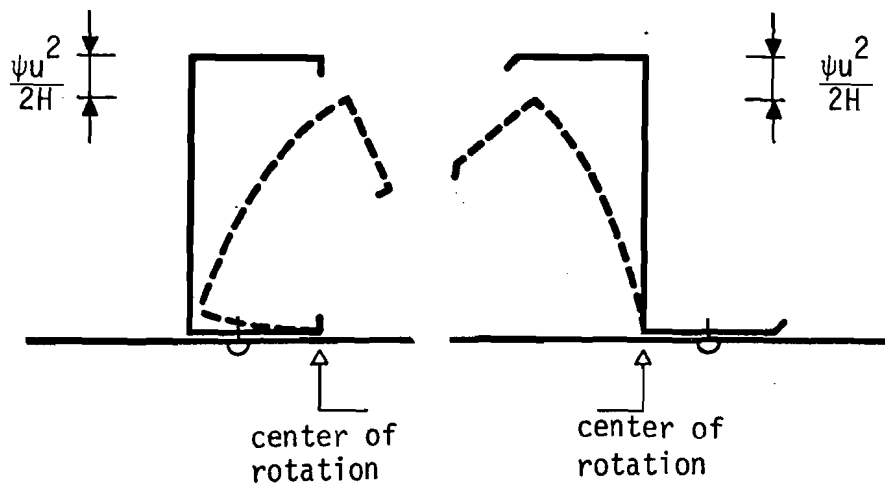
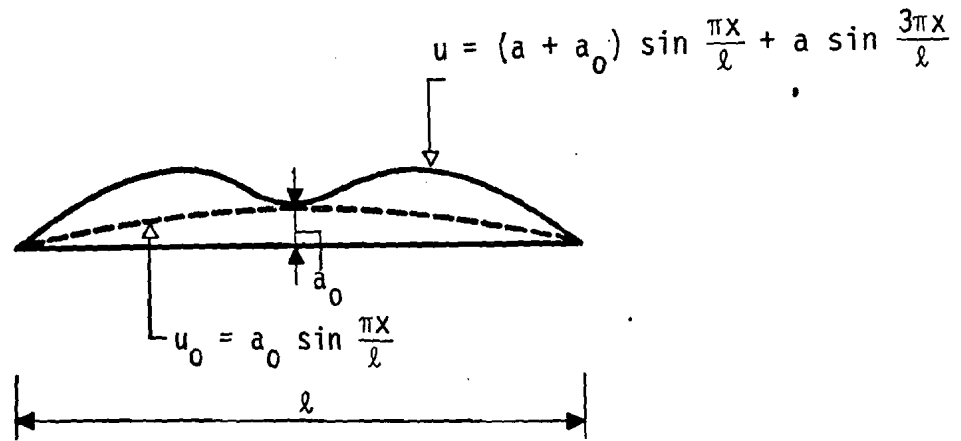
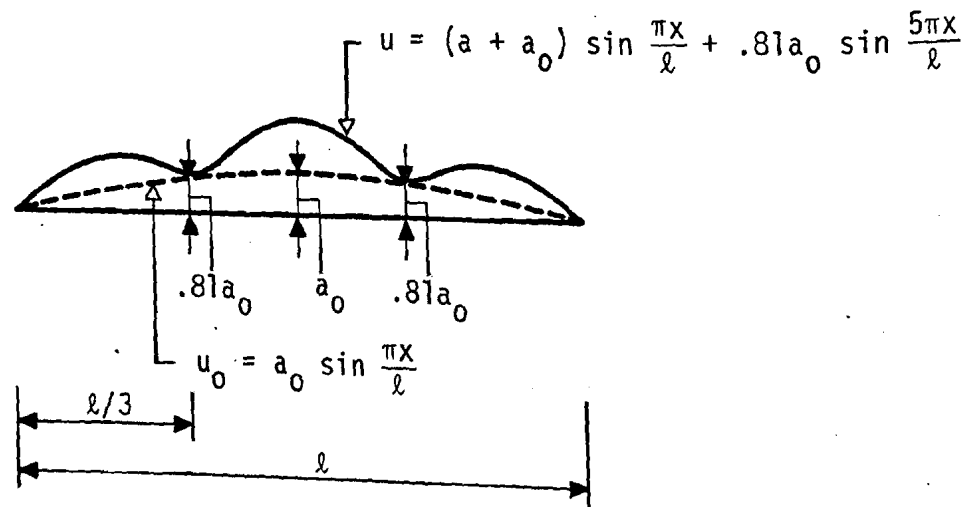


Fig. 2.5 Vertical deflection resulting from lateral deflection and twist
(Also refer to Fig. 3.3)



a. Purlin with midspan bracing



b. Purlin with third point bracing

Fig. 2.6 Initial sweep and deflected shapes

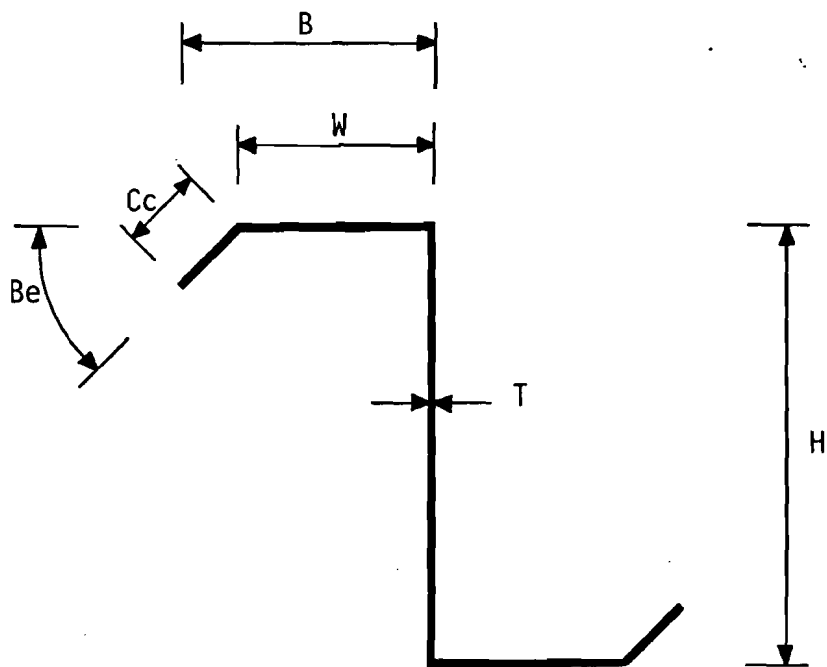
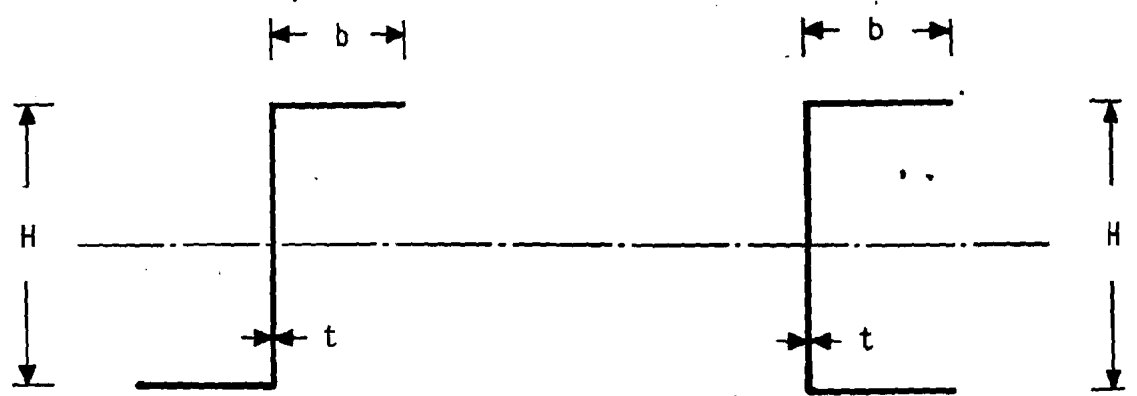
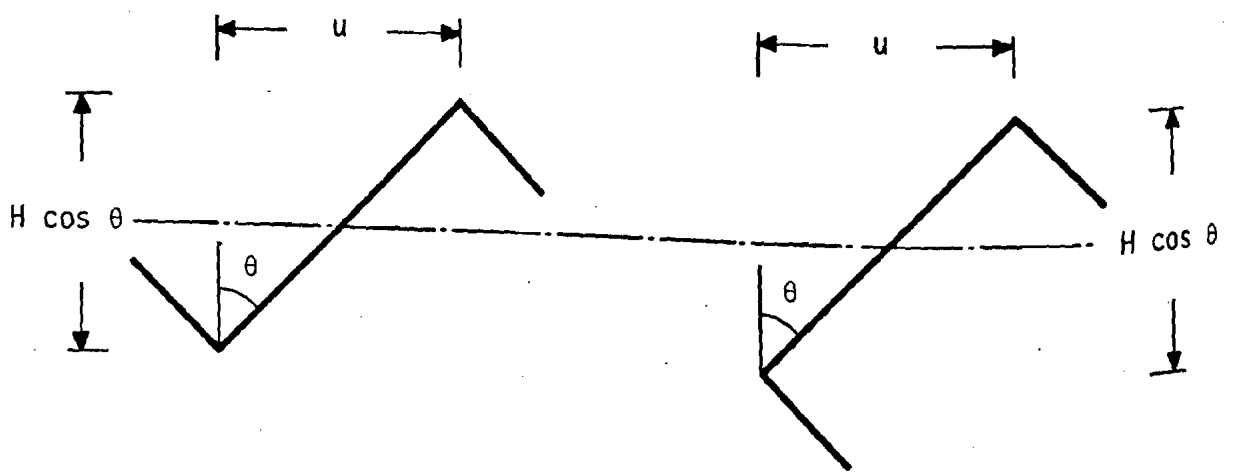


Fig. 3.1 Cross-sectional notation of the parametric studies



a. Original position



b. Position after lateral deflection and twisting

Fig. 3.2 Reduction of the moment of inertia due to lateral deflection and twisting.

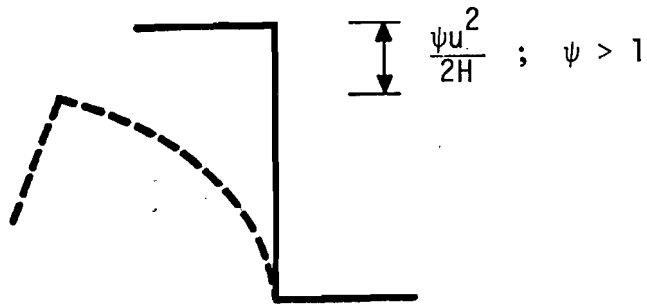
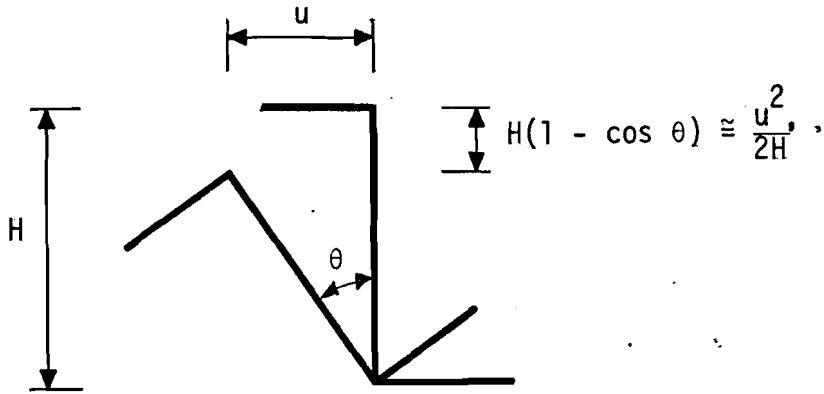


Fig. 3.3 The effect of cross-sectional distortion on the vertical deflection.

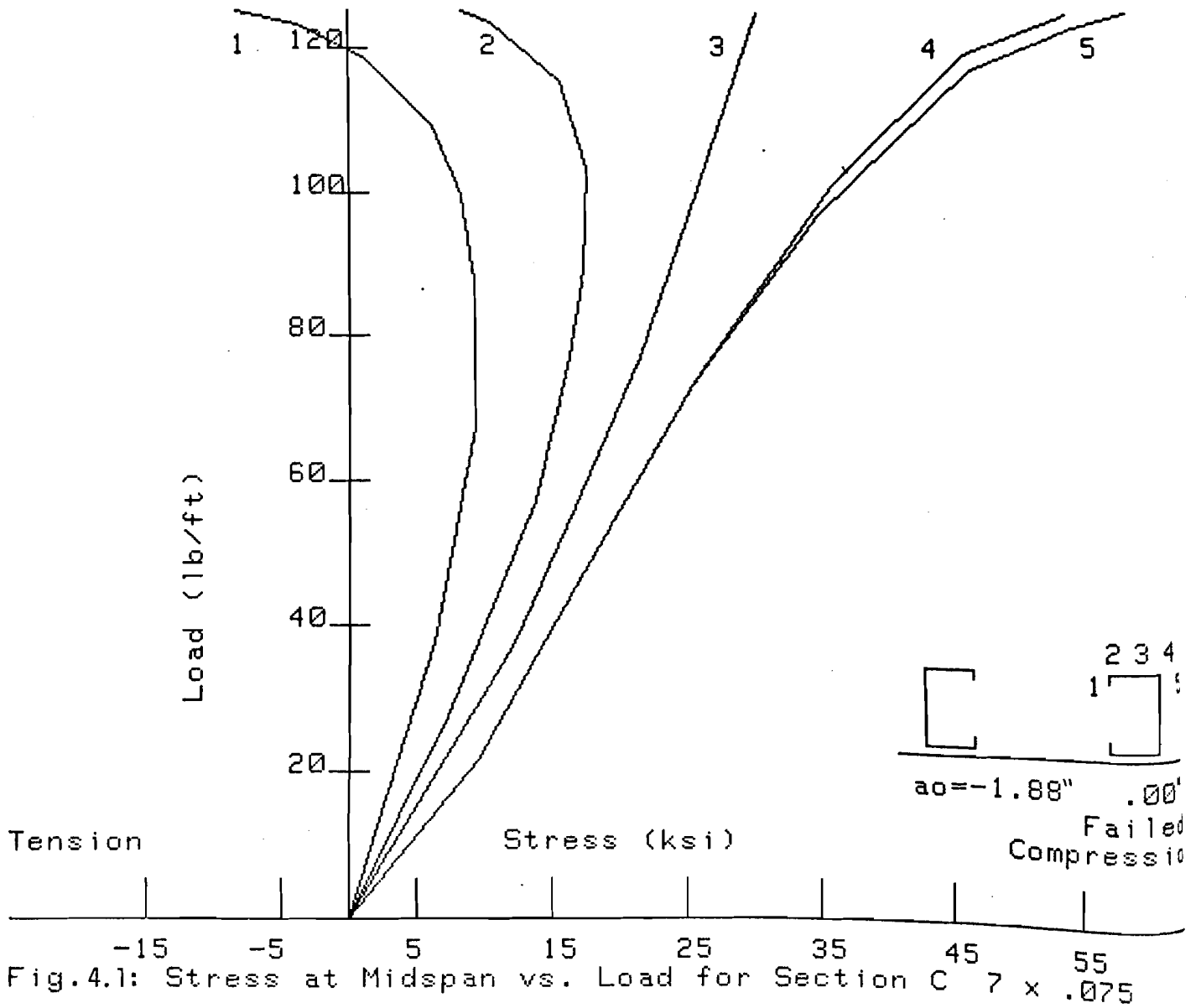


Fig.4.1: Stress at Midspan vs. Load for Section C 7 x .075

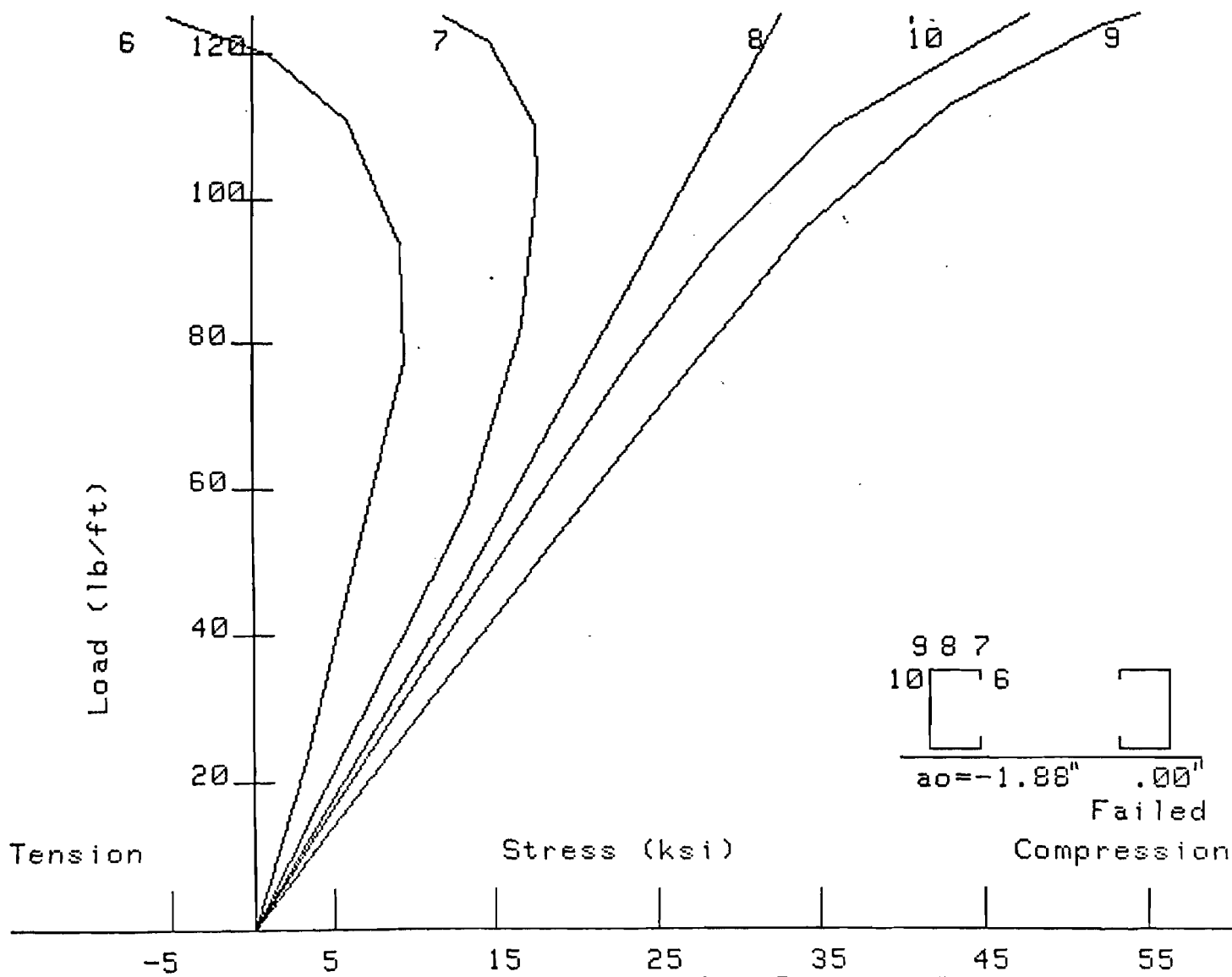


Fig.4.2: Stress at Midspan vs. Load for Section C 7 x .075

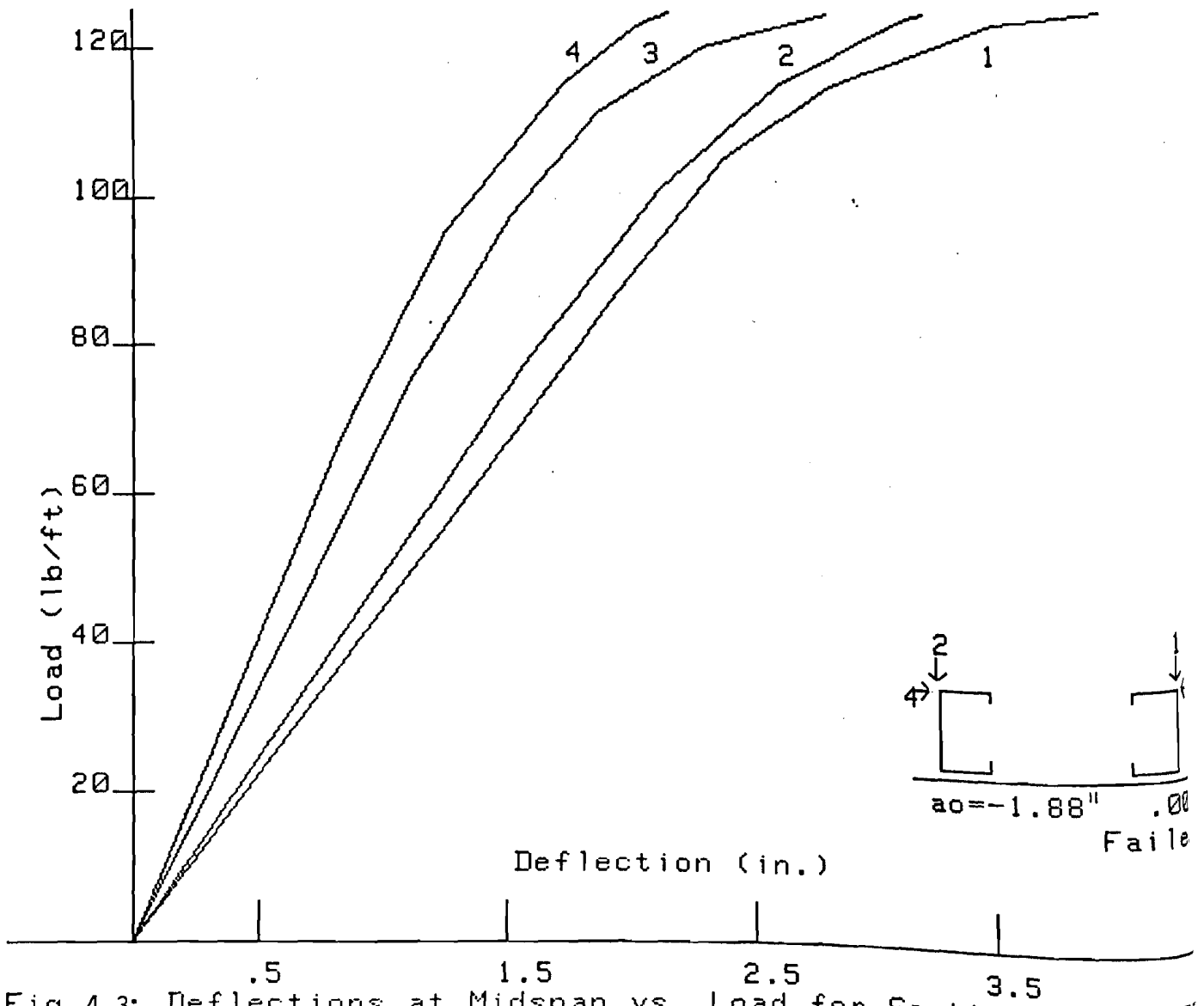


Fig.4.3: Deflections at Midspan vs. Load for Section C 7 x .0

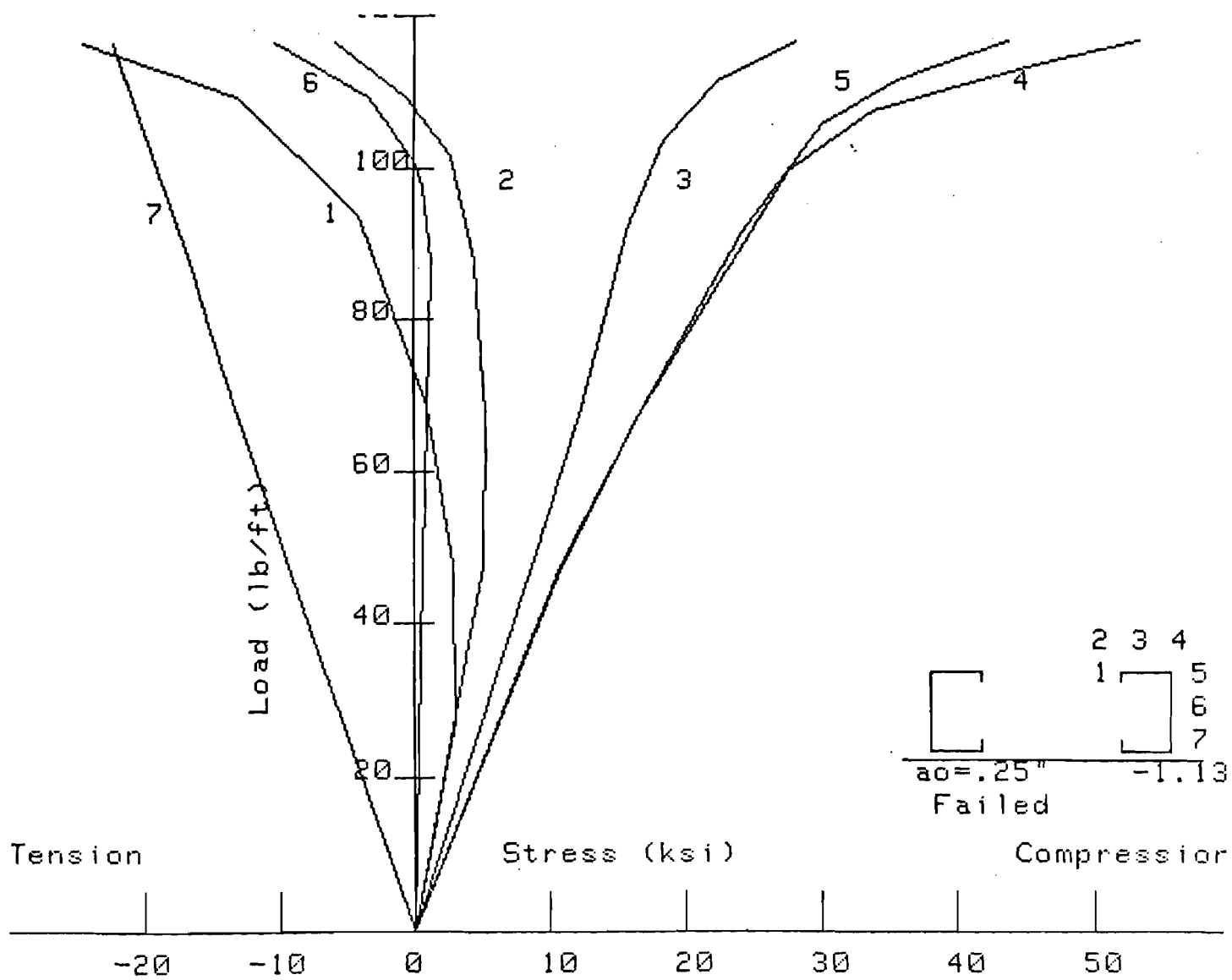
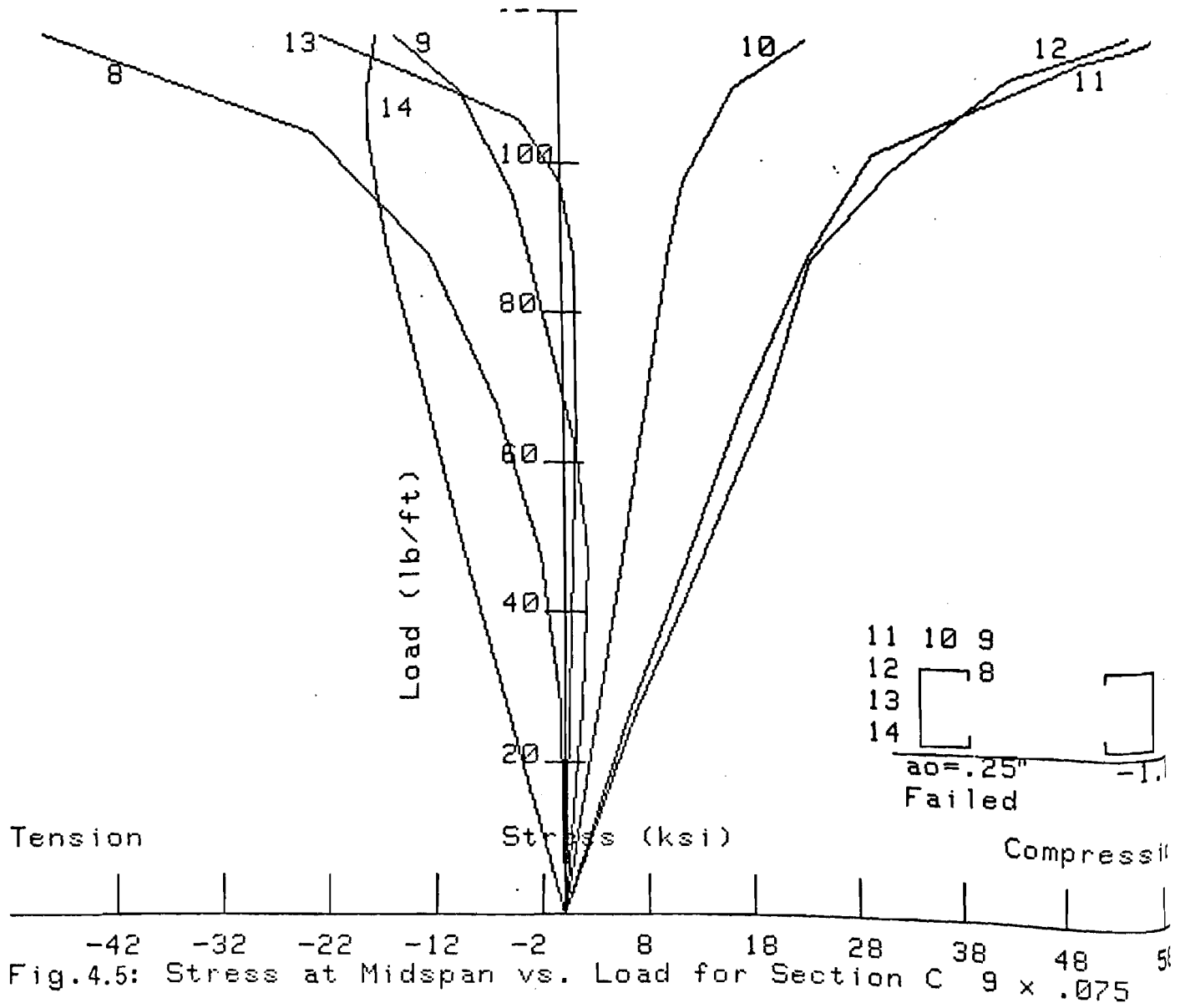


Fig.4.4: Stress at Midspan vs. Load for Section C 9 x .075



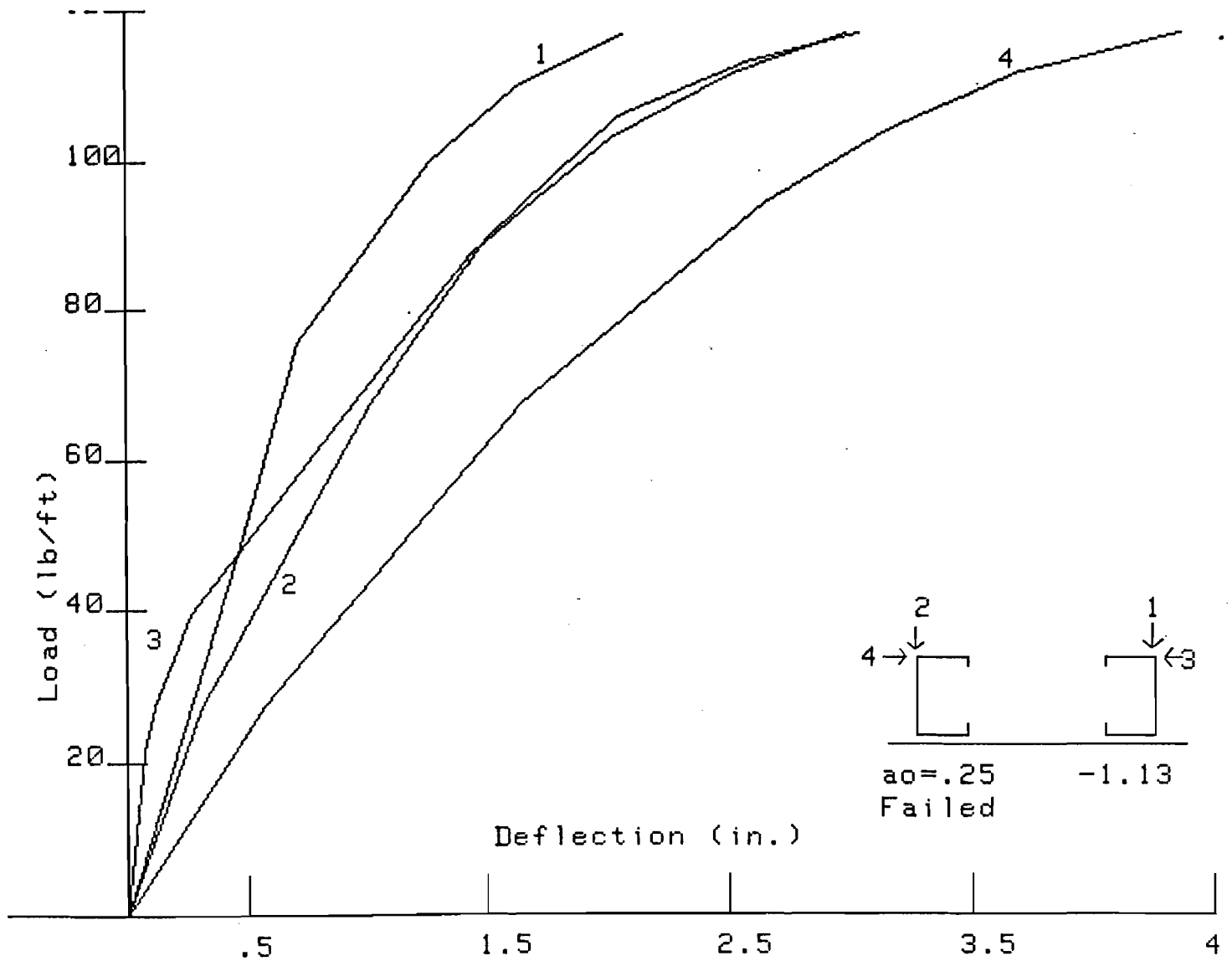


Fig.4.6: Deflections at Midspan vs. Load for Section C 9 x .075

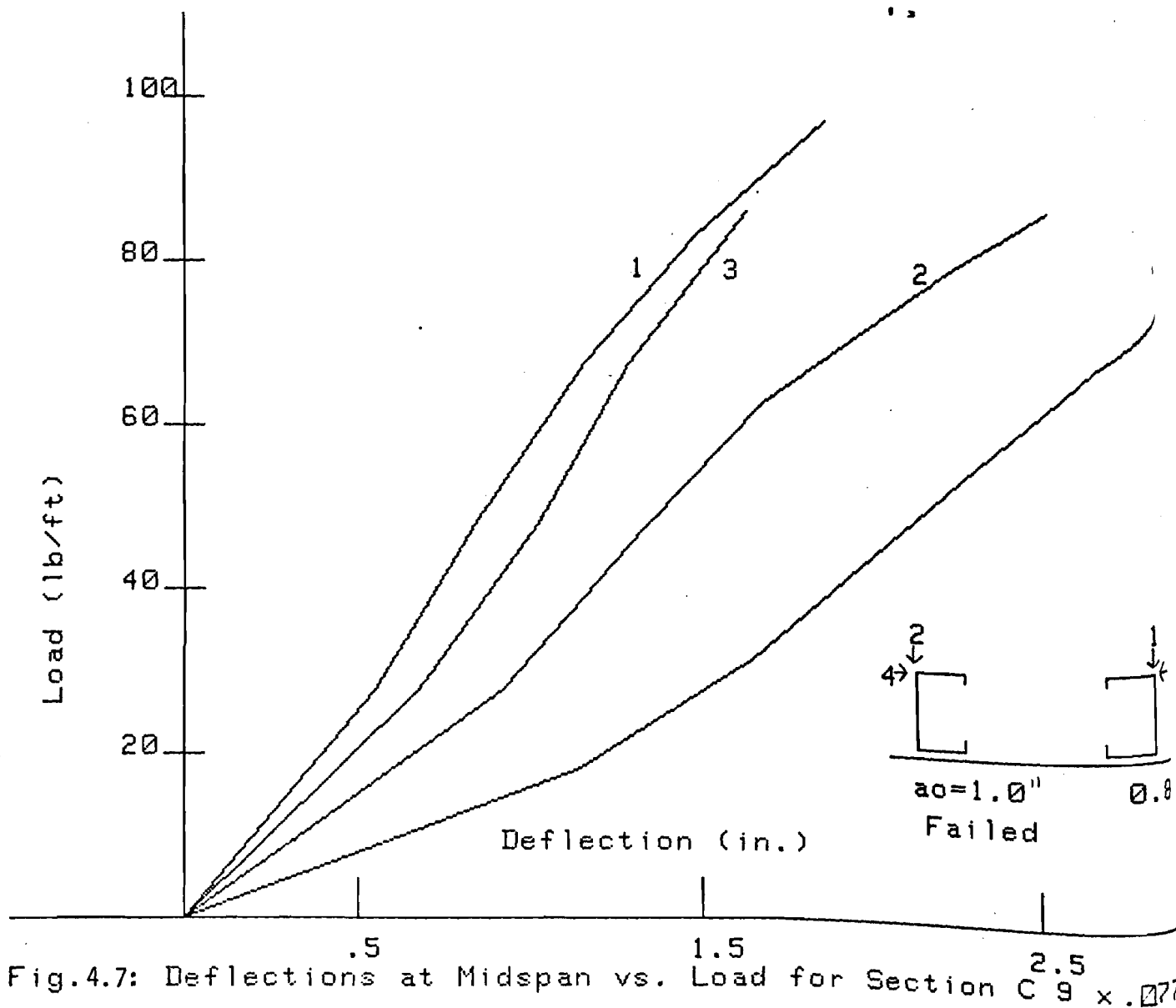


Fig.4.7: Deflections at Midspan vs. Load for Section C 9 x .071

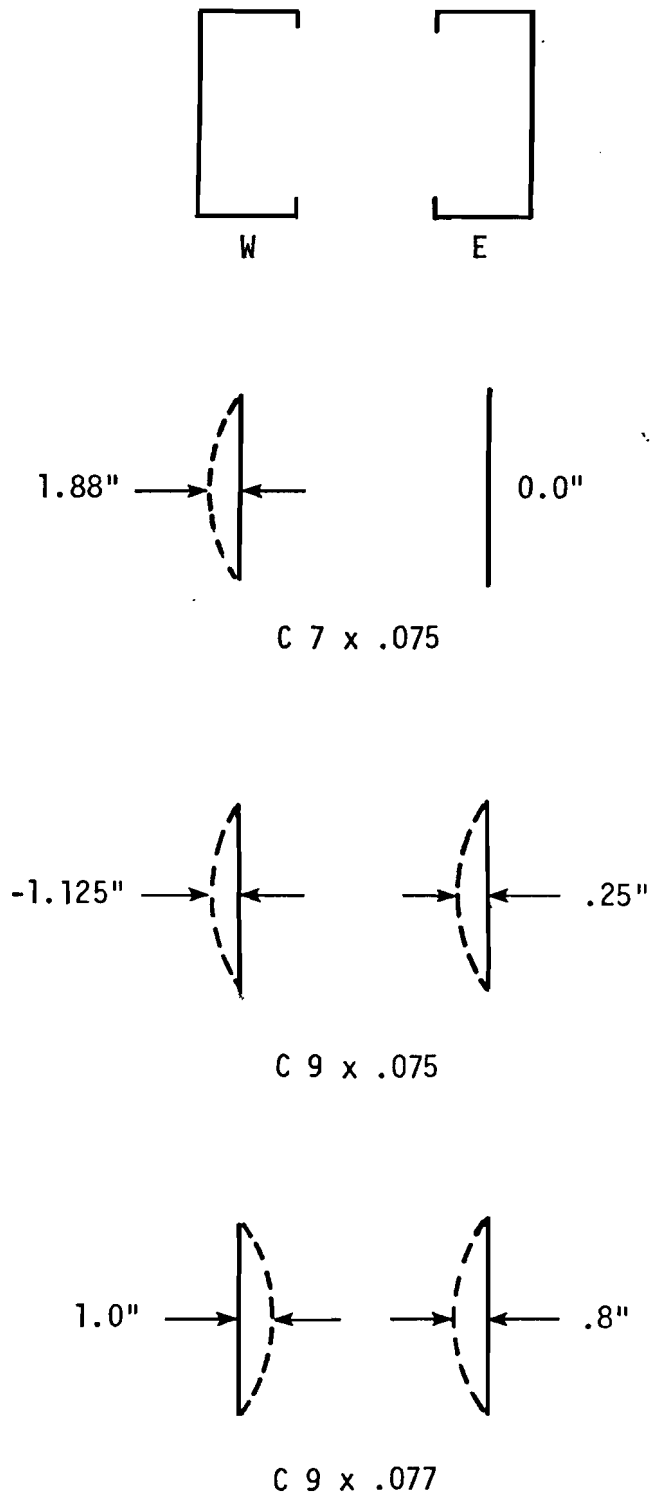


Fig. 4.8 Initial sweeps of the compression flanges of C-purlins

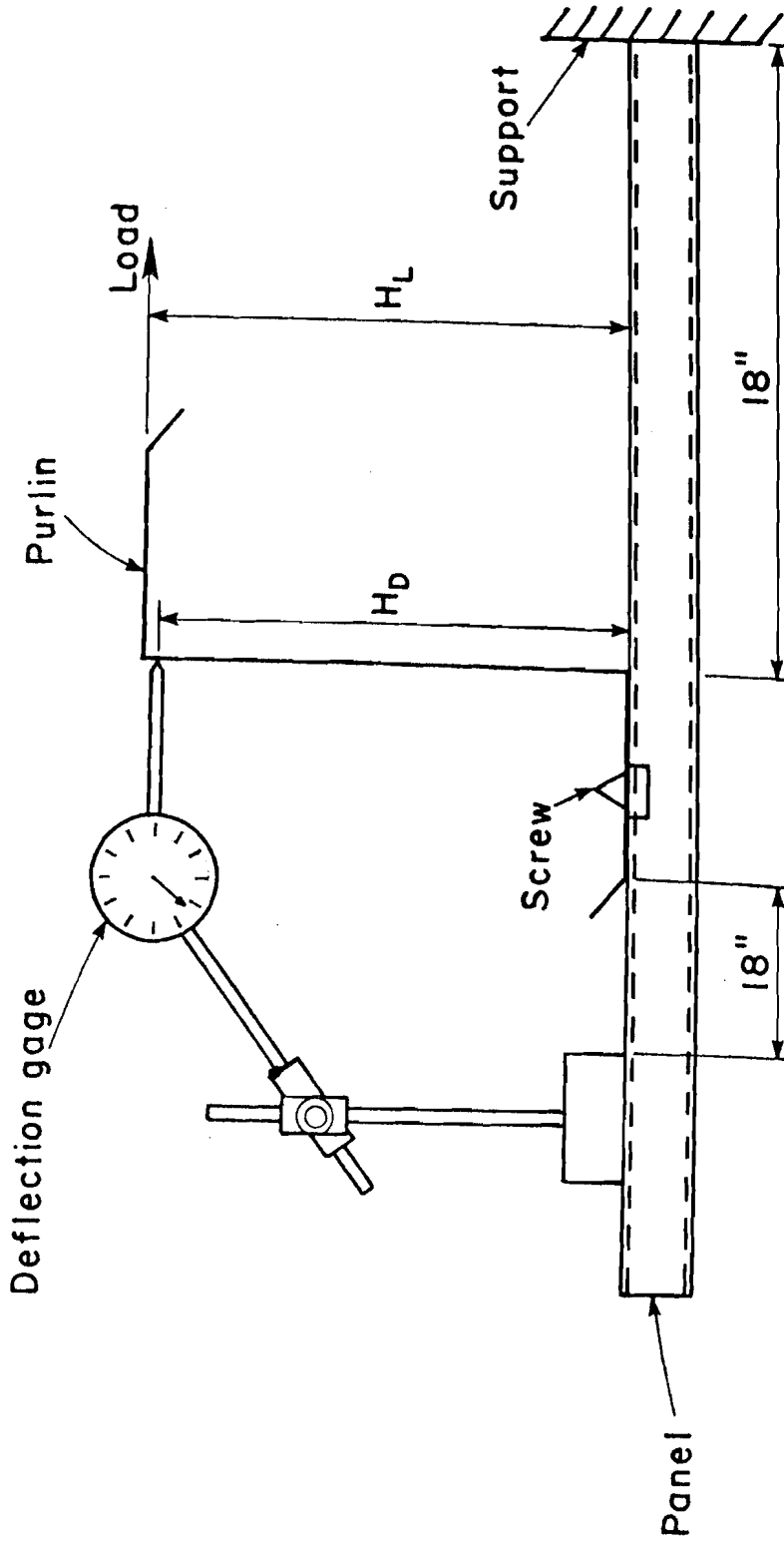


FIG. 4.9 F TEST: DIAPHRAGM-BRACED PURLIN

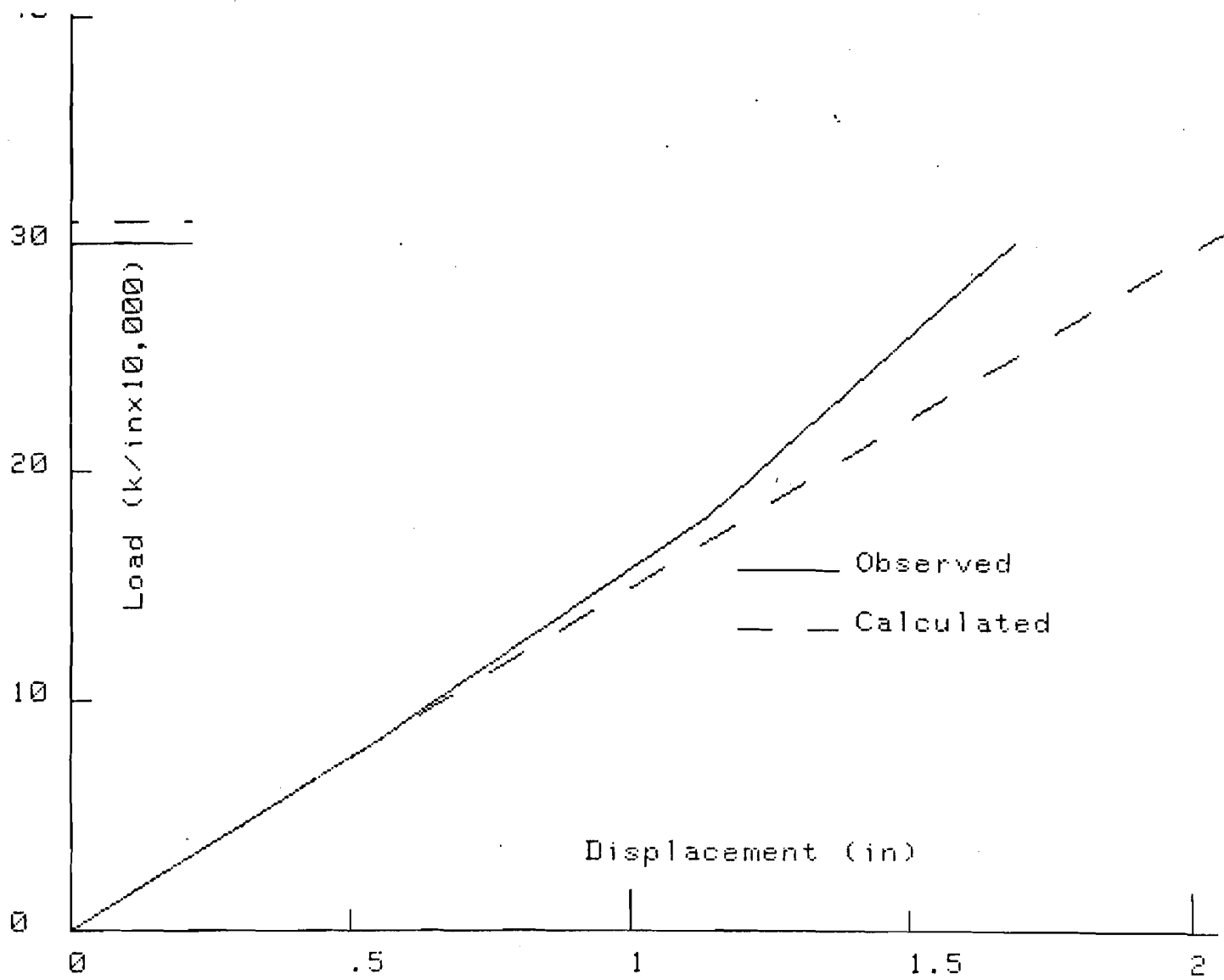


Fig.4.10: F test Results Z 8 x .073

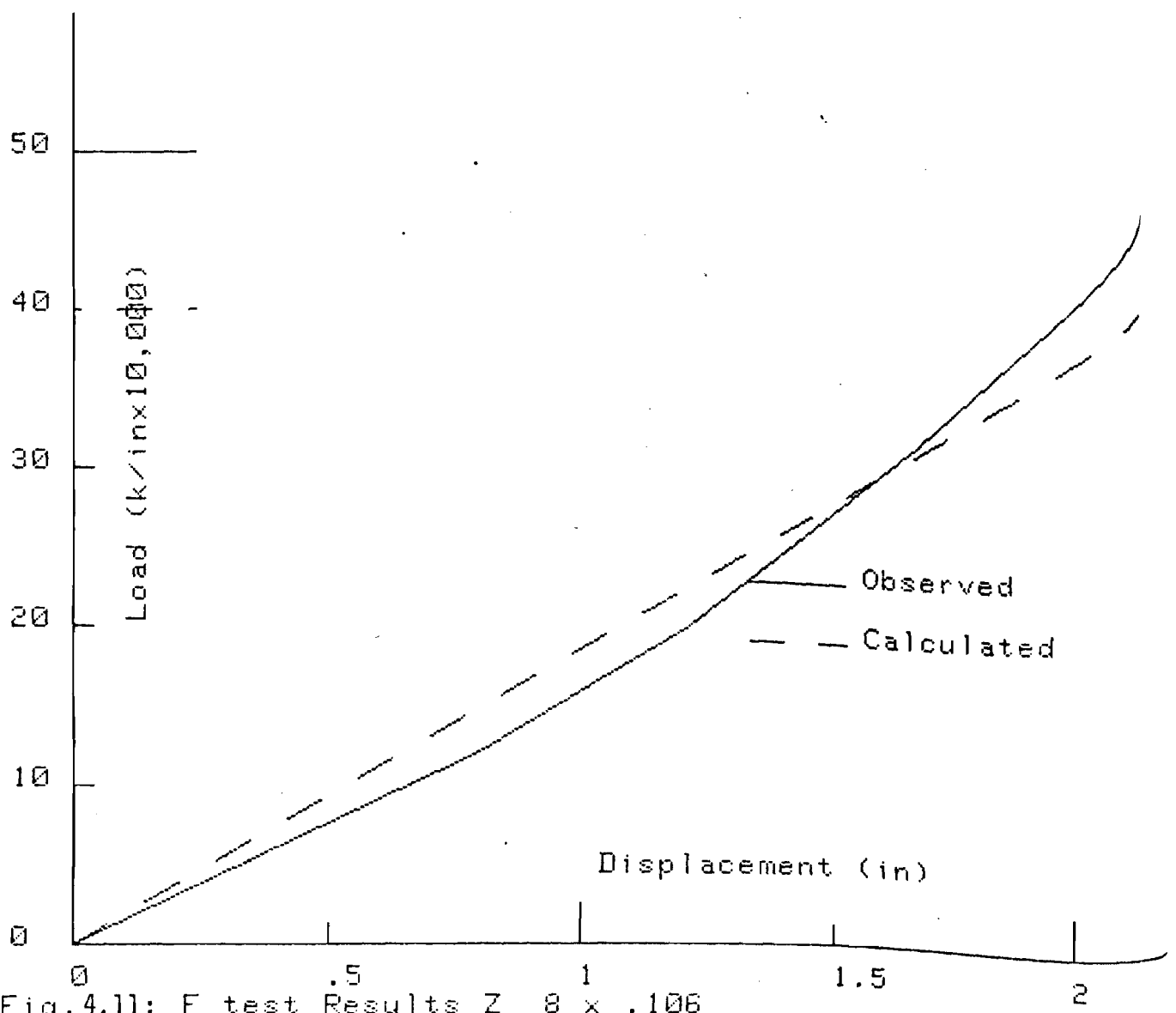


Fig.4.11: F test Results Z 8 x .106

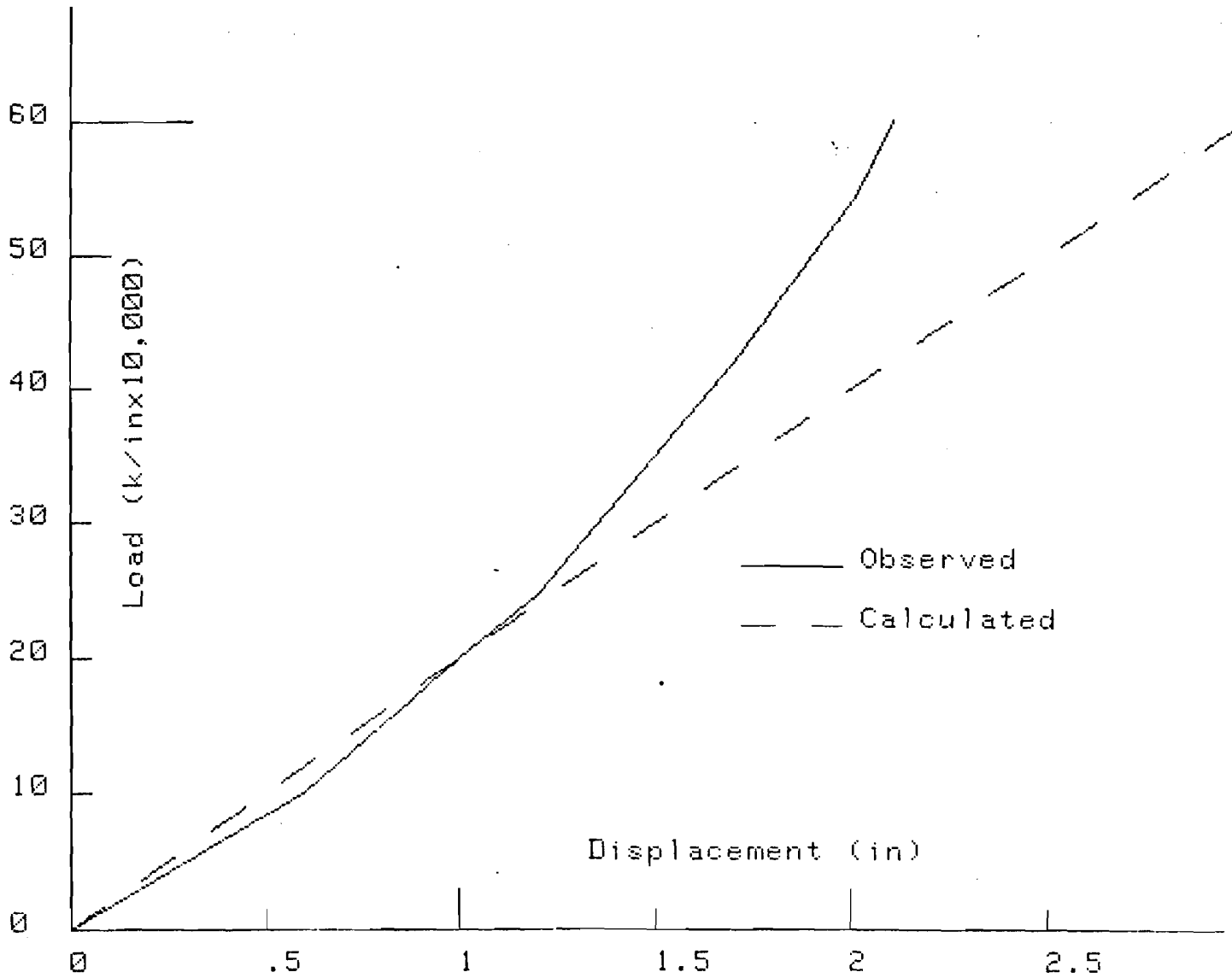


Fig. 4.12: F test Results Z 8 x .117

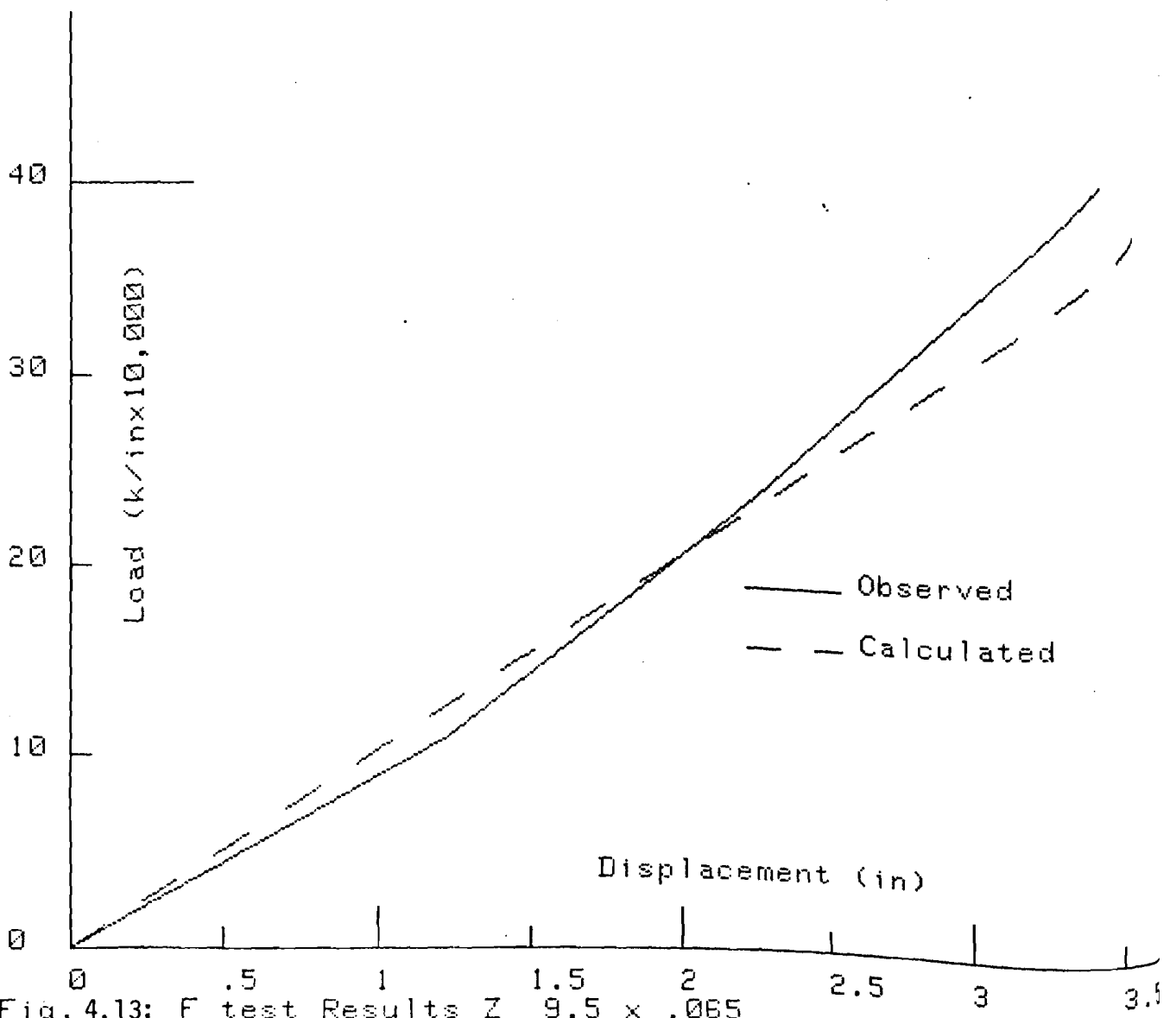


Fig. 4.13: F test Results Z $9.5 \times .065$

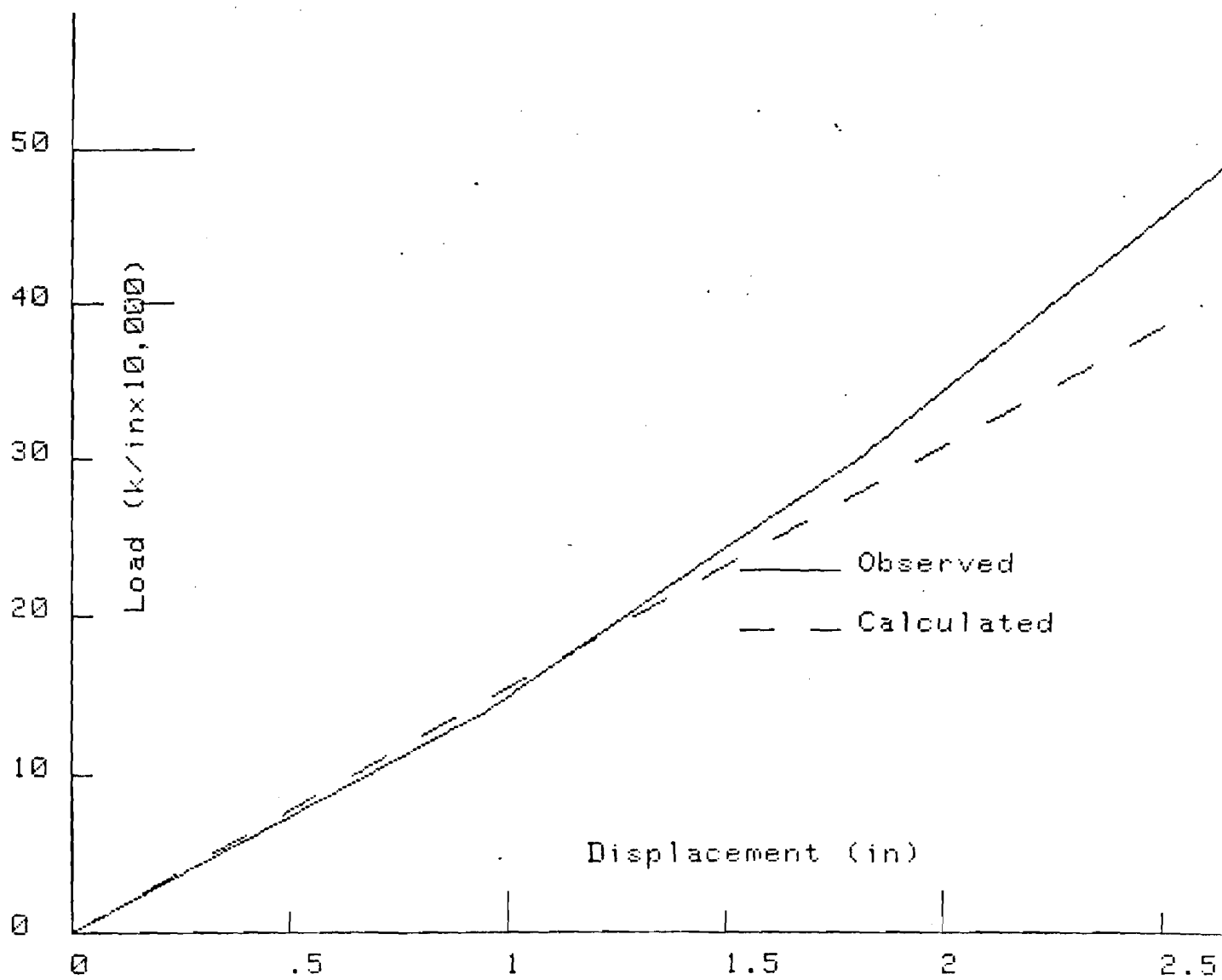


Fig. 4.14: F test Results Z 9.5×10^7

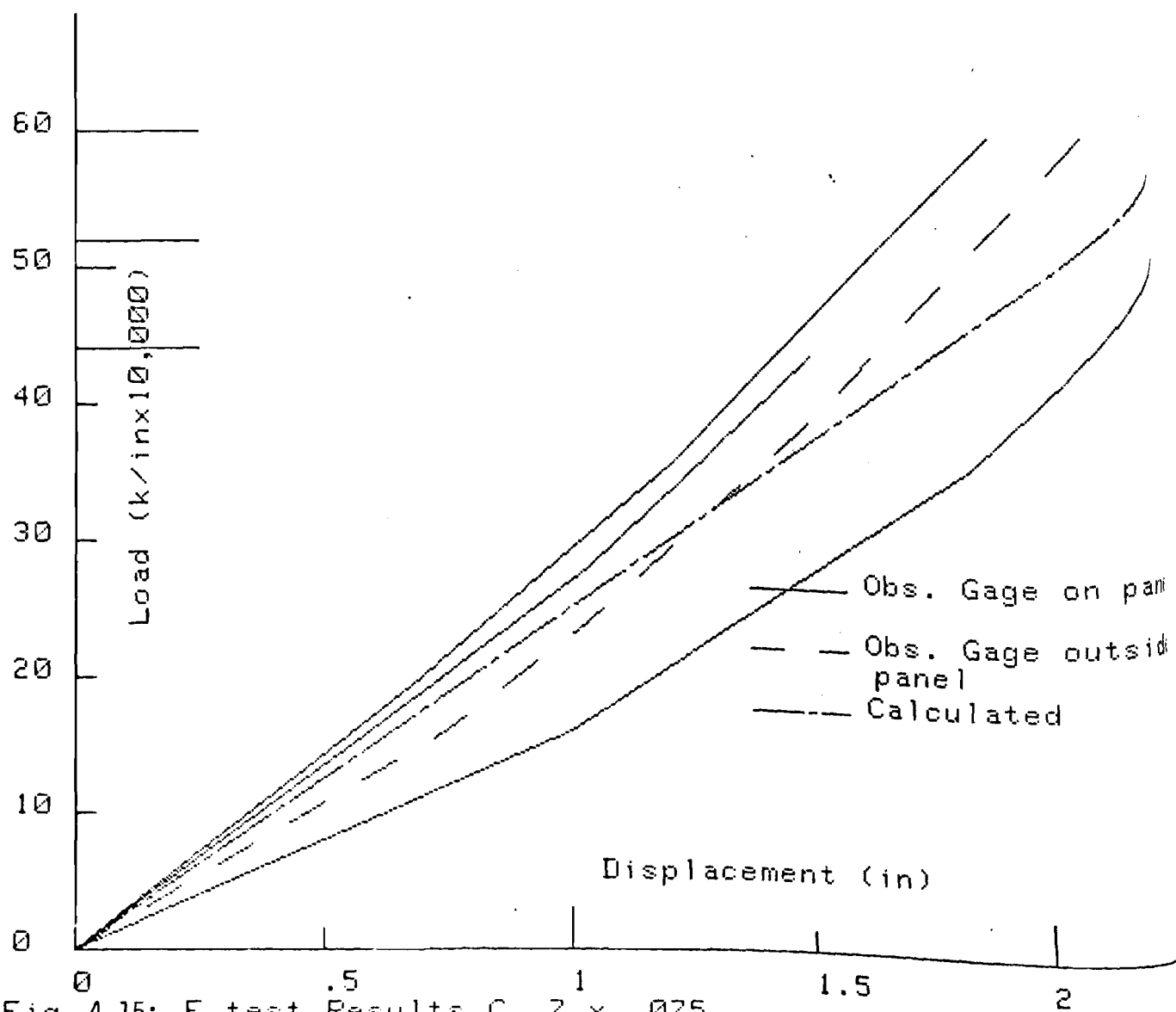


Fig. 4.15: F test Results C 7 x .075

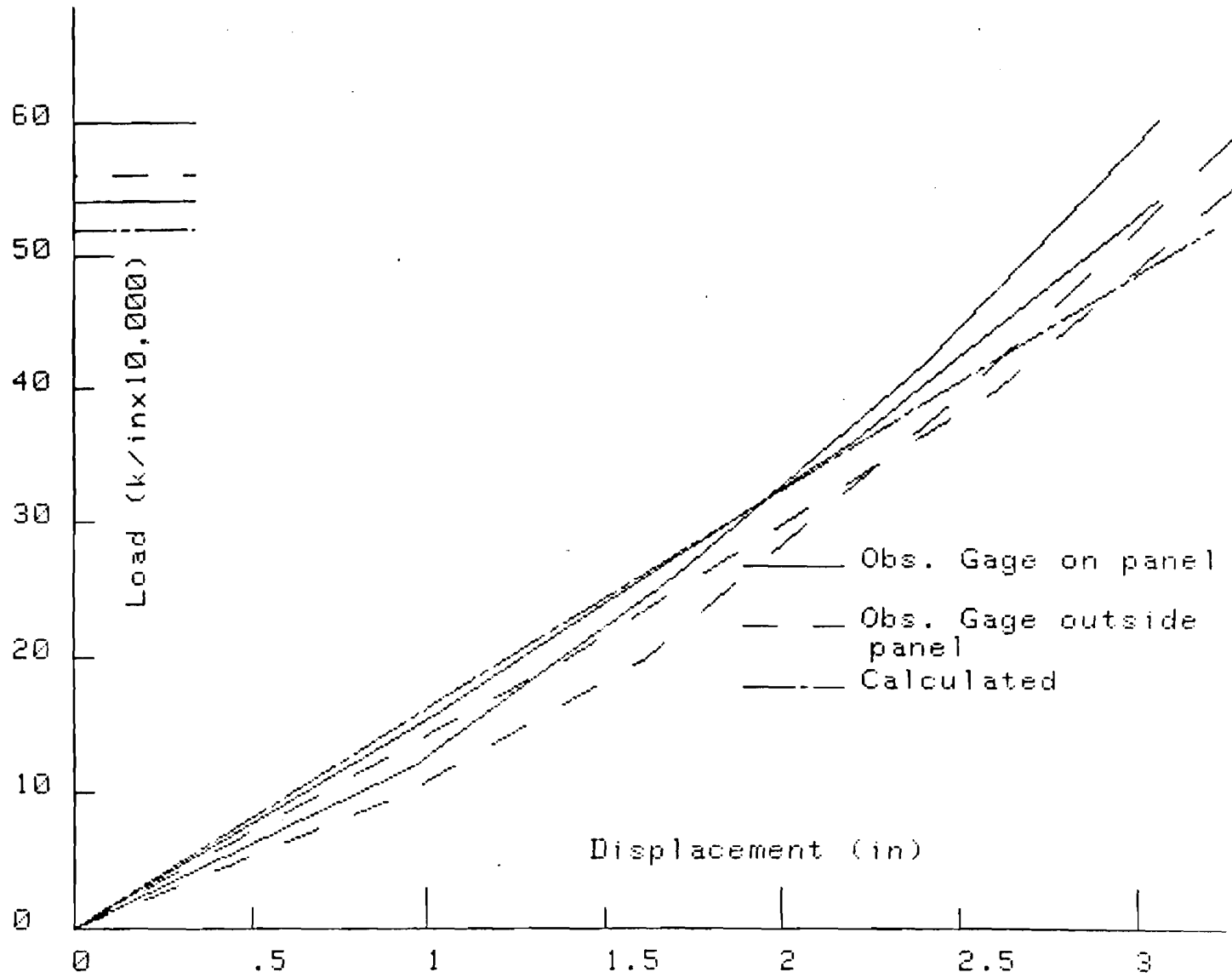


Fig. 4.16: F test Results C 9 x .075

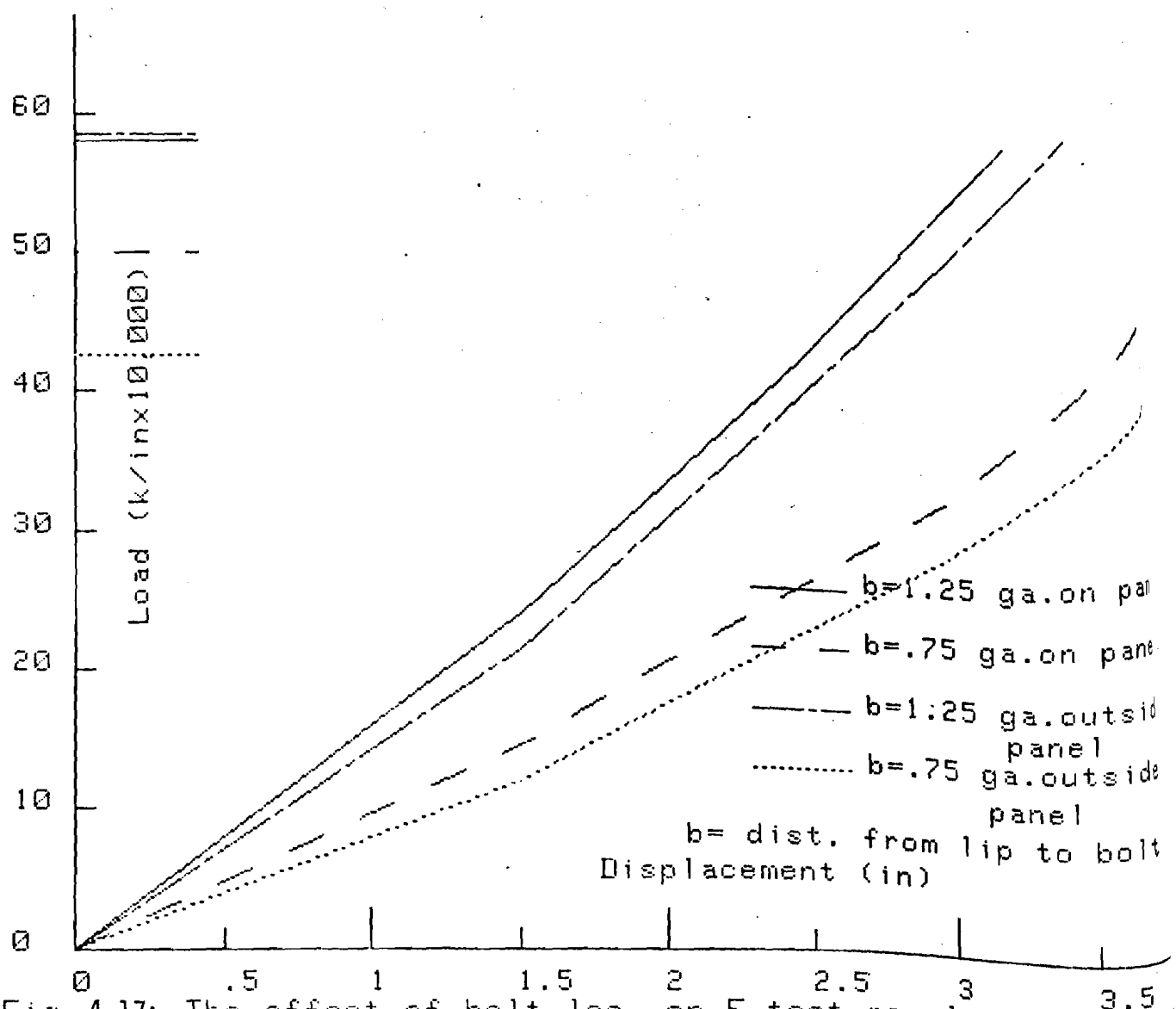


Fig. 4.17: The effect of bolt loc. on F test results $C_g \times .07$

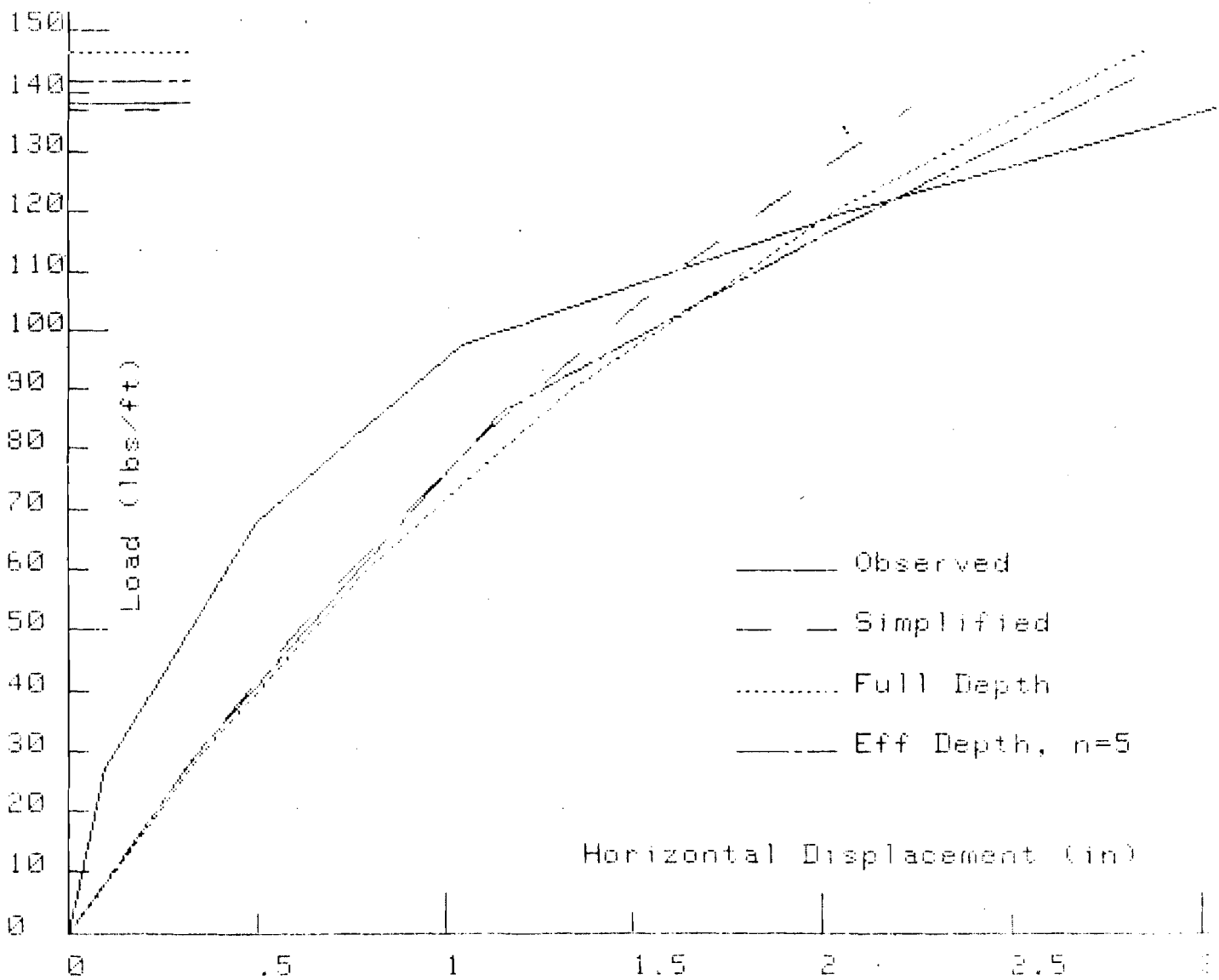


Fig. 5.1: Load vs. Displ. for Section Z $8 \times .075 \times .25$

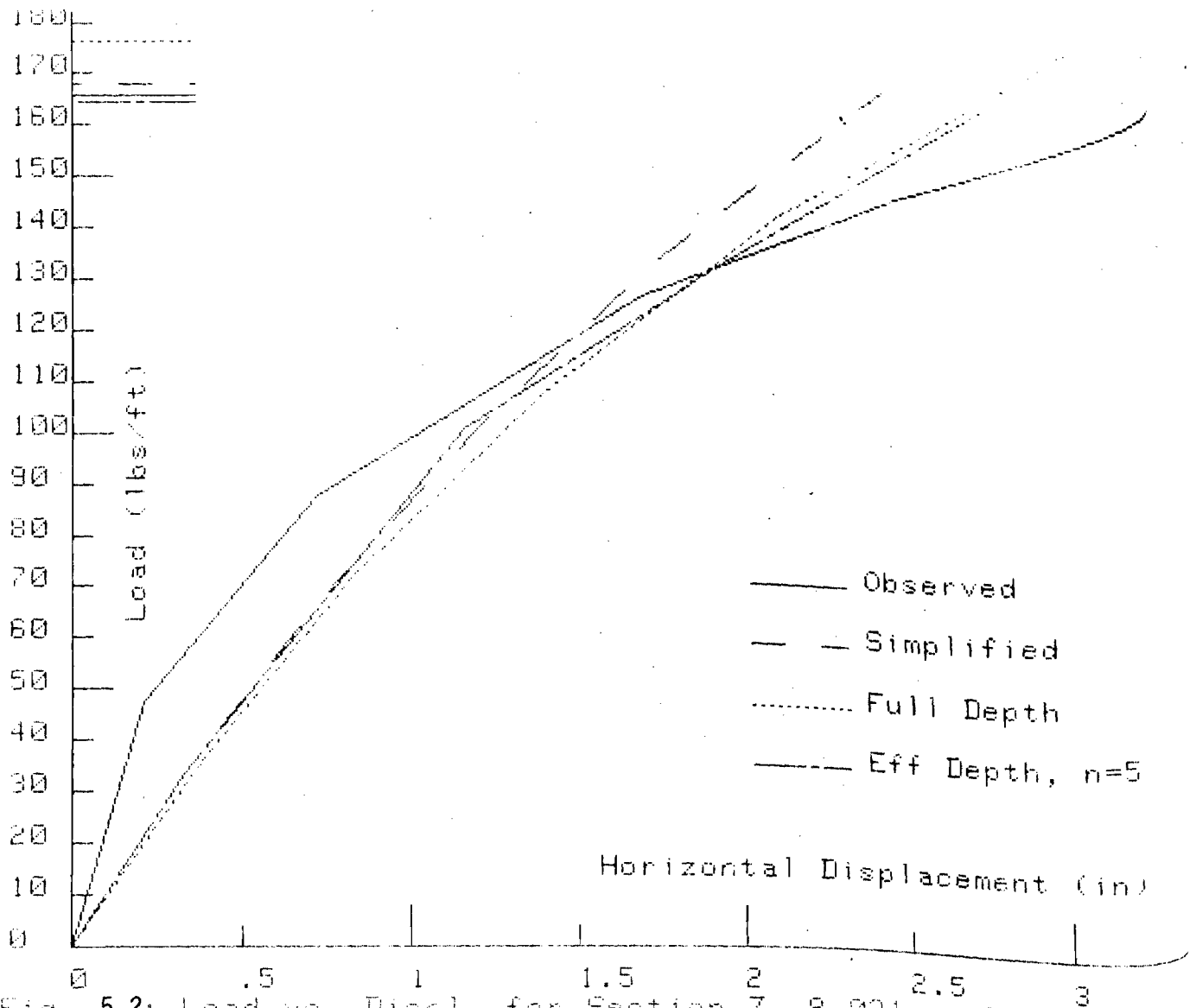


Fig. 5.2: Load vs. Displ. for Section Z $8.031 \times .088 \times .25$

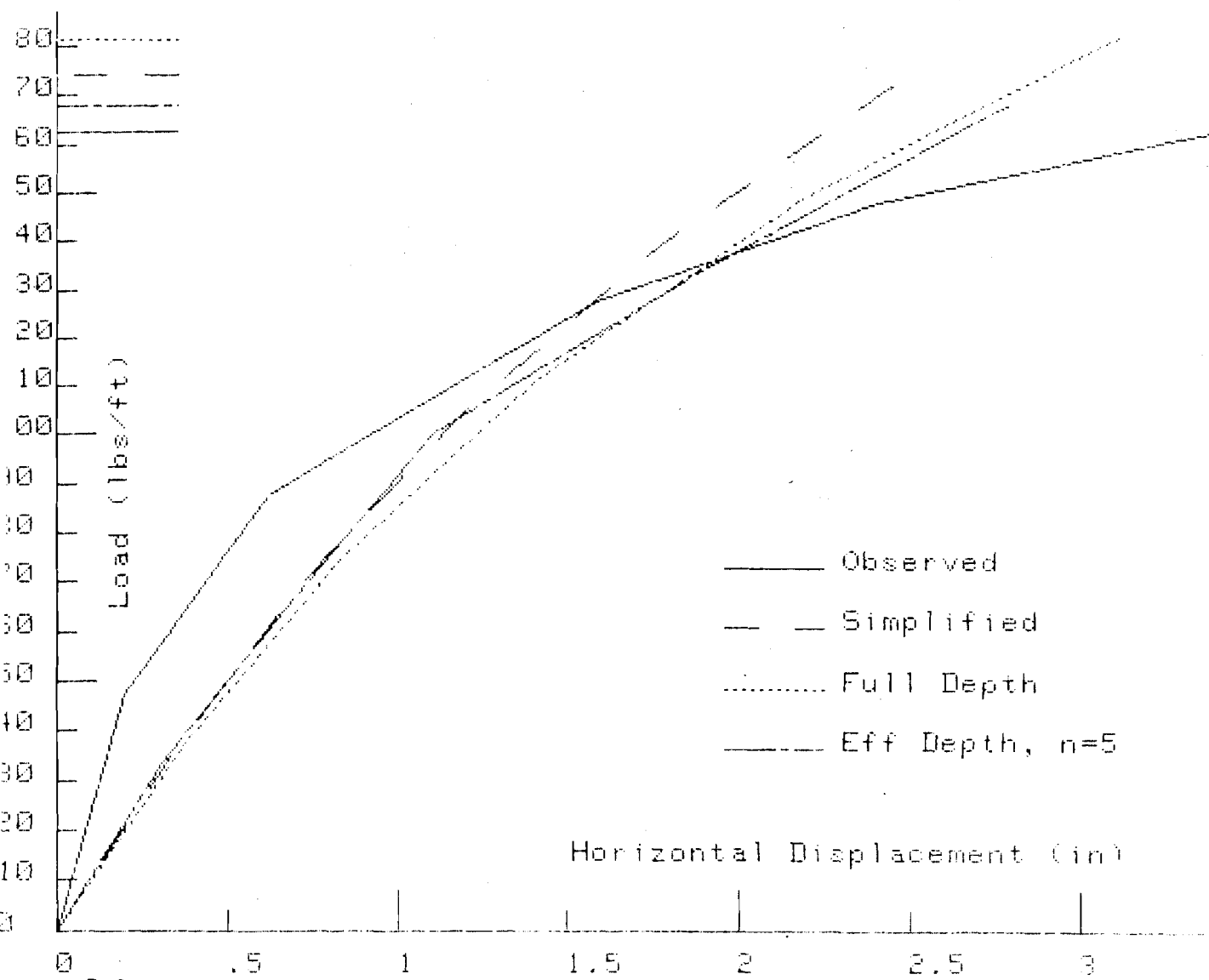


Fig. 5.3: Load vs. Displ. for Section Z $8 \times .089 \times 8$

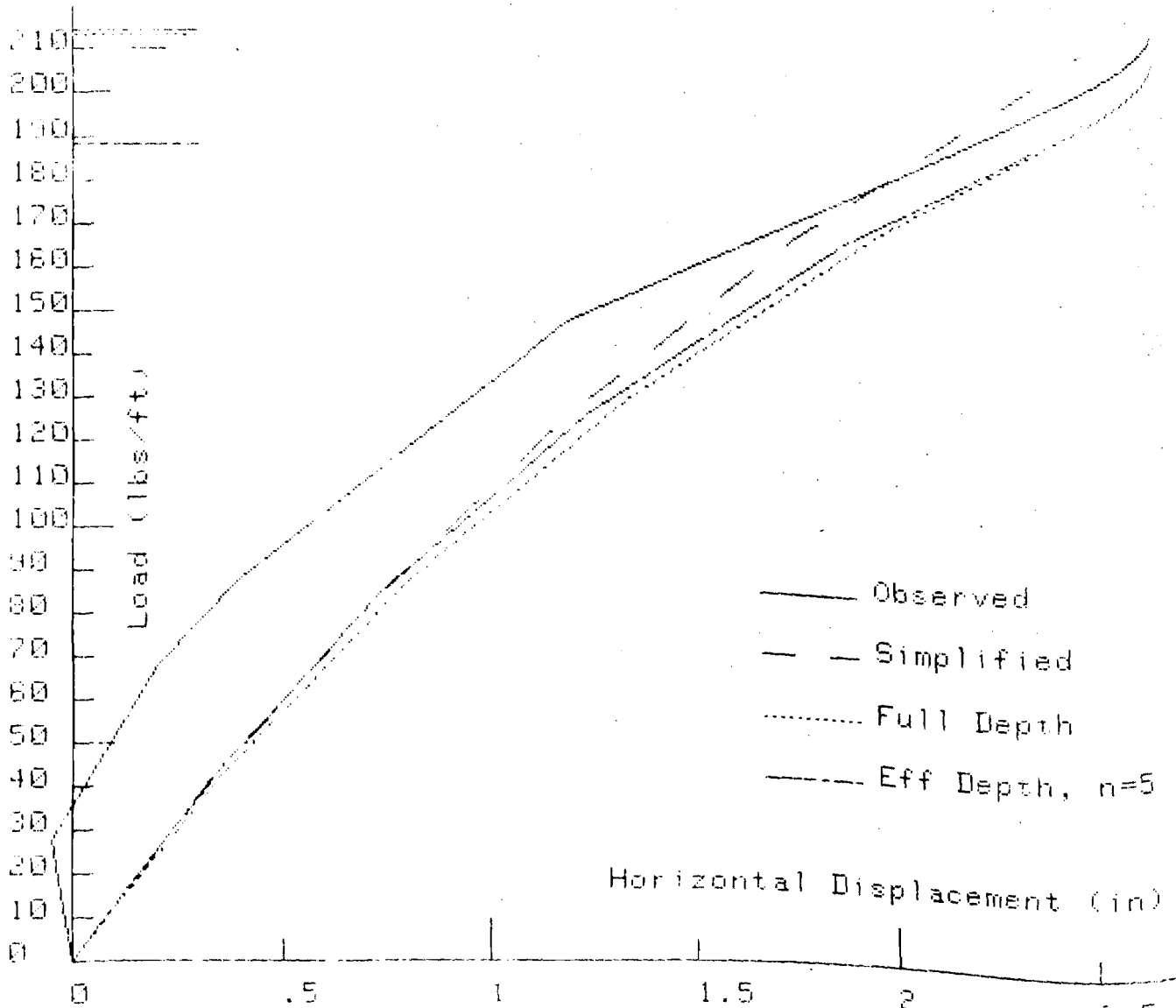


Fig. 5.4: Load vs. Displ. for Section Z $7.94 \times .114 \times .25$

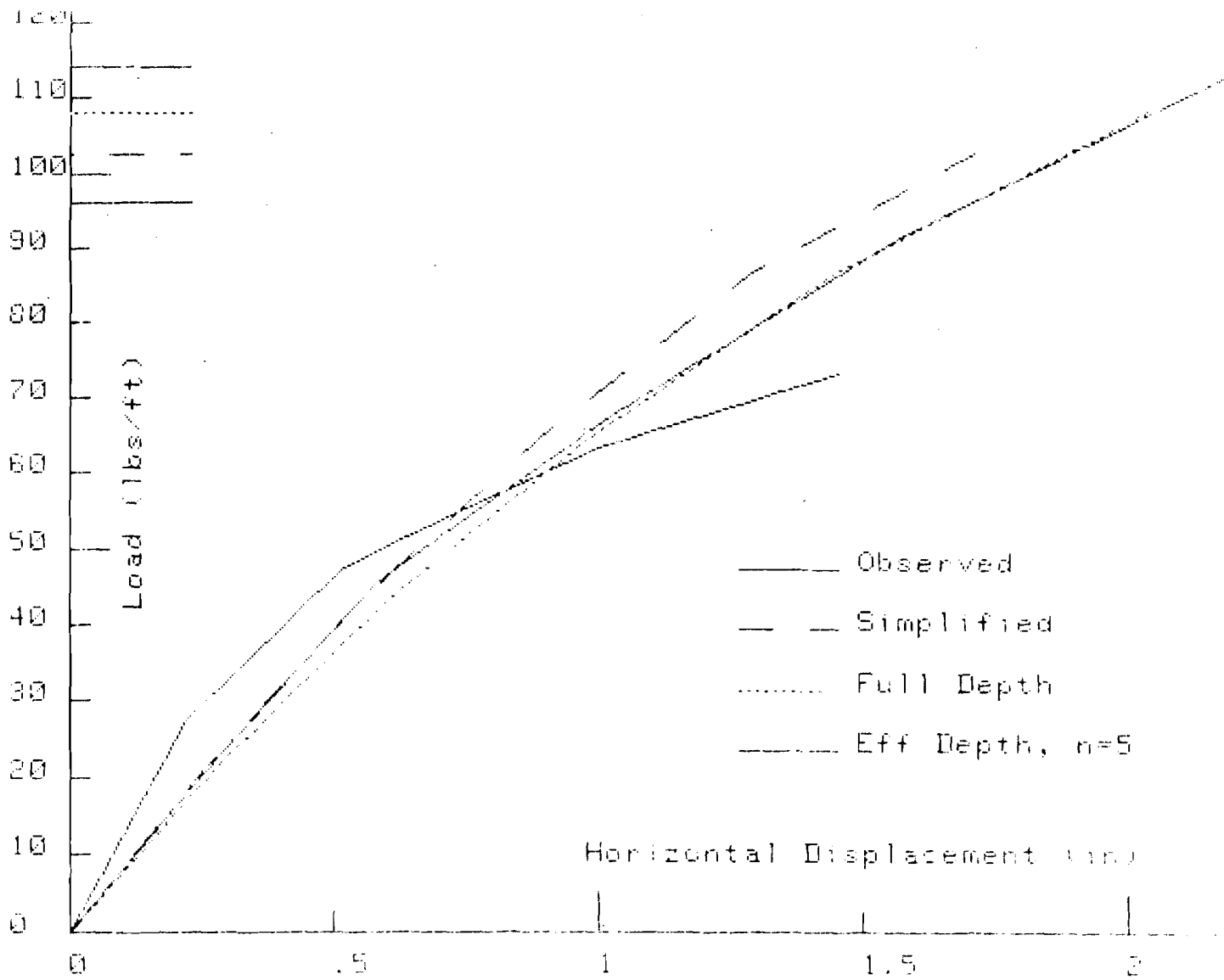


Fig. 5.5: Load vs. Displ. for Section Z $8.055 \times 10^3 \times .25$

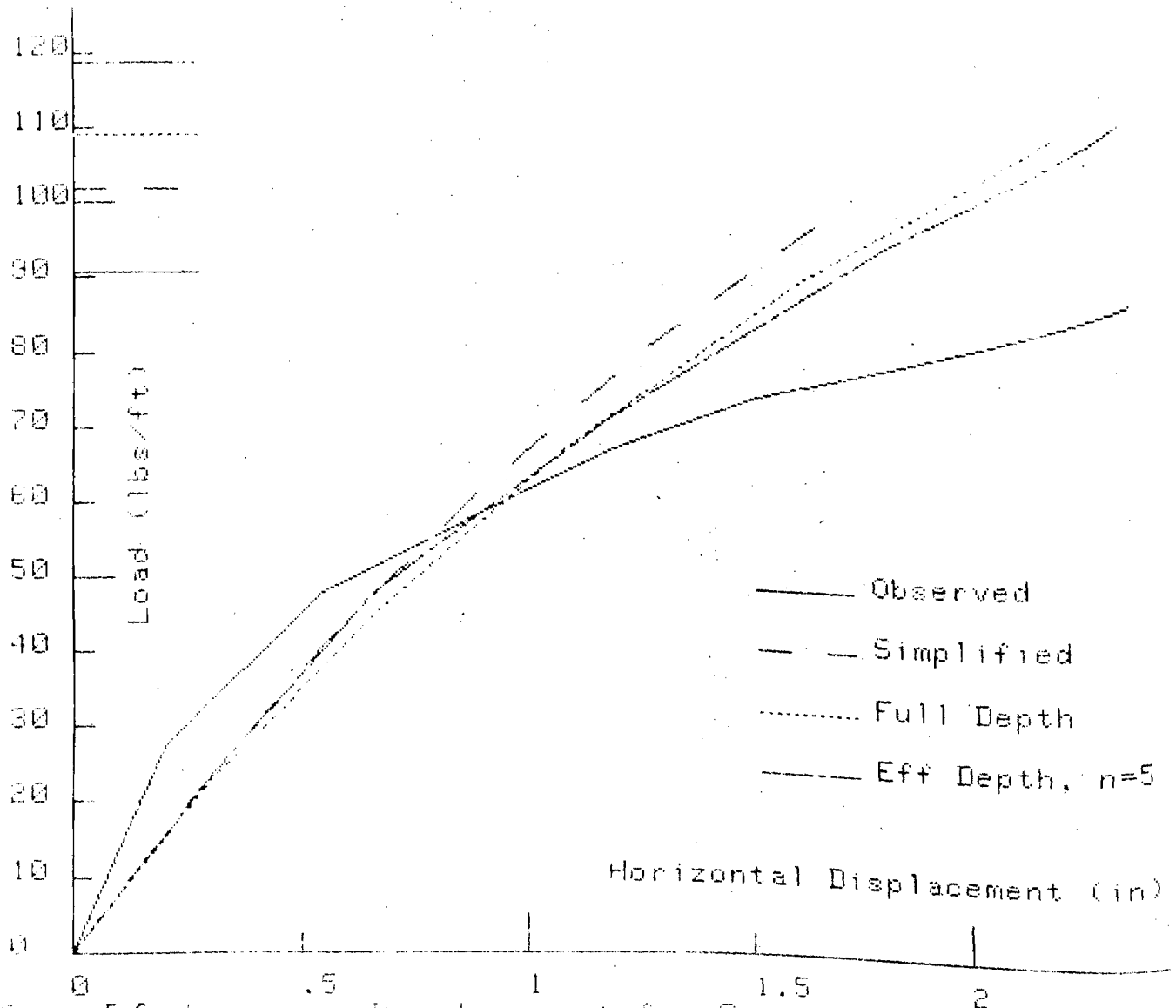


Fig. 5.6. Load vs. Displacement for Section Z $8 \times .059 \times .$

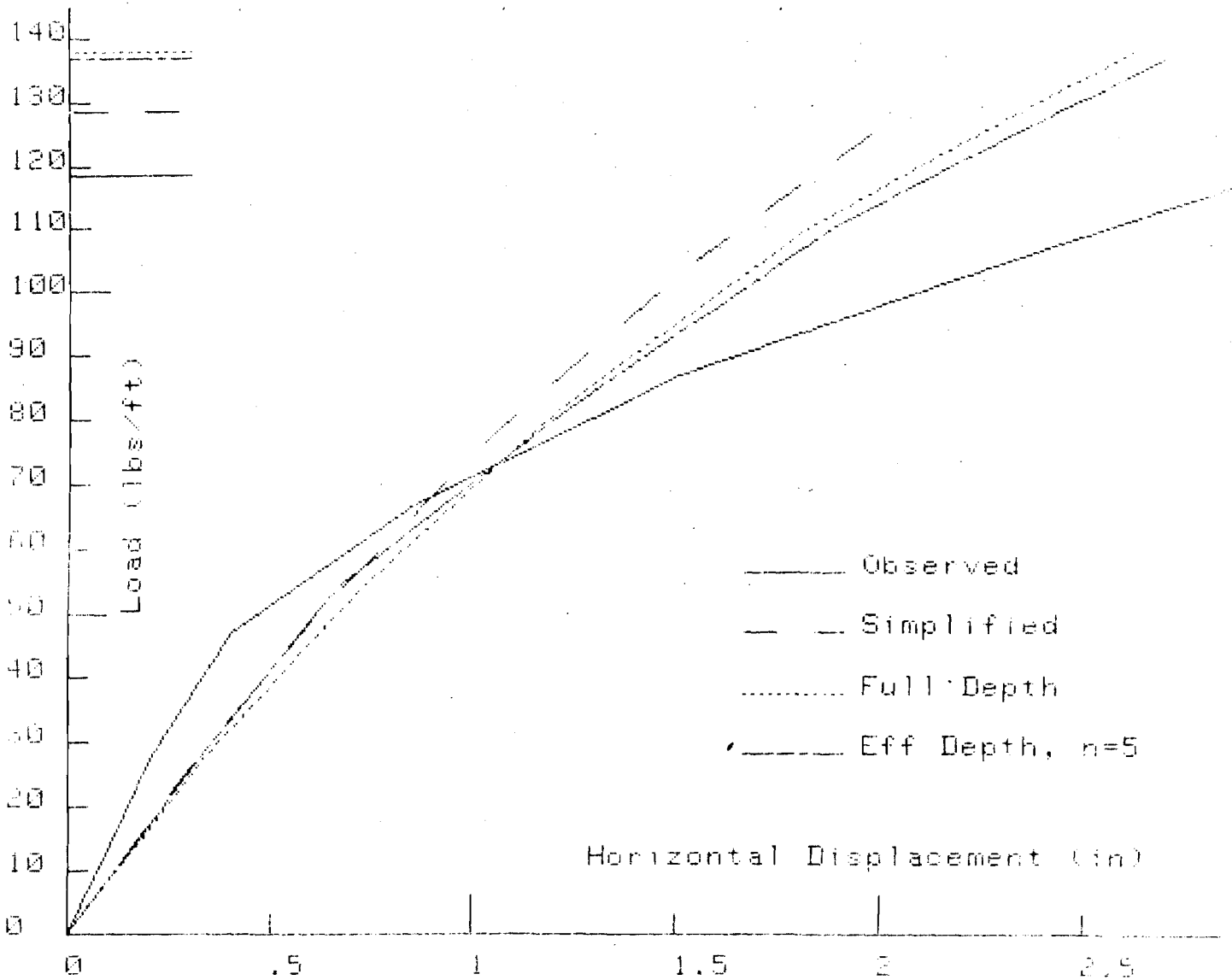


Fig. 5.7: Load vs. Displ. for Section Z $7.97 \times .07 \times .25$

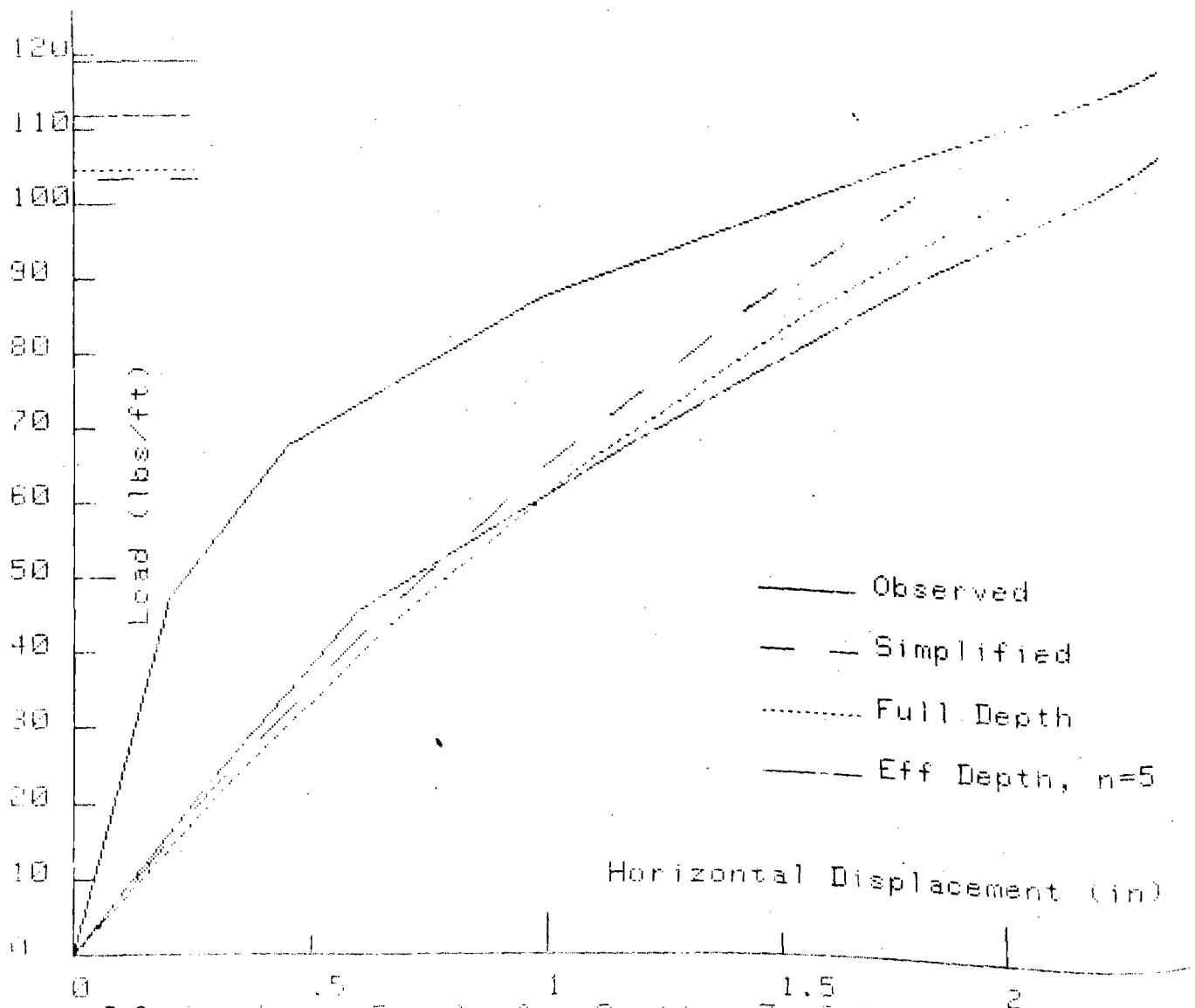


Fig. 5.8: Load vs. Displ. for Section Z $9.625 \times .062 \times .125$

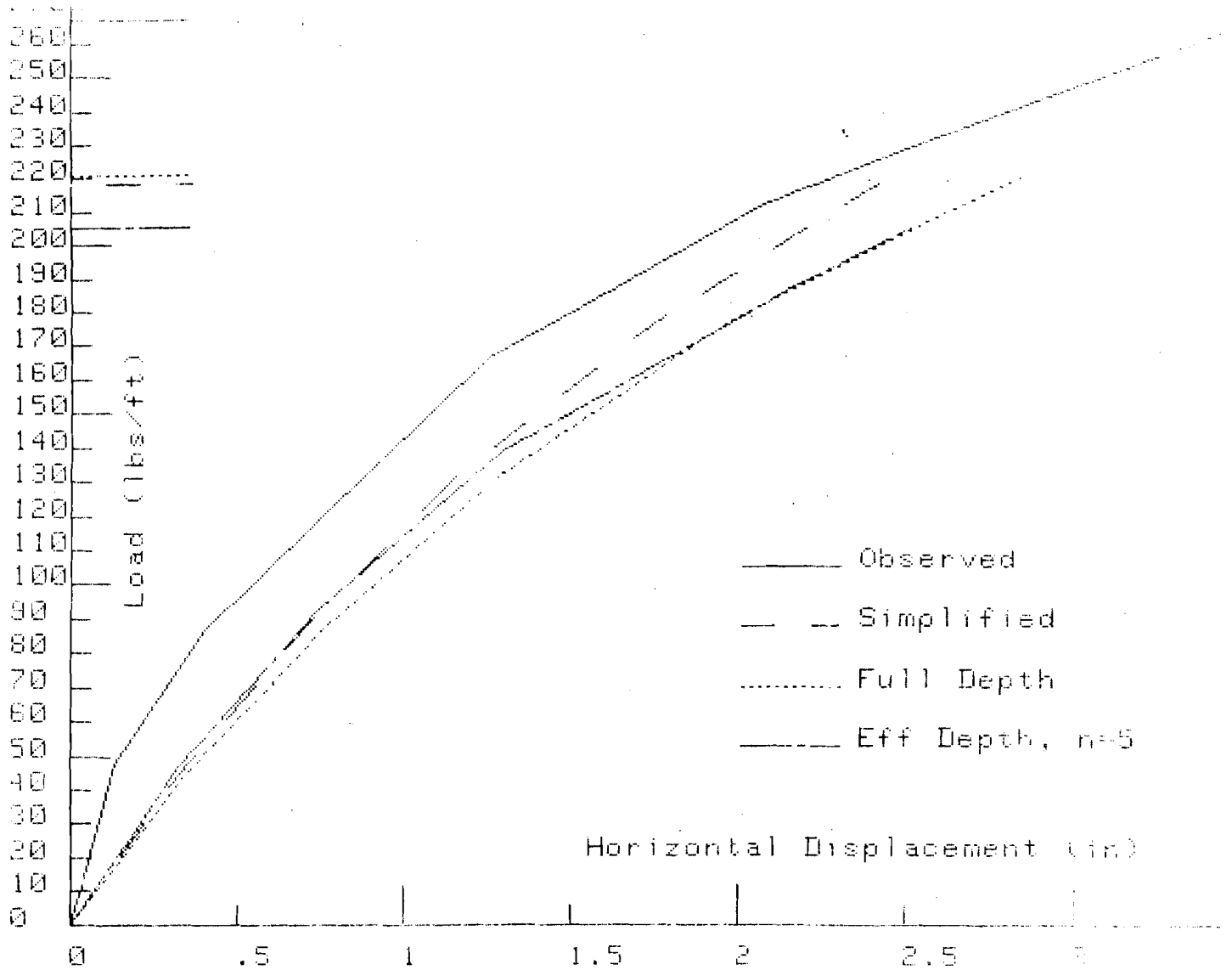
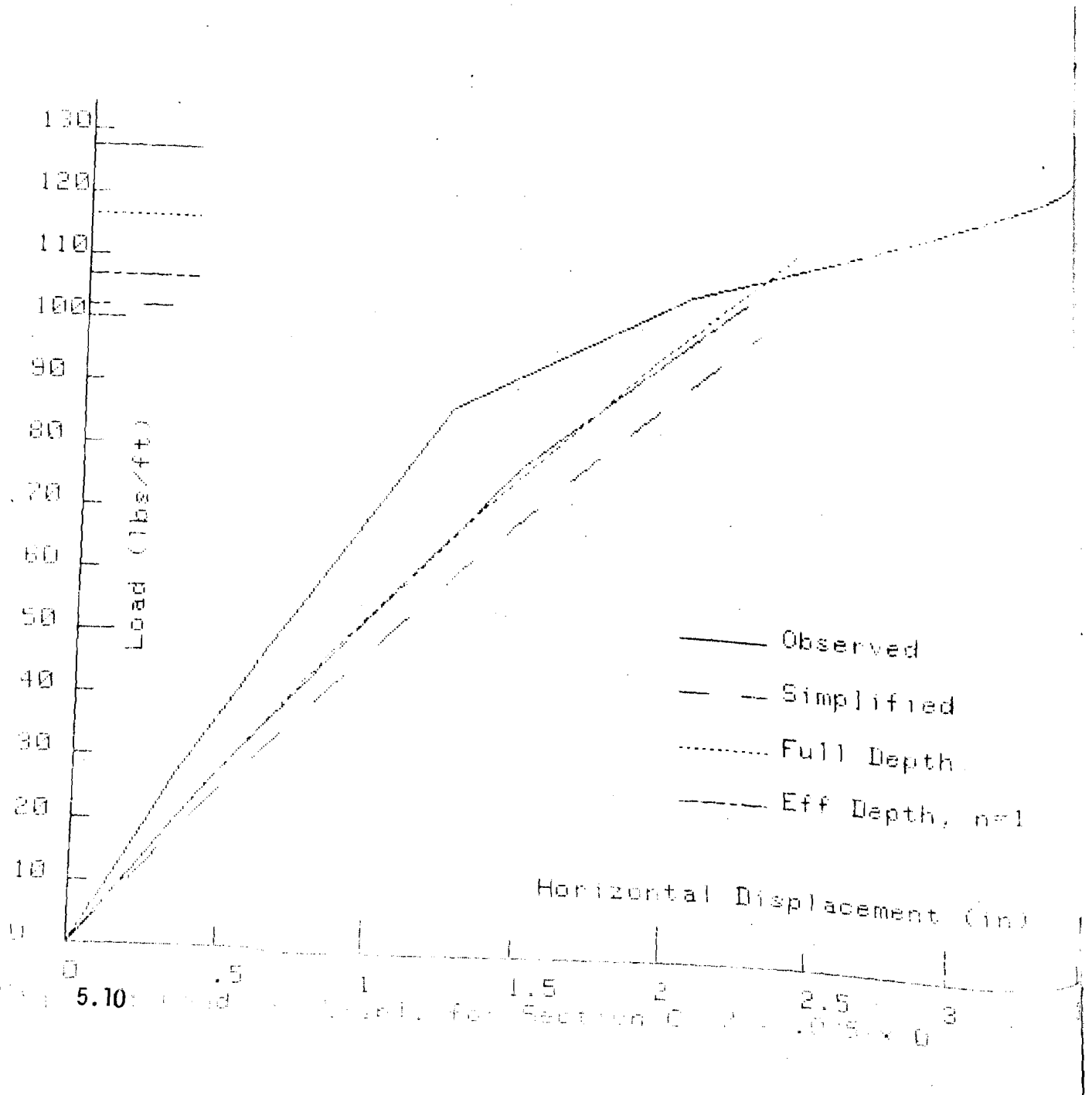


Fig. 5.9: Load vs. Displ. for Section Z $9.578 \times .100 \times .063$



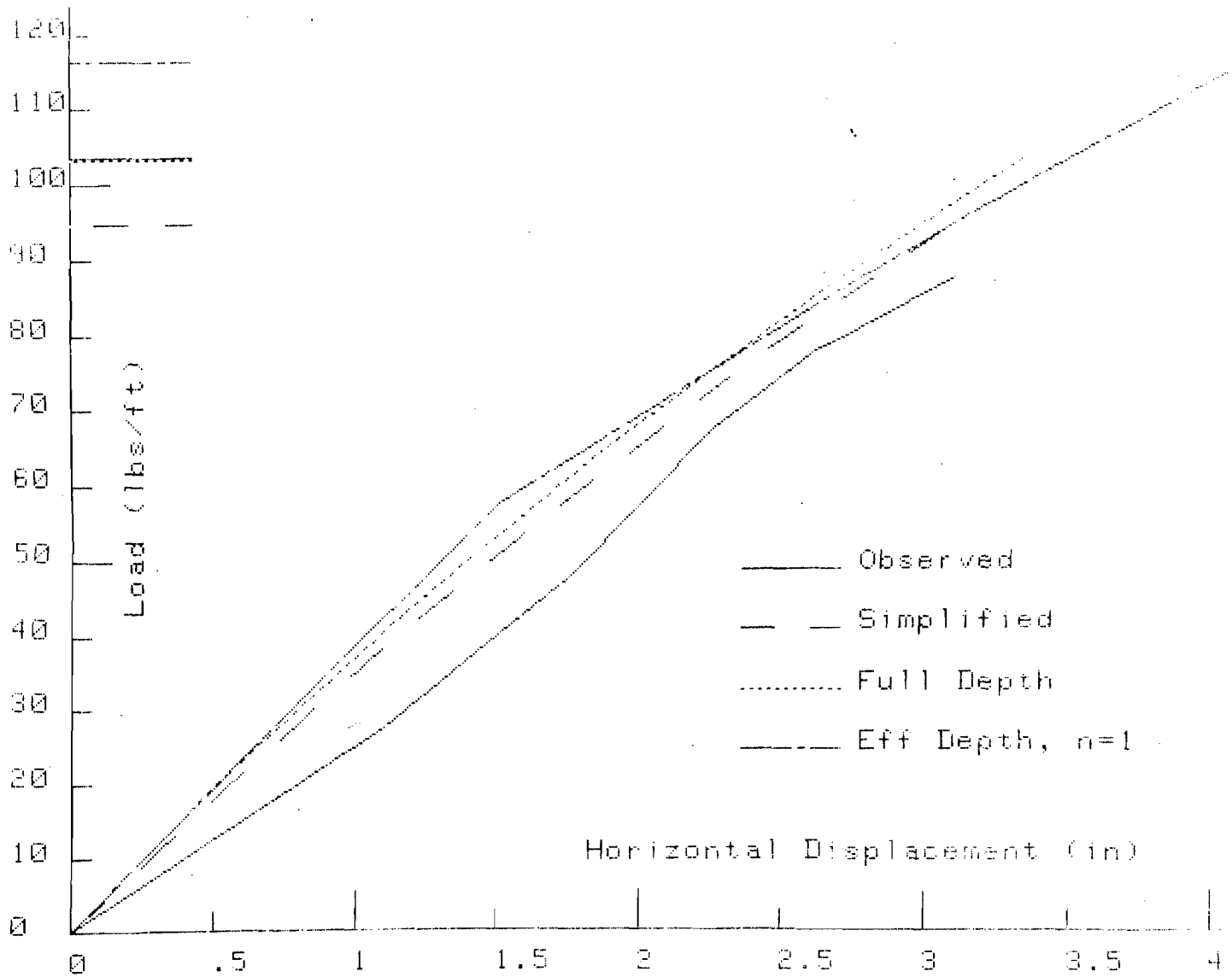


Fig. 5.11: Load vs. Displ. for Section C $9 \times .077 \times 1$

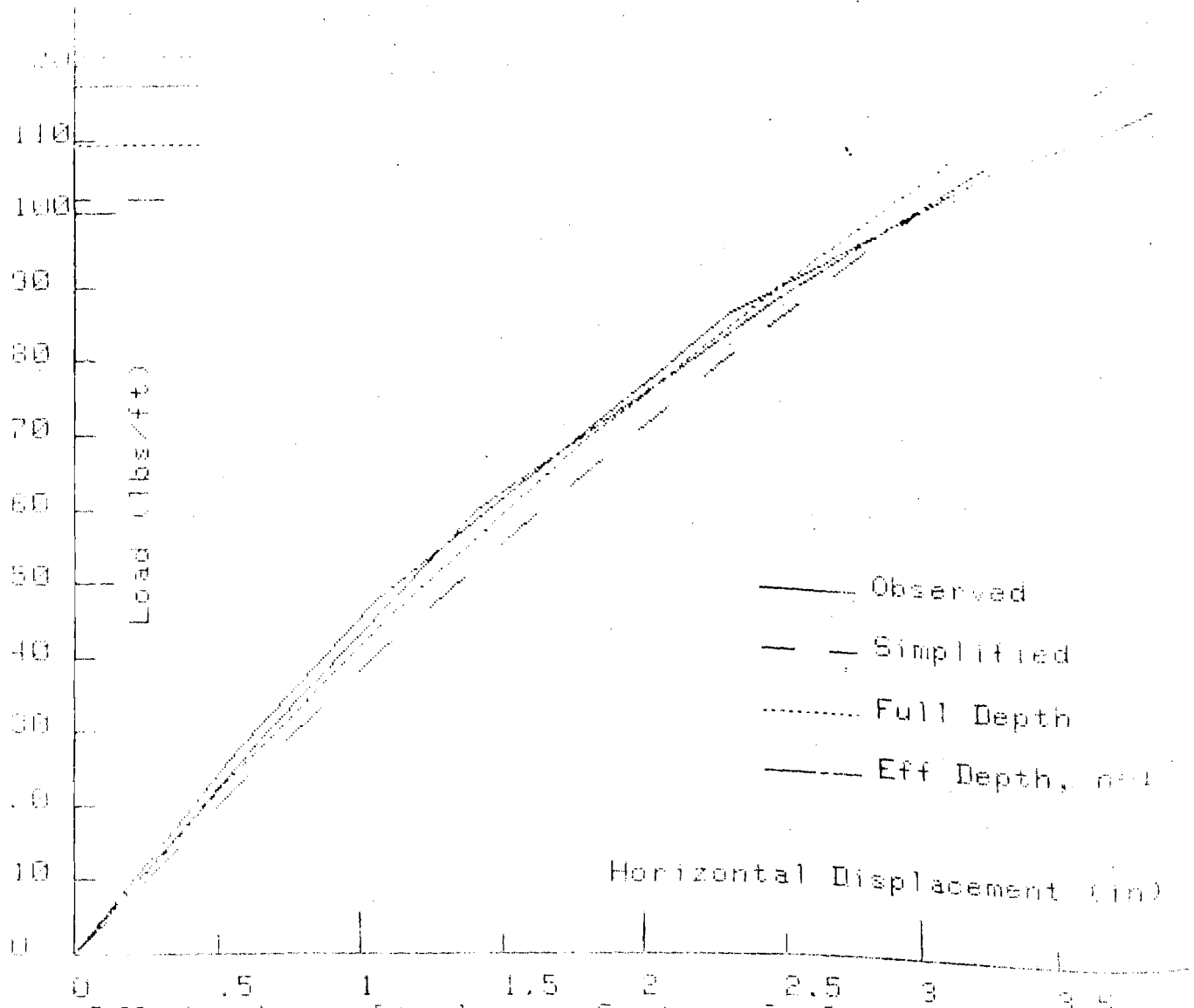


Fig. 5.12: Load vs. Displ. for Section C 9 x .075 x .25

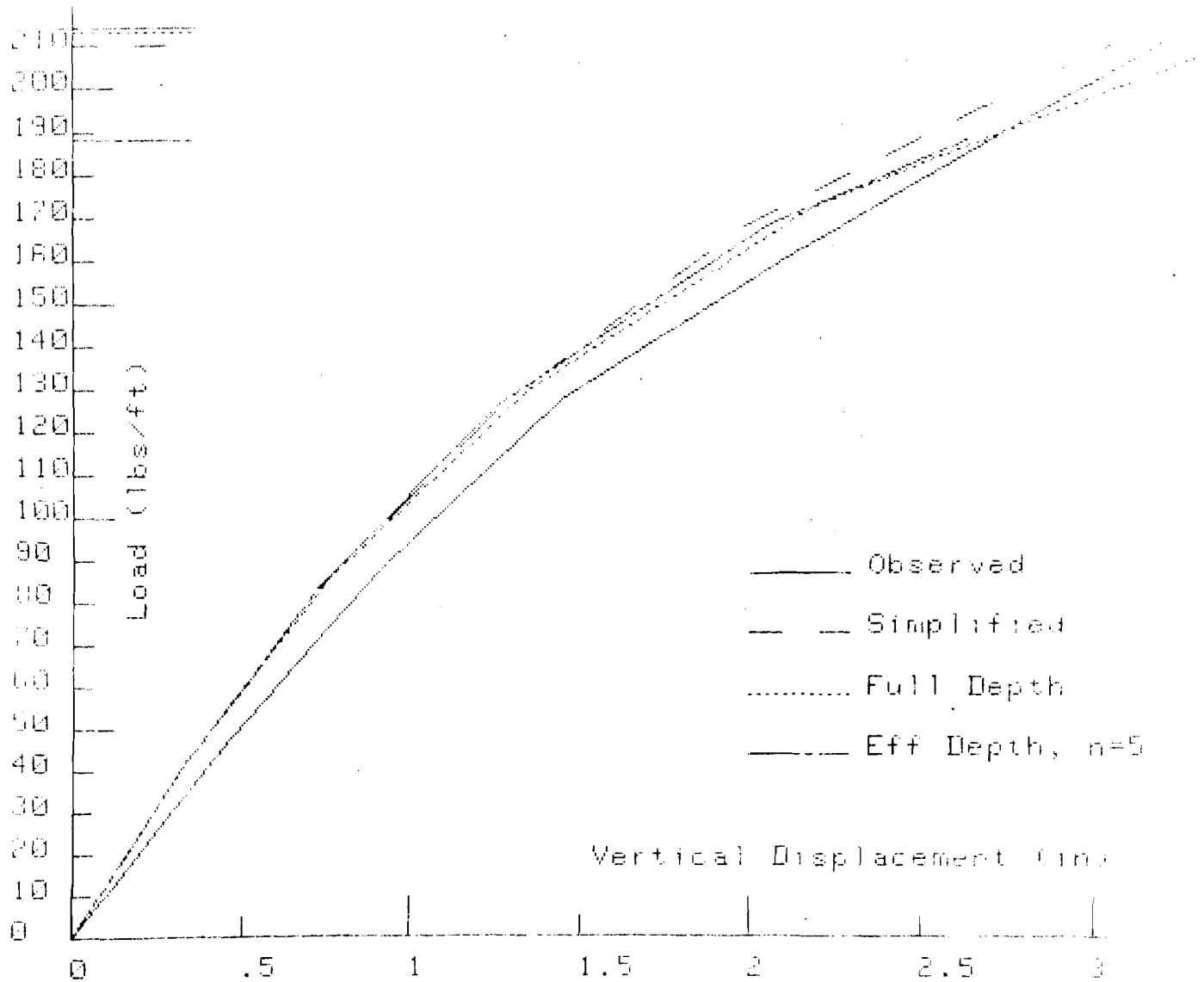


Fig. 5.13: Load vs. Displ. for Section Z $7.94 \times 10^{-4} \times 1.25$

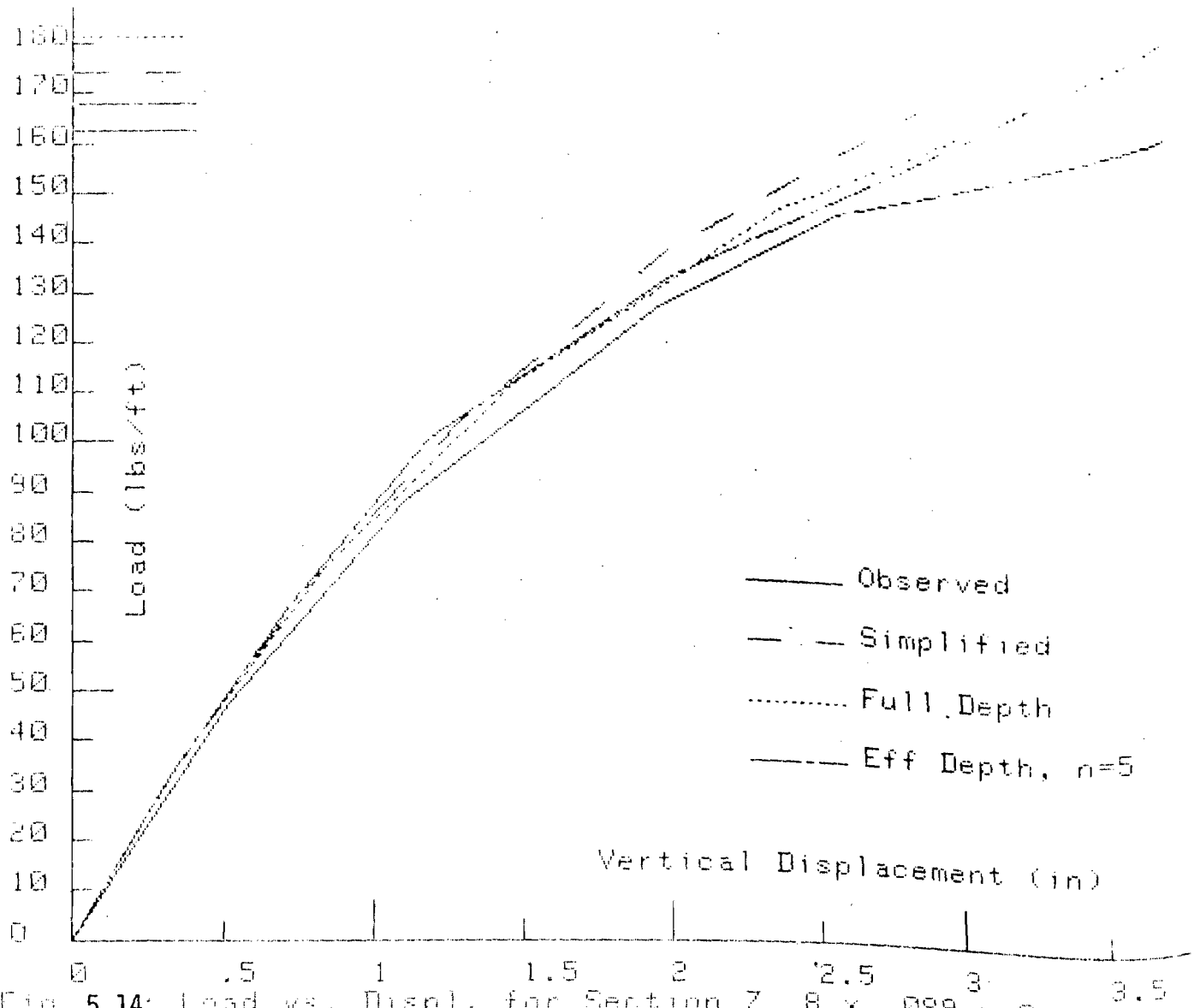


Fig. 5.14: Load vs. Displ. for Section Z 8 x .089 x 0

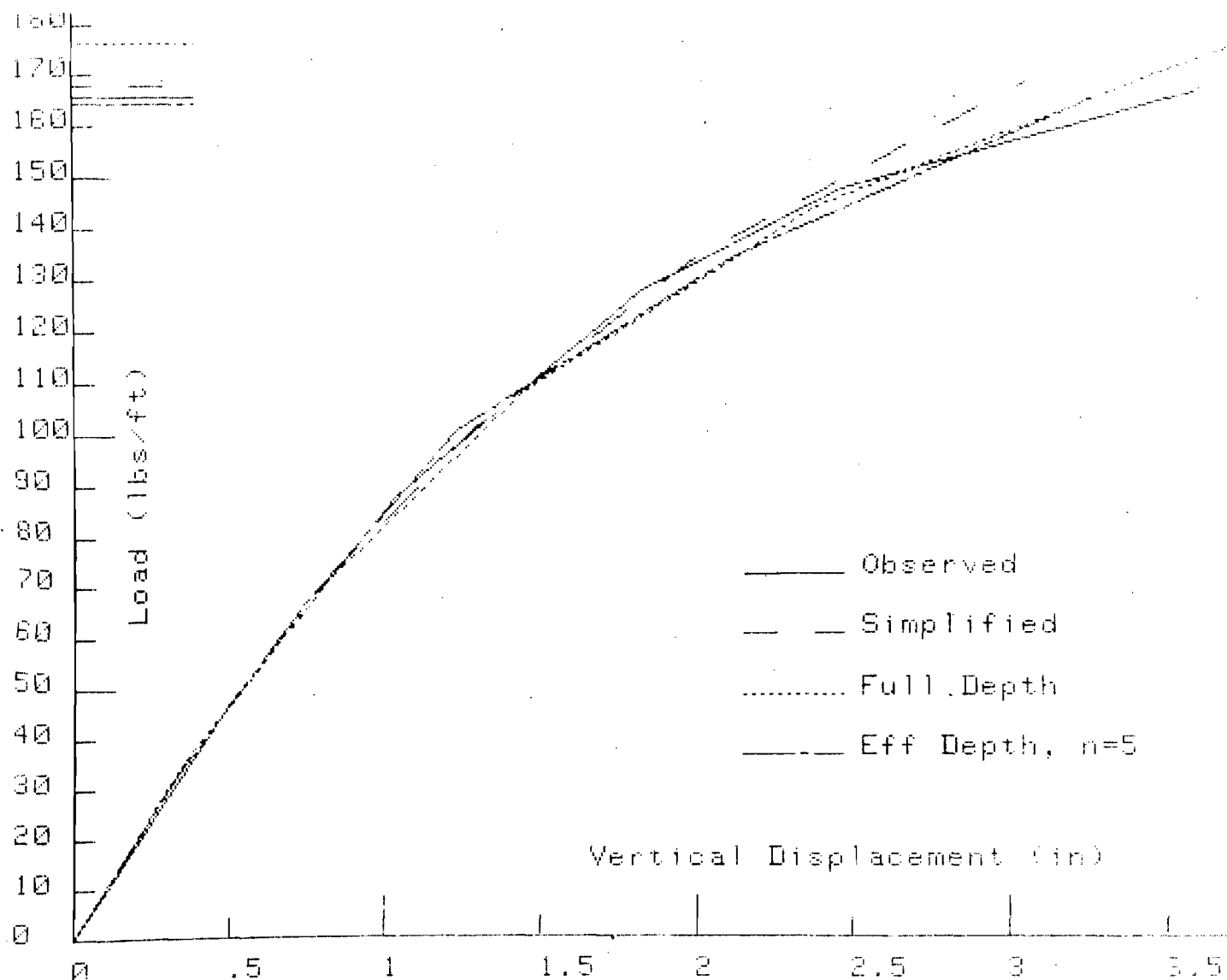
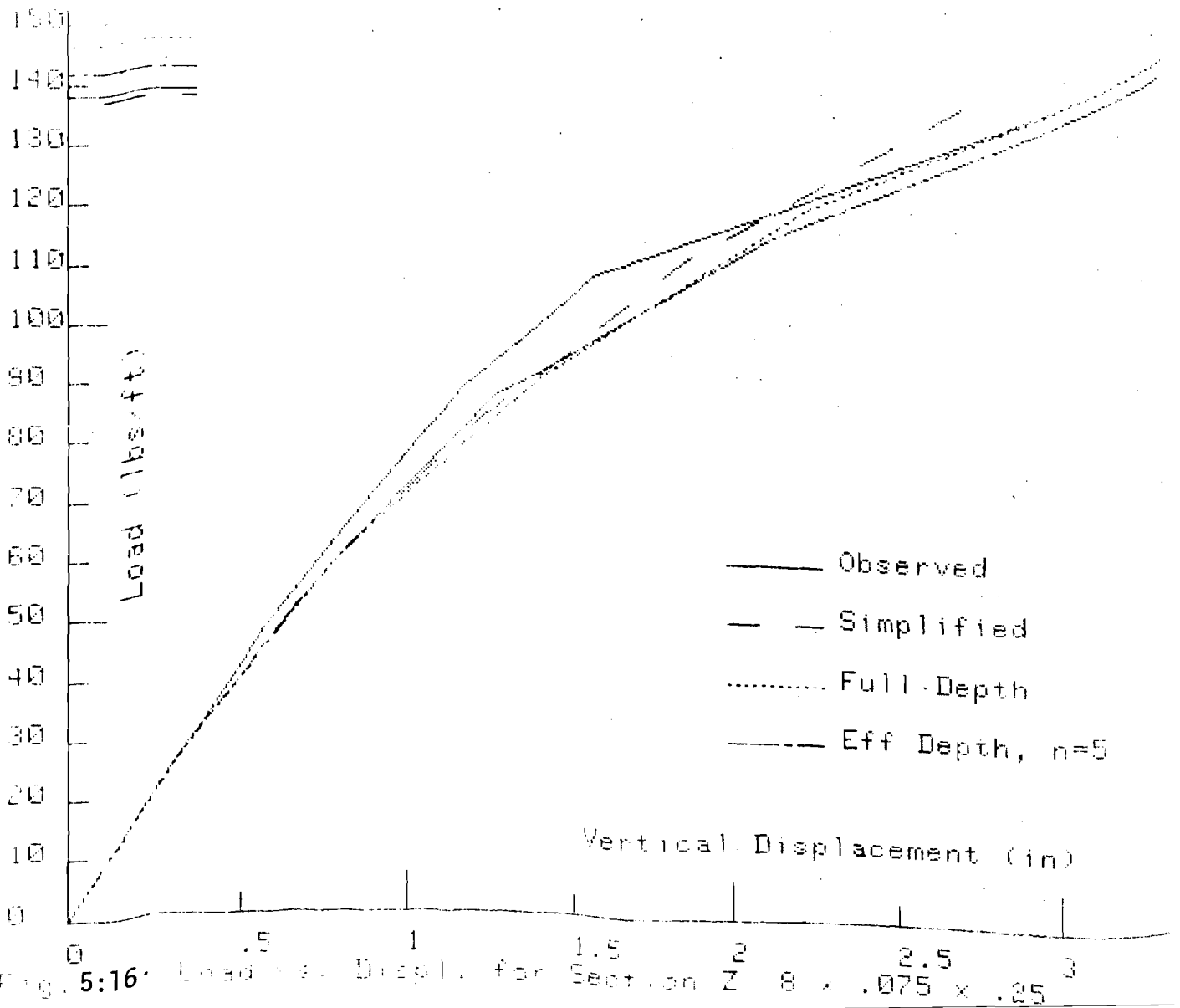


Fig. 5:15: Load vs. Displ. for Section Z 8.051 x .088 x .25



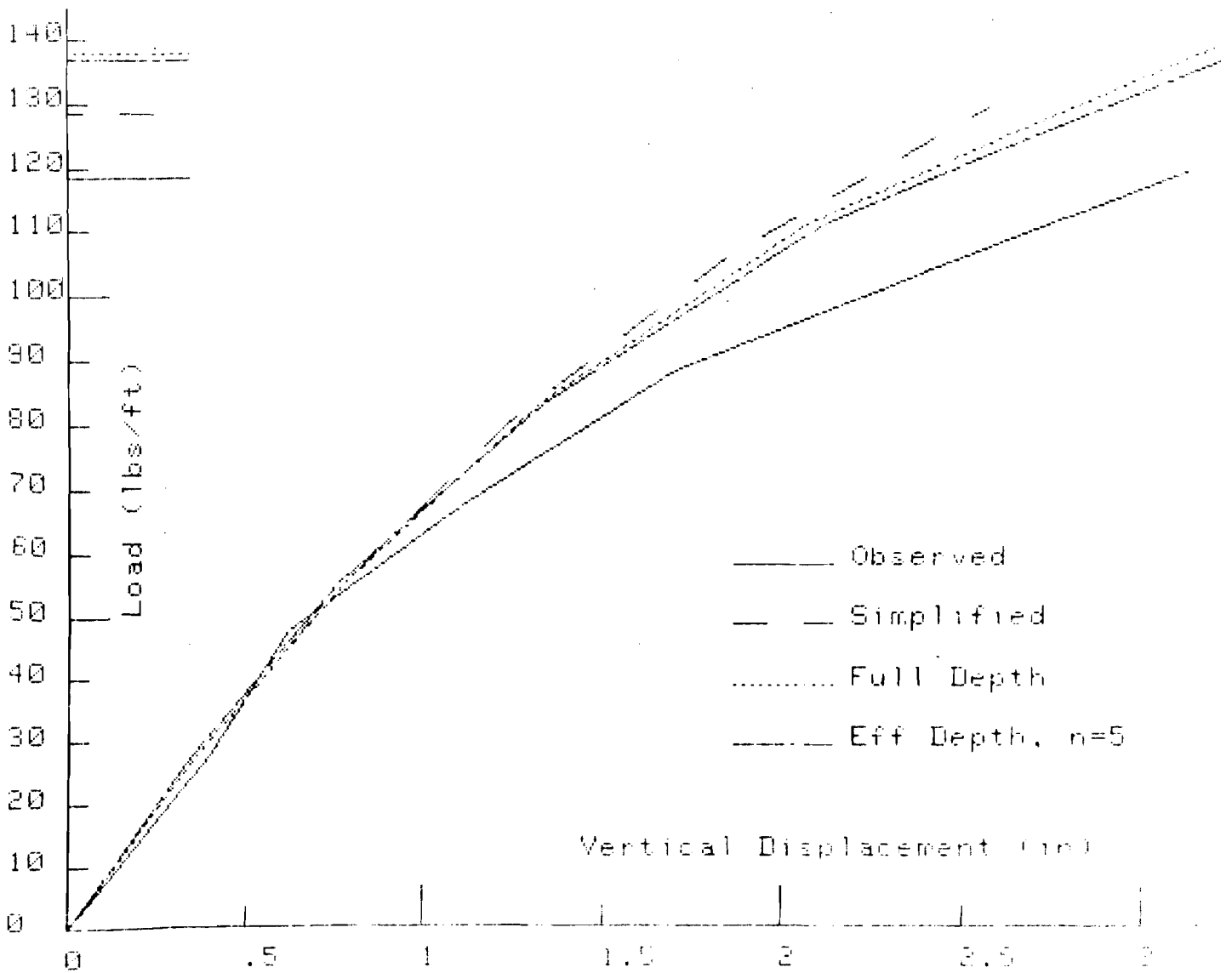


Fig. 5.17: Load vs. Displ. for Section Z 7.90×10^7 in-lb

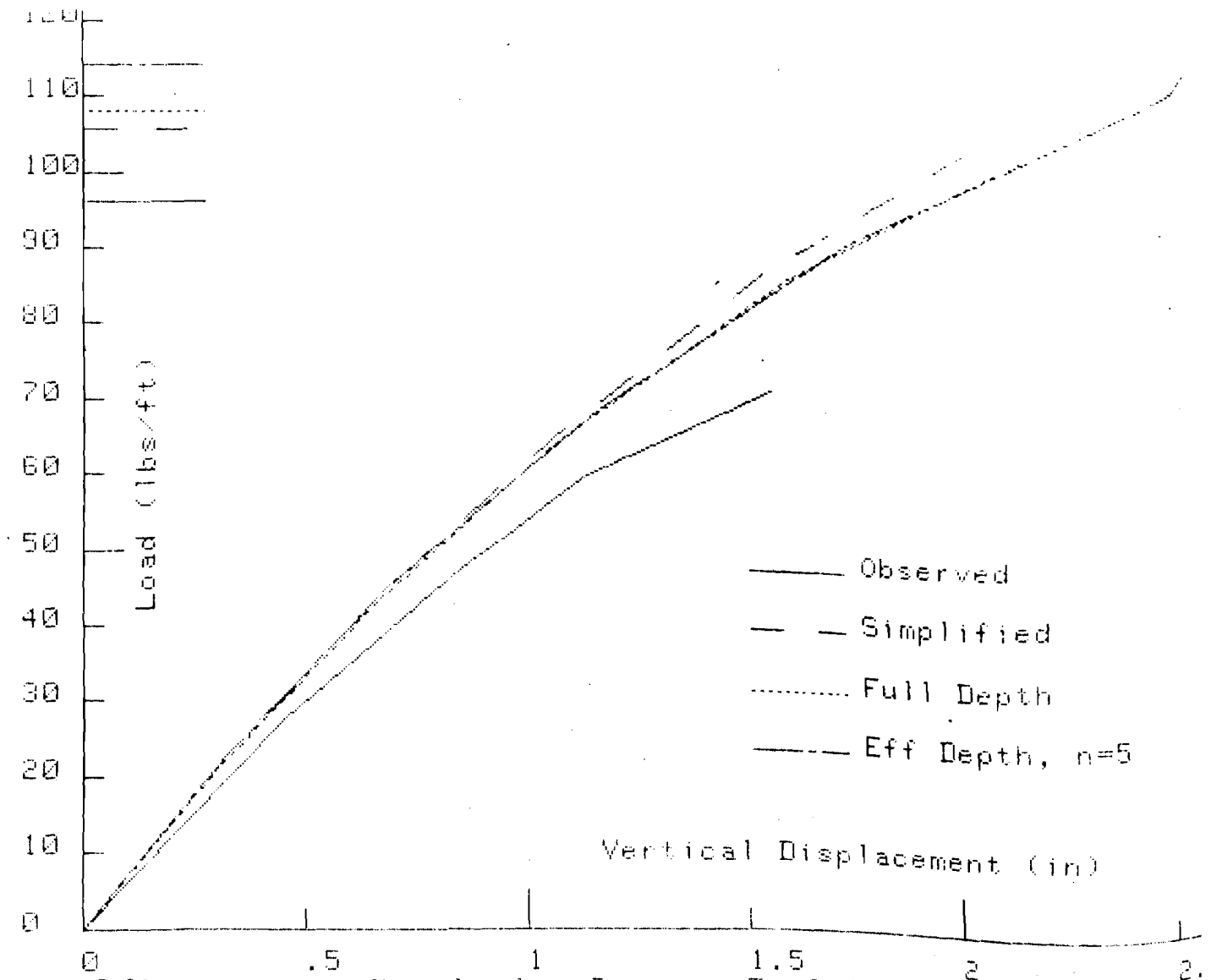


Fig. 5.18: Load vs. Displ. for Section Z $8.055 \times .063 \times .25$

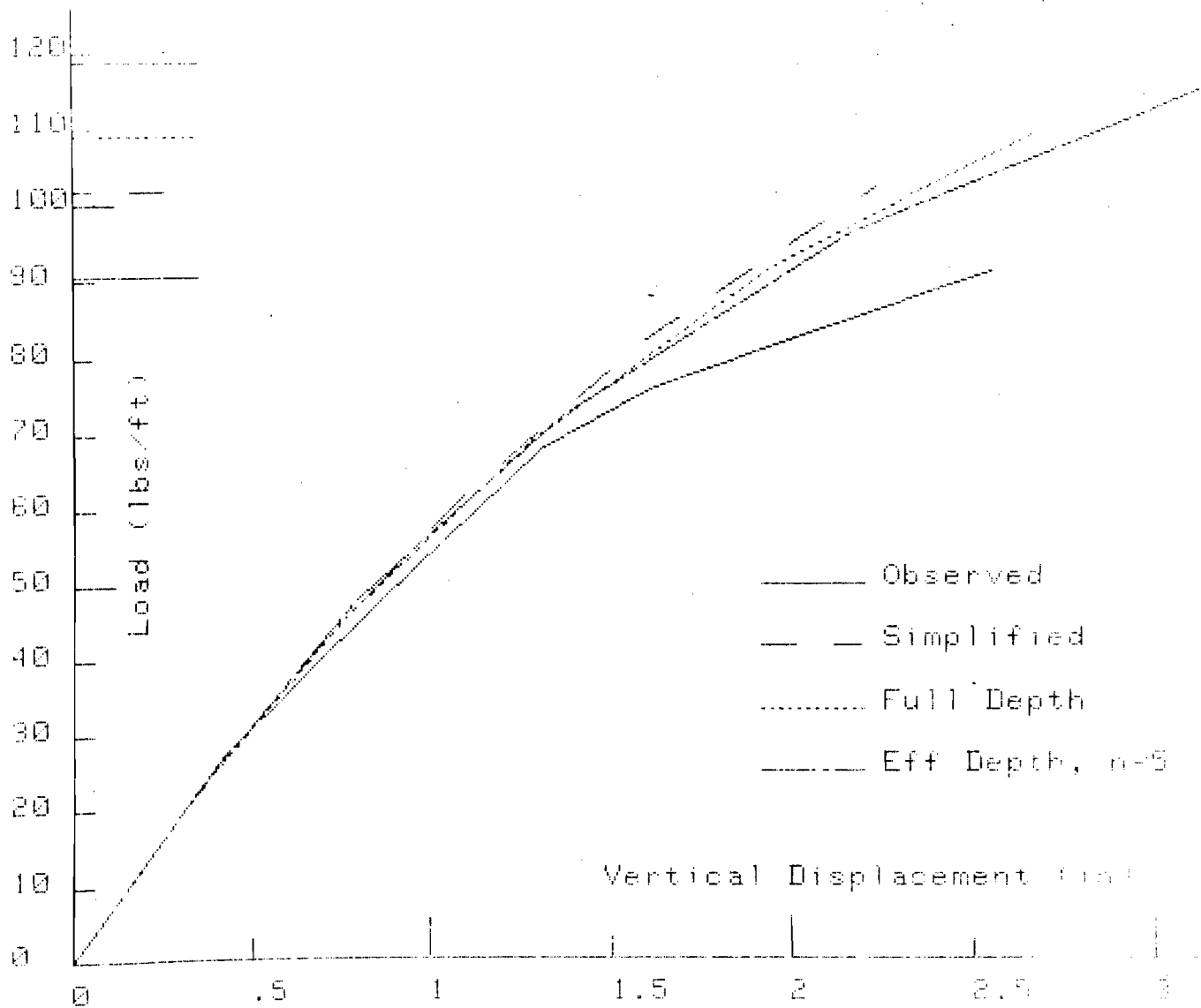


Fig. 5.19: Load vs. Displacement for Section Z. $\delta = 0.004$ in./lb.

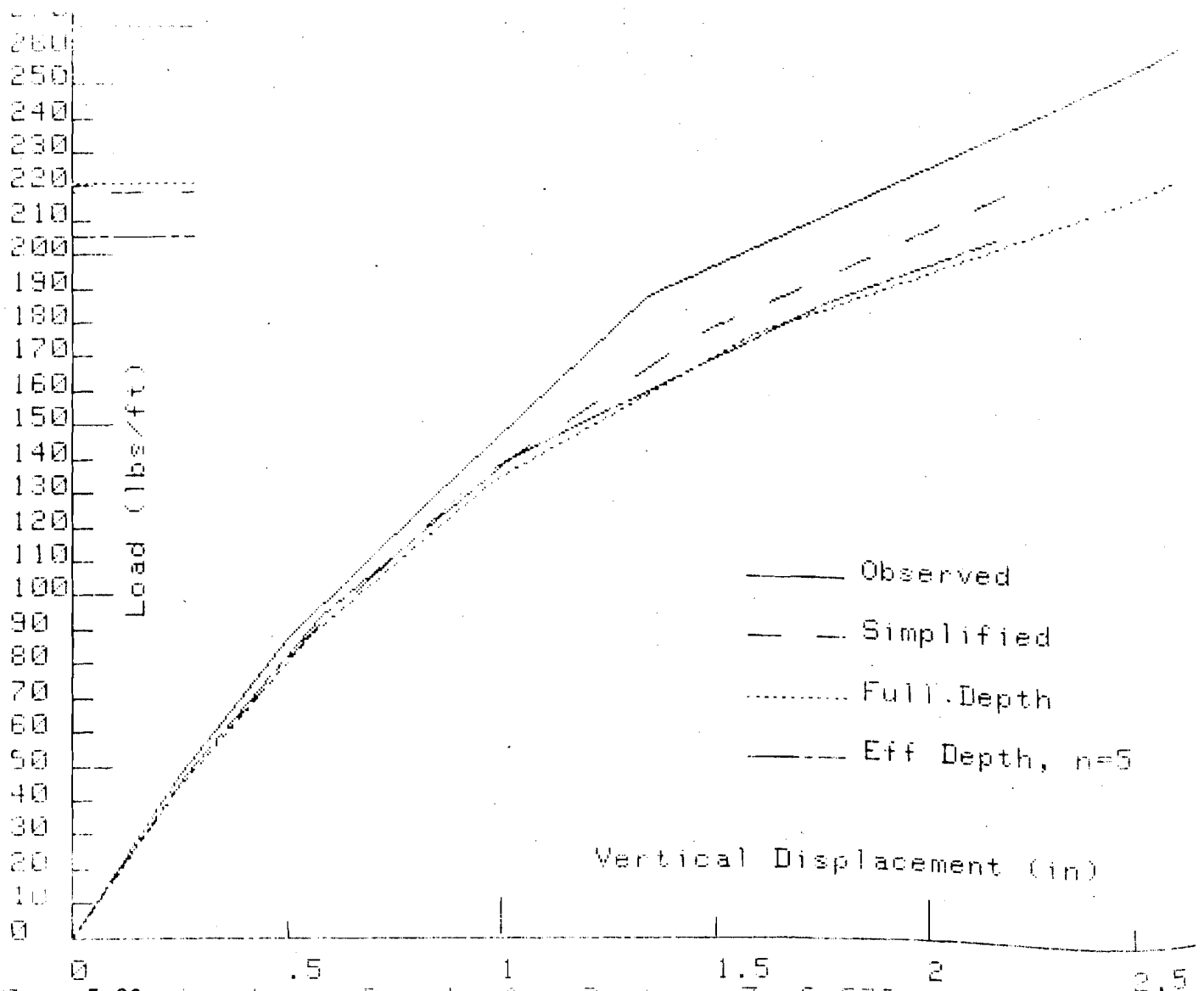


Fig. 5.20: Load vs. Displ. for Section Z $9.578 \times .106 \times -.063$

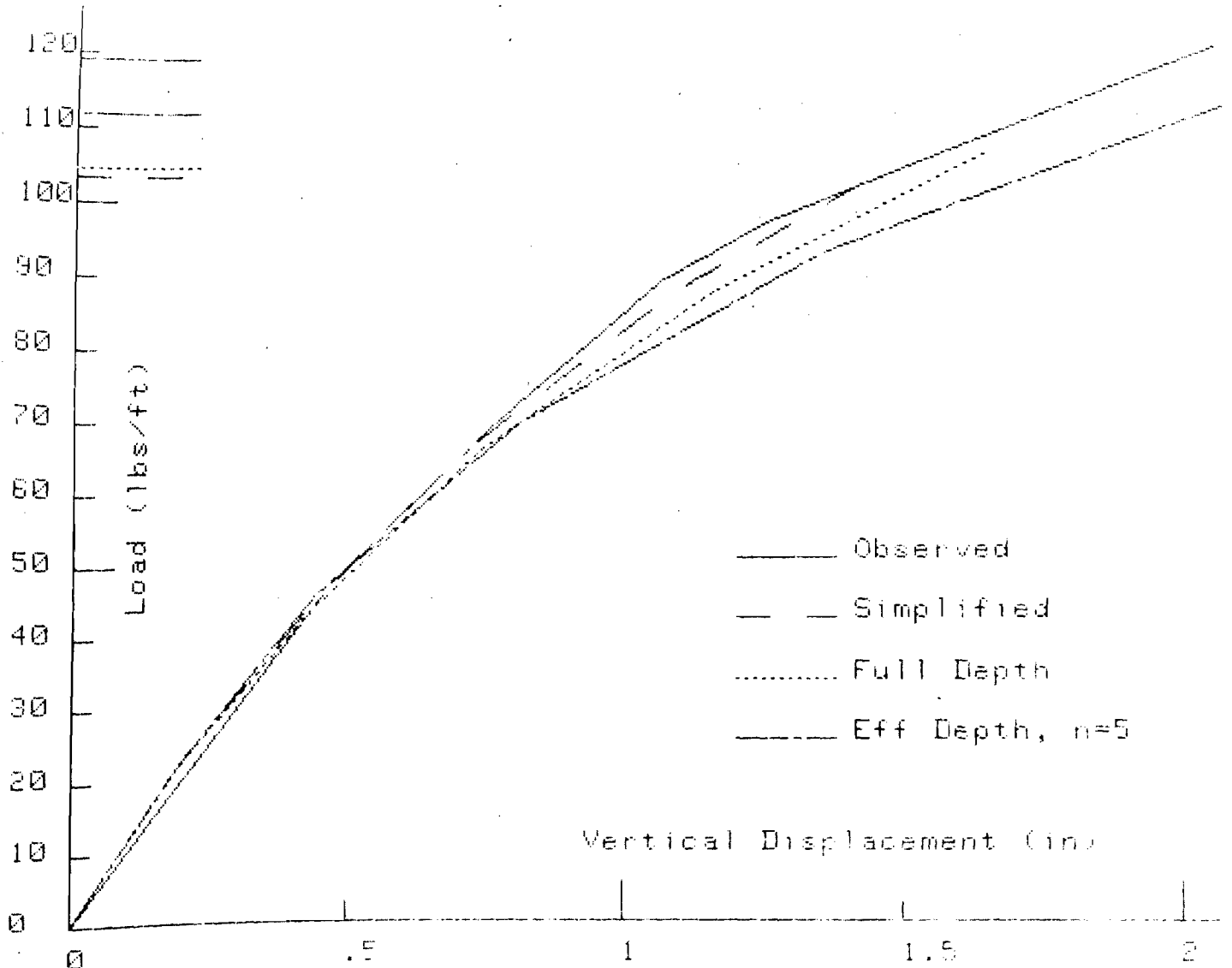


Fig. 5.21: Load vs. Displ. for Section Z 9.525 x .052 x .135

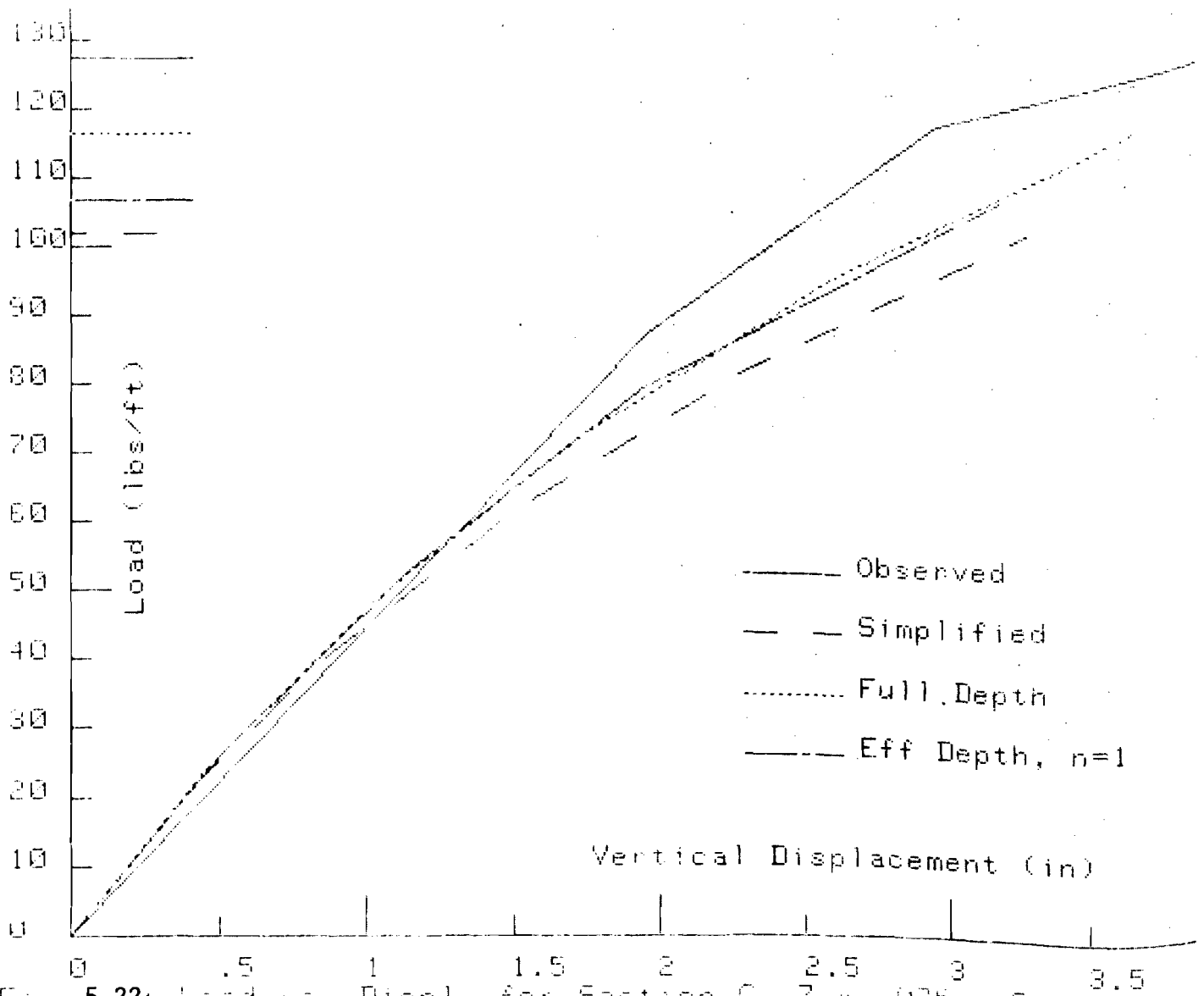


Fig. 5.22: Load vs. Displ. for Section C 7 x .075 x 0

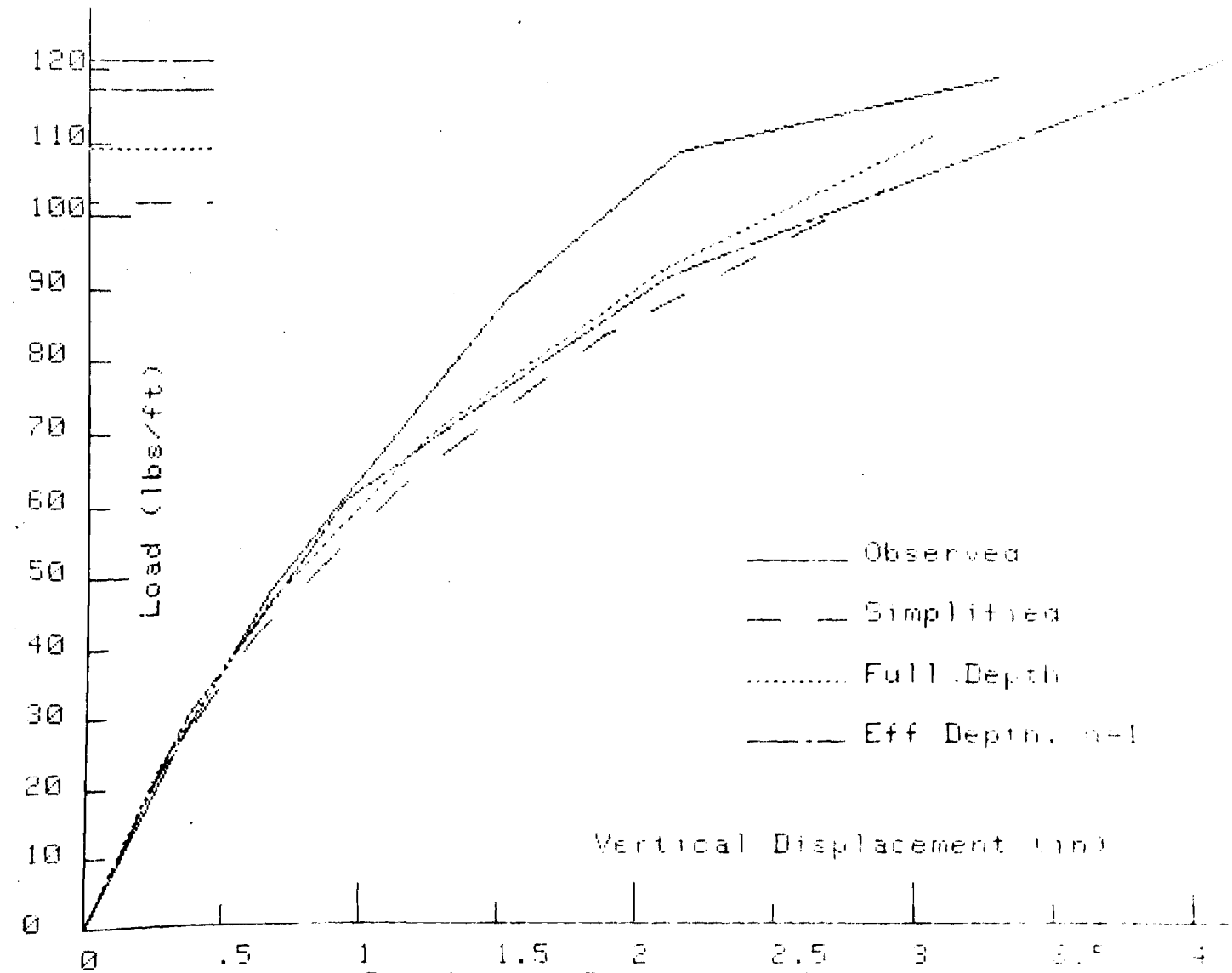


Fig. 5.23: Load vs. Displ. for Section 7-9, $\rho = 0.075$, $\rho = 0.32$

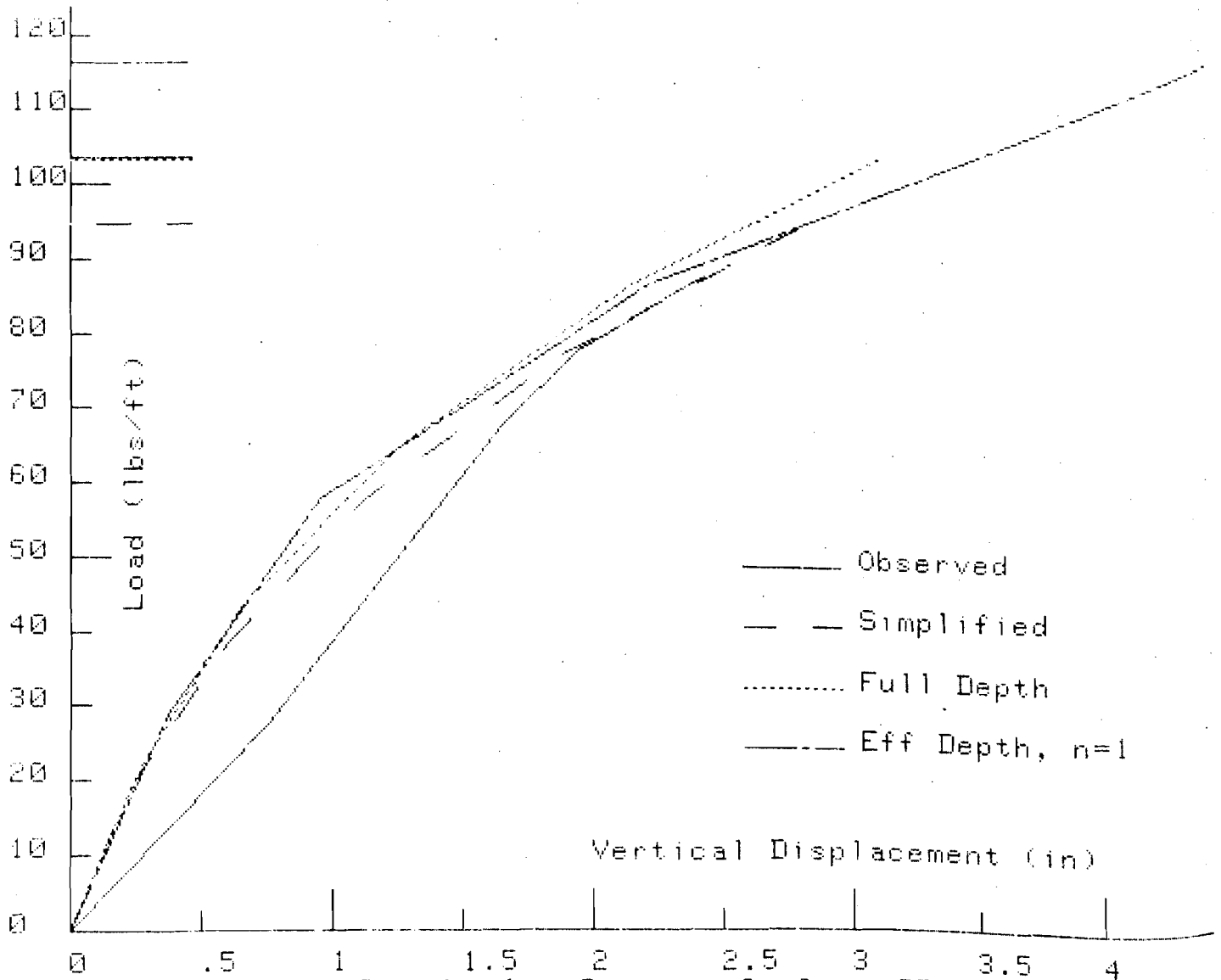


Fig. 5.24: Load vs. Displ. for Section C-9 x .077 x 1

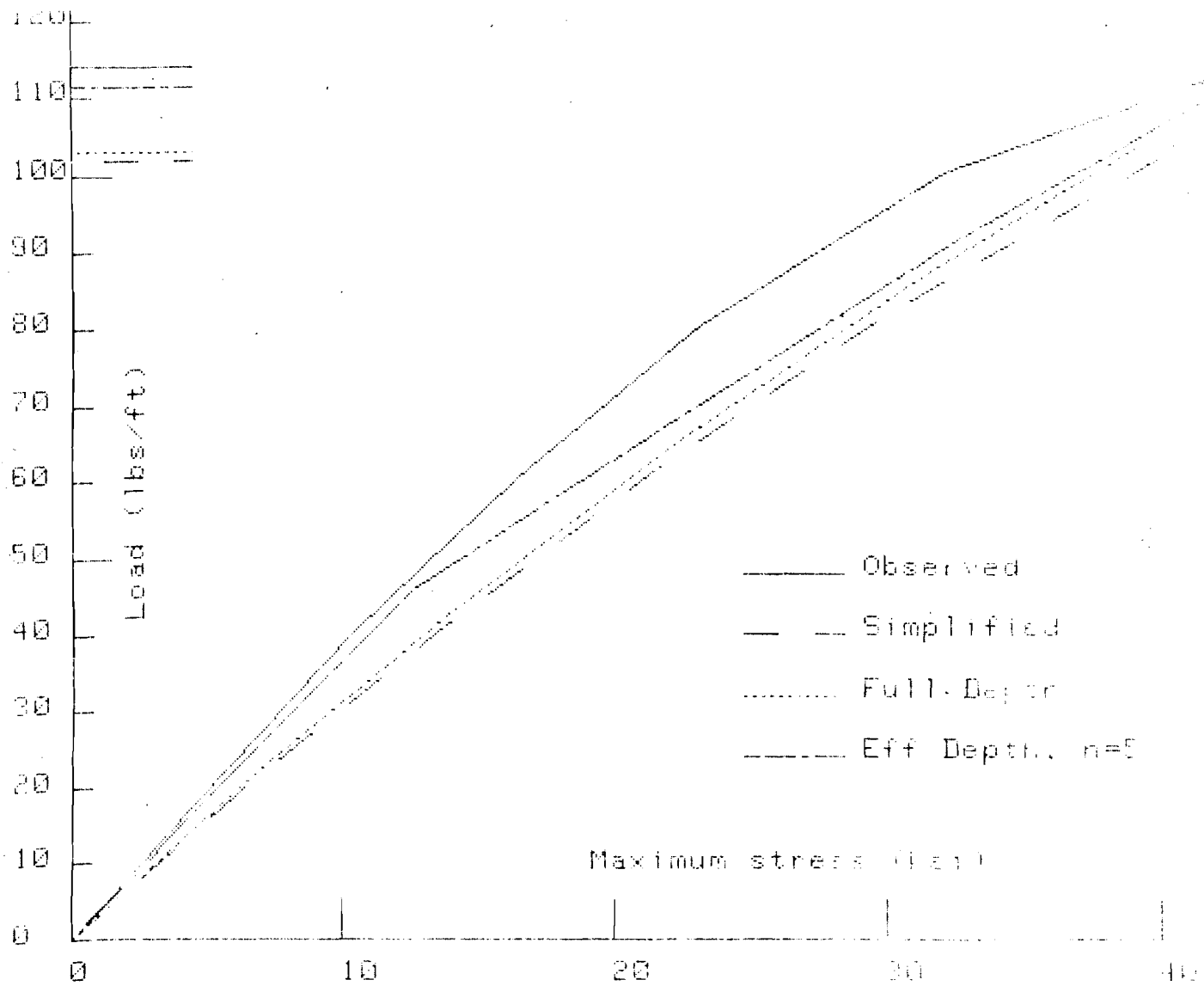


Fig. 5.25: Load vs. Stress for Section Z $\alpha=5$ $\beta=.053 \times .65$

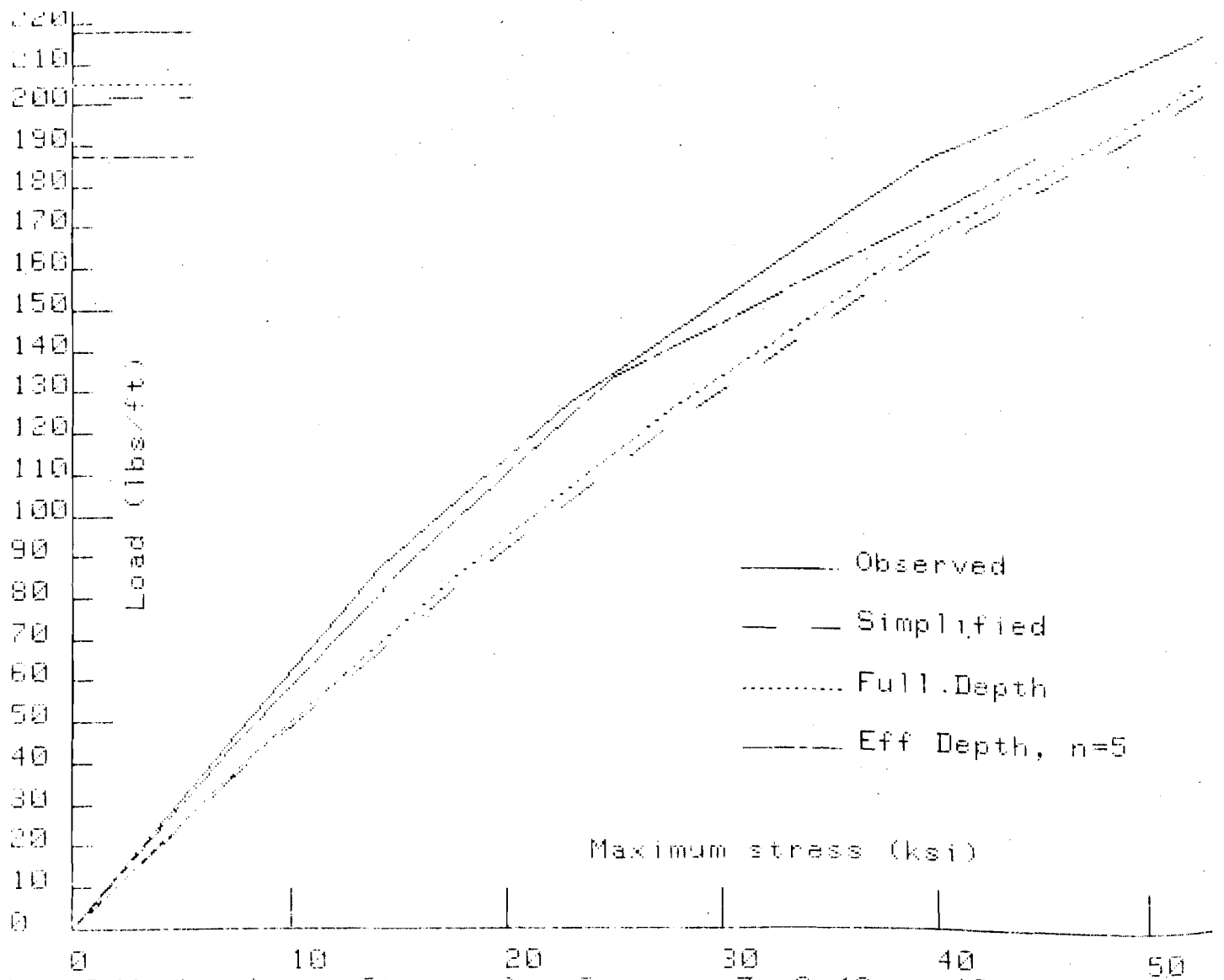


Fig. 5.26: Load vs. Stress for Section Z 9.49 x .109 x .94

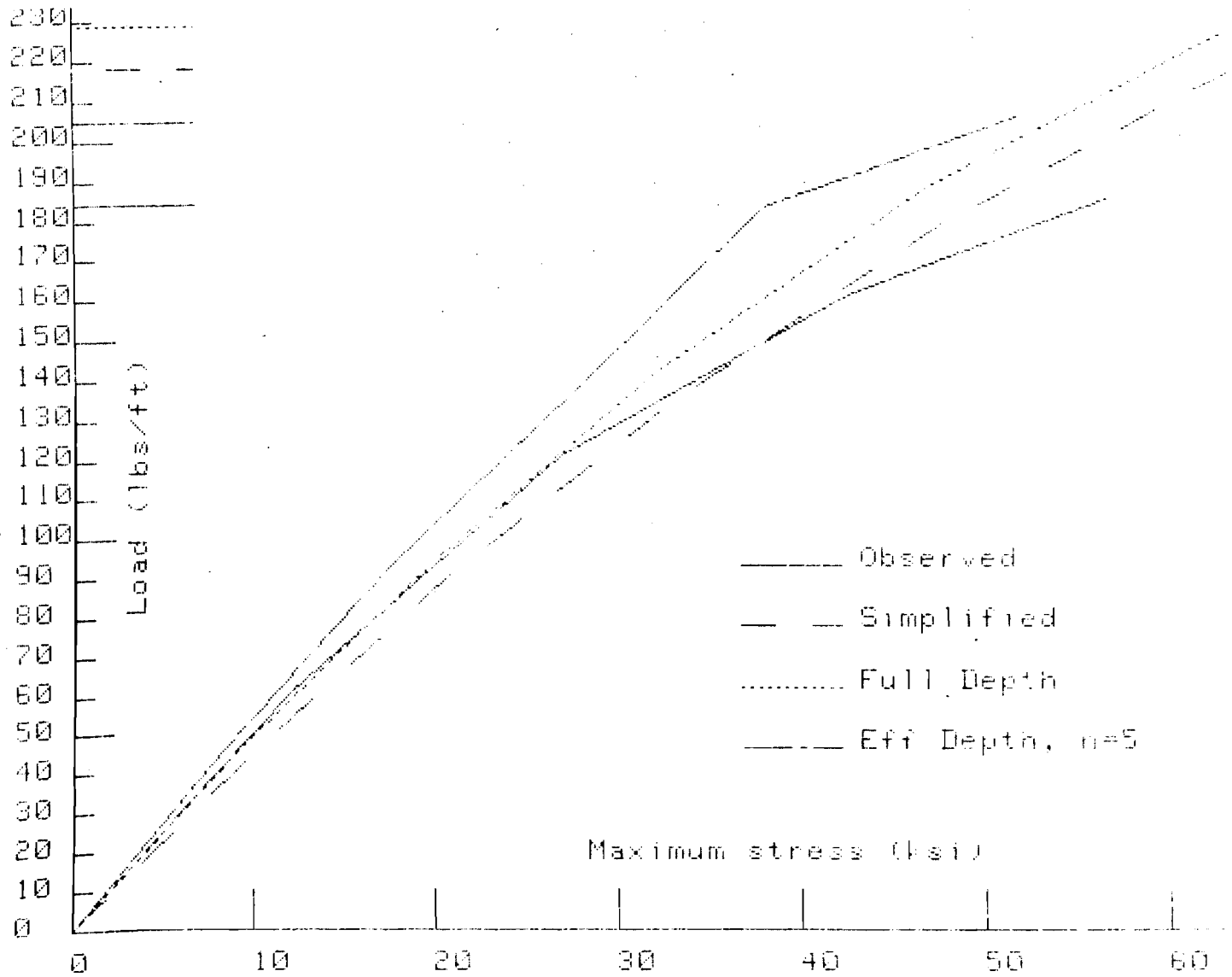


Fig. 5.27: Load vs. Stress for Section Z 7.93 x .115 x .47

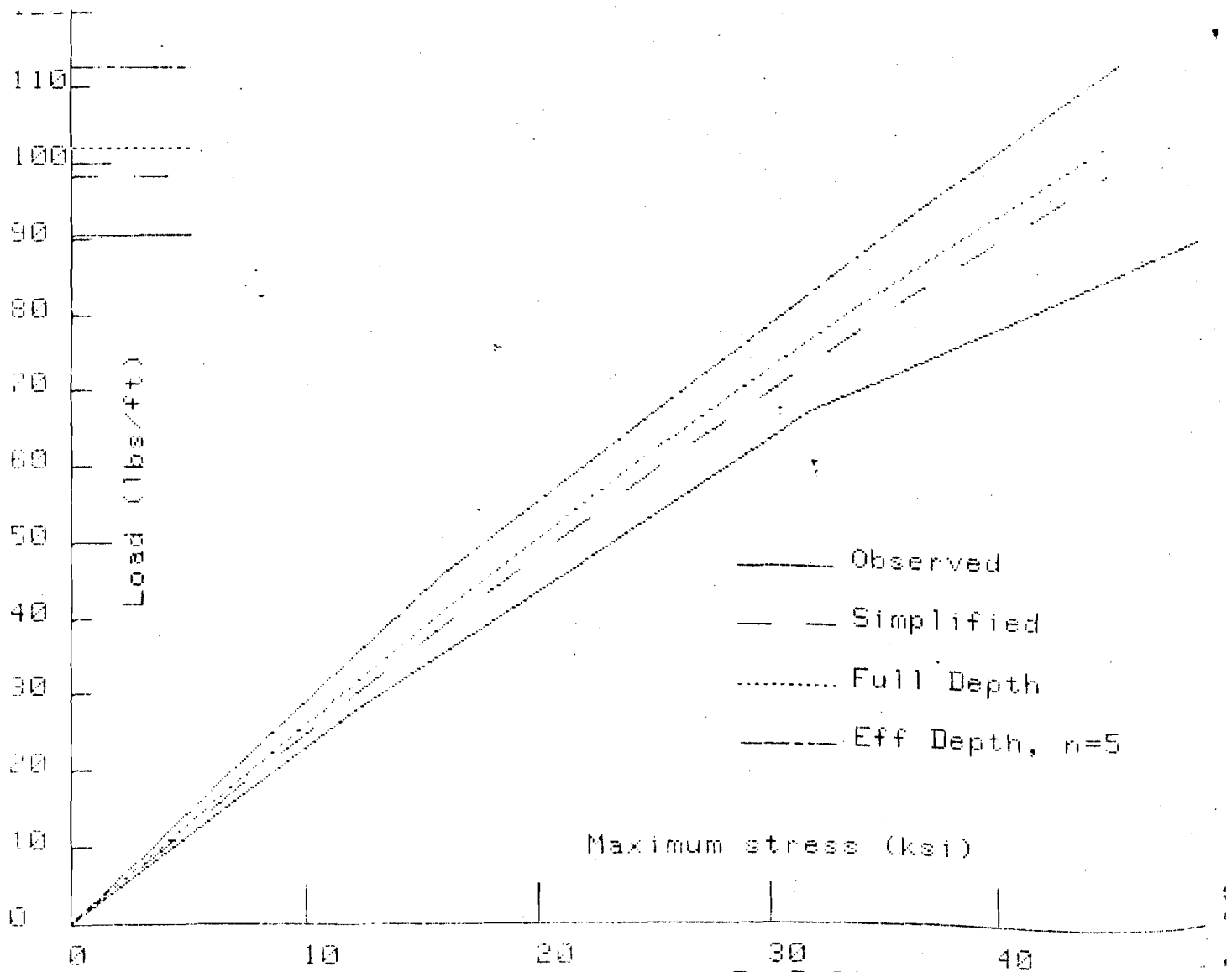


Fig. 5.28: Load vs. Stress for Section Z $7.92 \times .06 \times .56$

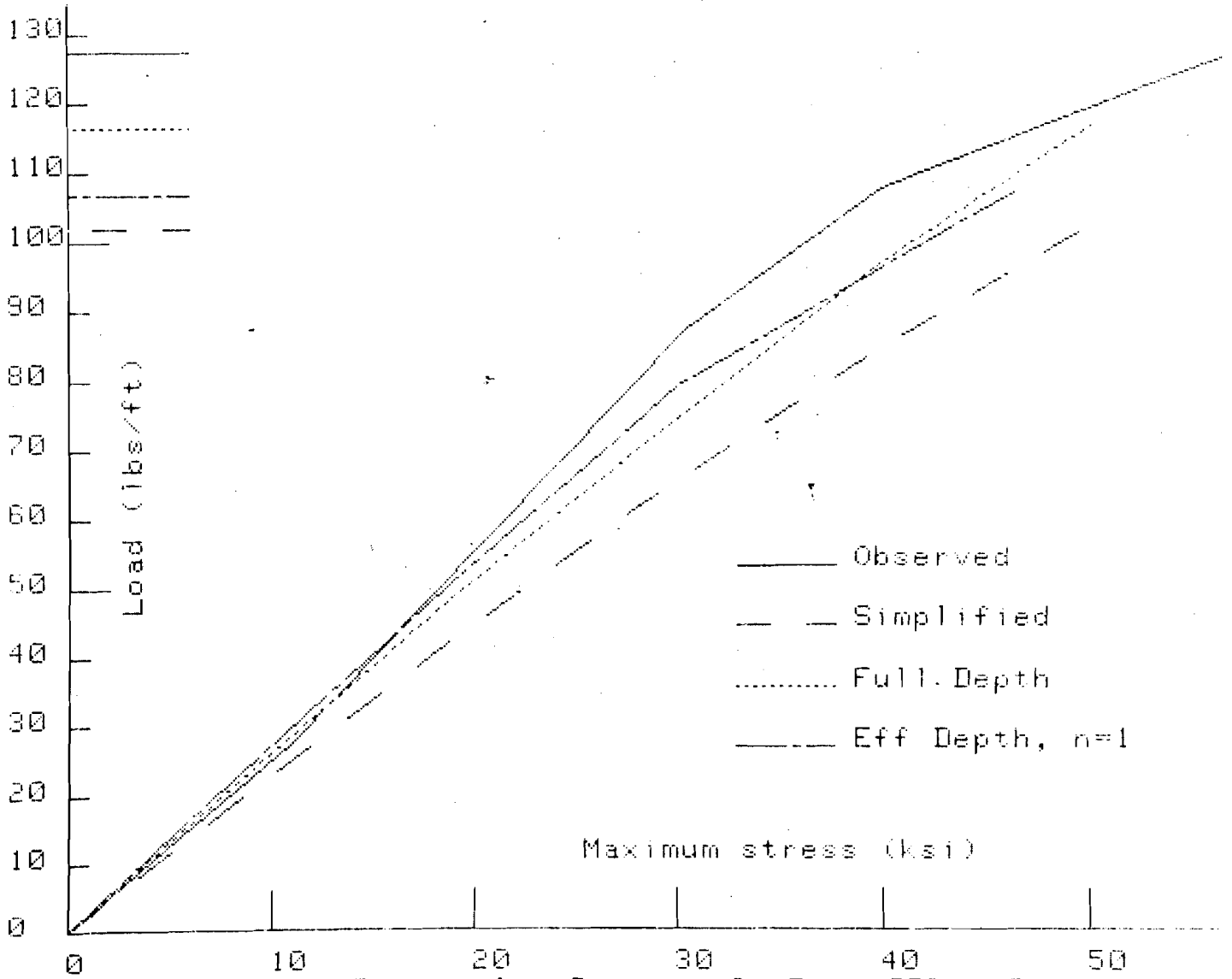


Fig. 5.29: Load vs. Stress for Section C 7 x .075 x 0

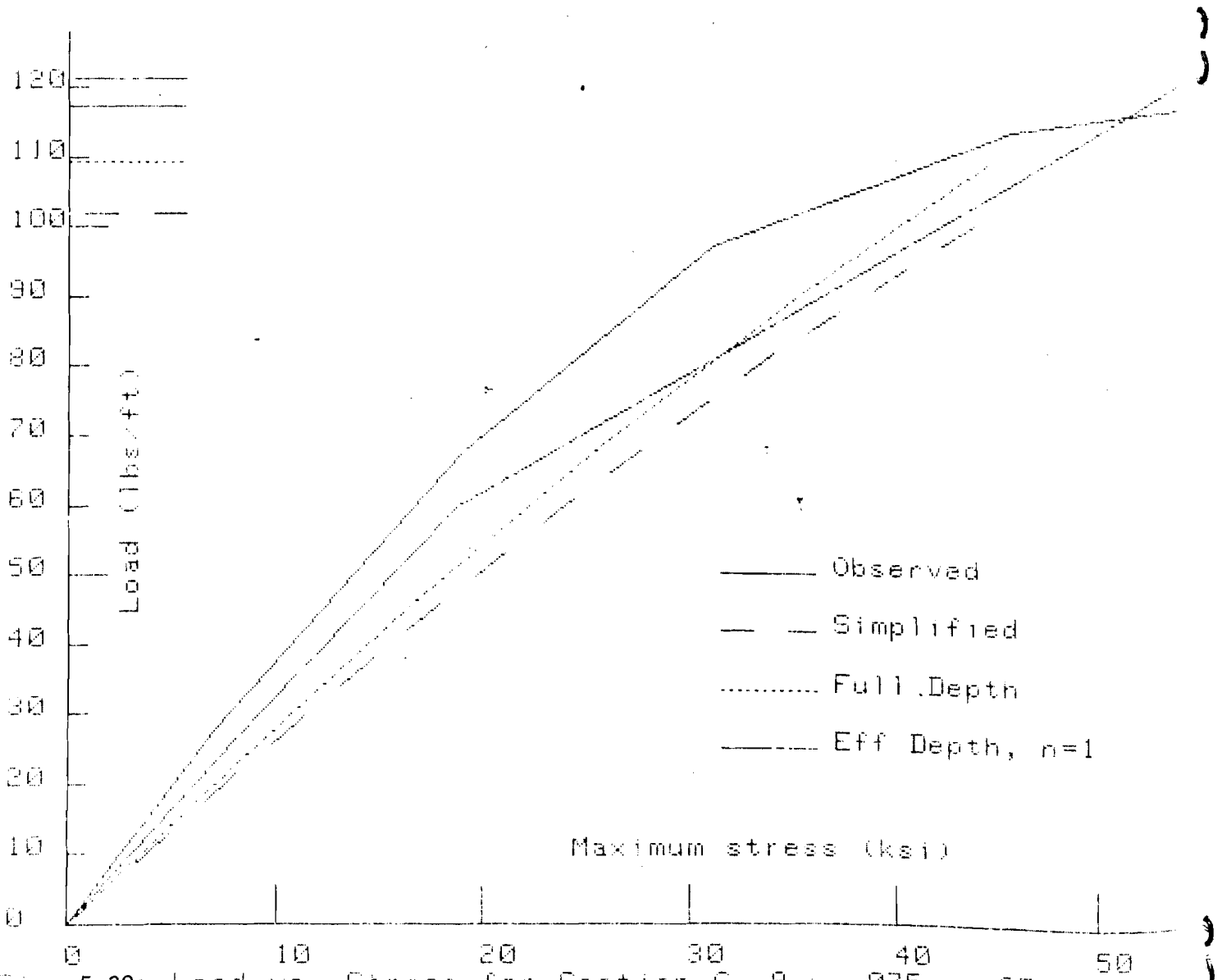


Fig. 5.30: Load vs. Stress for Section C 9 x .075 x .25